CONTROL OF TCR-MEDIATED T CELL ACTIVATION BY POLYCOMB REPRESSIVE COMPLEX 2

A Dissertation

Presented to the Faculty of the Weill Cornell Graduate School

of Medical Sciences

in Partial Fulfillment of the Requirements for the Degree of

Doctor of Philosophy

by

Joon Seok Park

August 2016

CONTROL OF TCR-MEDIATED T CELL ACTIVATION BY POLYCOMB REPRESSIVE COMPLEX 2

Joon Seok Park, Ph.D.

Cornell University 2016

ABSTRACT

The current view of signal transduction is that external stimuli trigger a series of cytosolic signaling events, which lead to the translocation of transcription factors, and changes in gene expression, which are dependent on the epigenetic landscape. Here, we discuss a paradoxical signaling paradigm in which a crucial chromatin modifier, Polycomb Repressive Complex 2 (PRC2), directly regulates receptor-proximal signaling. PRC2 catalyzes di/tri-methylation of histone 3 lysine 27 (H3K27me3), which correlates with transcriptional repression. While lysine methylation has largely been studied in the context of histone modification and epigenetic regulation, its role in the context of receptor-mediated signaling has rarely been described. In this study, we demonstrate that lysine methylation of cytosolic substrates by a cytosolic PRC2 complex plays an essential role in TCR-mediated T cell activation, independently from its nuclear function. Genetic ablation of essential PRC2 components in T cells had no effect on T cell development, loss of H3K27me3 or corresponding changes in gene expression. The resulting PRC2 deficient naïve T cells provided us with a good tool to study the signaling role of PRC2 in T cell

activation, without an altered epigenetic landscape. These PRC2-deficient T cells fail to proliferate upon TCR stimulation *in vitro* and *in vivo* and PRC2-deficient T cells have a specific defect in TCR-induced Erk phosphorylation. Pharmacological inhibition of PRC2 further substantiated that PRC2 directly controls TCR signaling and the methyltransferase activity of PRC2 is required for TCR-induced Erk phosphorylation. To understand the mechanism(s) by which PRC2 controls TCR signaling, we examined the complex composition and identified cytosolic substrates of Ezh2. We found that cytosolic PRC2 (cPRC2) contains the core components of the nuclear PRC2 complex, indicating that its methyltransferase activity is present. Additionally we found that cPRC2 is associated with the TCR signaling components Vav1 and Nck1. We predicted Nck1 *in silico* as a PRC2 substrate by screening for target consensus-sequences among Vav1-interacting proteins. We show that Nck1 is methylated *in vivo* and Ezh2 is responsible for methylation of lysine 64 in Nck1 *in vitro*. In addition to Nck1, we also found Ezh2 is self-methylated, suggesting that cPRC2 may assemble a signaling complex through the methylation of several sites within the complex. This possibility was supported by data showing altered interactomes of Nck and Ezh2 upon inhibition of Ezh2 enzymatic activity. In summary, this study sheds light on an underappreciated role for lysine methylation of non-histone substrate by PRC2 in receptor-mediated signaling.

To my Mother, Father, Brother and Love

ACKNOWLEDGEMENTS

First of all, I would like to deeply and sincerely thank my father Mr. Dae Beum Park, my mother Mrs. Mikyung Lee and my brother Mr. Junho Park who supported my goals of pursuing a scientific career with their unlimited love. I also thank Ms. Dayoung Hong for her invaluable support and encouragement at the later stage of graduate study. I believe that God drove me to this pathway and I am always grateful for his fathomless love.

In the course of graduate work, I would like to express my deepest gratitude to my mentor, Dr. Sasha Tarakhovsky, who trained me to become a real scientist. Under his supervision, I have learned how to think differently and critically for detail-oriented research.

I am also highly thankful to Dr. Carl Nathan, Dr. Sasha Rudensky and Dr. David Artis, who served as my committee. Without their help, support and advice, I would have not been able to finish my graduate work.

I would like to acknowledge the unlimited support from my colleagues. Dr. Marc-Werner Dobenecker gave me scientific advice on my thesis and provided various supports for finishing my thesis work. Also, he cheered me up whenever I was facing difficulties. I would also like to thank to Dr. Uwe Schaefer, Dr. Jessica Ho and Dr. Heuijoon Park who helped me adapt to the lab when I joined. I am also grateful to Jonas Marcello for our earlier collaboration. Additionally, I want to thank Dr. Diego Mourão-Sá, Dr. Brandon Razooky, and Dr. Armin Lahiji for our scientific discussion and their advice.

In addition, I would like to thank the other faculty members in the immunology program such as Dr. Morgan Huse and Dr. Jayanta Chaudhuri who gave me scientific and academic advice. Particularly, Dr. Huse taught me imaging of the immunological synapse. In addition, I thank Dr. Joseph Sun for experimental reagents such as LCMV and Listeria. Also, I would like to thank my earlier advisor Dr. James P. Allison, who gave me an opportunity to learn in his lab at the beginning stages of my PhD before he moved to Texas.

I also thank Brian Dill at Rockefeller proteomics facility for helping me with Mass spectrometric analysis. I am always grateful to Dr. Pedro Lee from Dr. Danny Reinberg's lab at NYU School of Medicine for teaching me biochemical techniques and for his friendship. And I would like to thank Dr. Poncharoen for Nck1/2 knockdown shRNA and Dr. Larry Samelson for the J.Vav cell line. Also, I would thank NIH tetramer facility for LCMV peptide MHC class I monomers.

I would like to express my gratitude to Dr. Sang-Jun Ha, who initially taught me how to do immunology research and encouraged me every time I had a hard time during my studies. In addition, I'd like to especially thank all the scientists and mentors who helped me to build myself as an independent scientist. Finally, I'd like to acknowledge Cornell University, Memorial Sloan Kettering Cancer Center and Rockefeller University, which provided me with PhD training opportunity, research facilities and scientific communities.

TABLE OF CONTENTS

FIGURES AND TABLES

CHAPTER 1: INTRODUCTION

1.1 Signaling through T cell receptor

T cells are essential cellular components of the immune system that play an important role in protecting the body from pathogens. They function by recognizing antigens through the T cell receptor (TCR) and along with co-receptors, they form a TCR signaling complex. These receptors bind to short peptides of 8-10 (for class I) or 14-20 (for class II) amino acids in length in the context of the major histocompatibility complex (MHC) that is present in the antigen presenting cells (APCs). T cells express unique TCRs after rearrangements of their germ-line encoded TCR-locus, which creates diversity allowing them to recognize a vast number of different antigens. Each T cell recognizes only a small number of antigens with their TCR and this feature creates specificity in their immune response.

A series of signaling events is initiated upon binding of the TCR to the peptide-MHC complex. The intracellular domains of the TCR undergo a conformational change that allows the Src family kinase, Lck, which is associated with the co-receptors CD4/CD8, to phosphorylate the TCR (Barber et al., 1989). The TCR contains ten Immunoreceptor Tyrosine-based Activation Motifs (ITAMs), whose tyrosine residues are phosphorylated by Lck. The phosphorylation of the ITAMs recruits the Spleen Tyrosine Kinase (Syk) kinase family member, Zap70 (Zeta-Chain associated protein Kinase 70kDa) (Chan et al., 1991; Chan et al., 1992). Zap70 gets activated through phosphorylation by Lck and in turn phosphorylates the integral membrane adaptor protein Linker for Activation of T-cells (LAT), which recruits

signaling molecules such as GRB2 related adaptor protein downstream of Shc (GADS), Inducible T-cell kinase (Itk), SH2 domain-containing leukocyte protein of 76 kDa (Slp76) and Phospholipase Cγ1 (PLCγ1) (Bunnell et al., 2000; Liu et al., 1999; Weiss et al., 1991; Zhang et al., 1998). The phosphorylation of Slp76, a scaffold protein that contains phospho-tyrosines, promotes its binding to Non-catalytic region of tyrosine kinase (Nck) and Vav (Bubeck Wardenburg et al., 1998; Tuosto et al., 1996; Wu et al., 1996). Activation of PLCγ1 by Itk results in hydrolysis of phosphatidylinositol 4,5-biphosphate (PIP2) into inositol 1,4,5-triphosphate (IP3) and diacylglycerol (DAG), which activate downstream signaling pathways (Secrist et al., 1991).

IP3 induces Ca^{2+} release from the endoplasmic reticulum (ER), followed by further influx of extracellular Ca^{2+} through calcium release-activated channels (CRAC) (Fasolato et al., 1993). This process enables Ca^{2+}-bound calmodulin to activate calcineurin to de-phosphorylate nuclear factor of activated T-cells (NFAT), which then translocates into the nucleus (Clipstone and Crabtree, 1992; Hogan et al., 2003; Shaw et al., 1988).

DAG, produced from the hydrolysis of PIP2, recruits and activates Ras guanyl nucleotide-releasing protein (RasGRP) and protein kinase C (PKC) (Downward et al., 1990; Ebinu et al., 1998). RasGRP converts Ras-GDP into Ras-GTP, which binds to Raf1. Activated Raf1 phosphorylates mitogen-activated protein kinase kinase1/2 (Mek1/2) (Huang et al., 1993). Activated Mek1/2 phosphorylates extracellular-signal regulated kinase1/2 (Erk1/2), whose translocation induces phosphorylation of many downstream effectors such as early growth response 1 (Egr1), ETS domain-containing

protein (Elk), mitogen- and stress-activated protein kinase (Msk) and ribosomal S6 kinase (Rsk) (Anjum and Blenis, 2008; Deak et al., 1998; Hodge et al., 1998; Seger et al., 1992; Yang et al., 1999). Among the targets of Erk are kinases that activate transcription factors, which is why Erk phosphorylation has such a large impact on gene expression downstream of the signal transduction cascade. Chief among them is the DAG bound PKCθ, which activates the mitogen-activated protein kinase (MAPK) pathway and the nuclear factor kappa-light-chain-enhancer of activated B cells (NF-kB) pathway (Baier-Bitterlich et al., 1996; Bi et al., 2001; Kishimoto et al., 1980; Monks et al., 1997).

Collectively, several transcription factors are activated downstream of the TCR and induce transcriptional programs including the binding of activator protein 1 (AP-1) (Fos/Jun), NF-kB, NFAT and Elk that bind to the promoter of the IL-2 gene, a hallmark of T cell activation (Jain et al., 1995). In short, the TCR signaling pathway represents a general receptor-mediated signaling mechanism (Figure 1.1). First, a ligand, the peptide-MHC complex, binds to the TCR. Second, the binding of TCR:pMHC results in the phosphorylation of tyrosine-residues in intracellular tail of the receptor. Third, recruitment of adaptors and enzymes such as kinases and GTPases to the receptor are involved in the formation of signaling clusters, where downstream molecules are sequentially activated. Lastly, downstream signaling intermediates translocate/activate transcription factors to induce transcriptional changes. This last step is usually subject to further modulation by chromatin modifications.

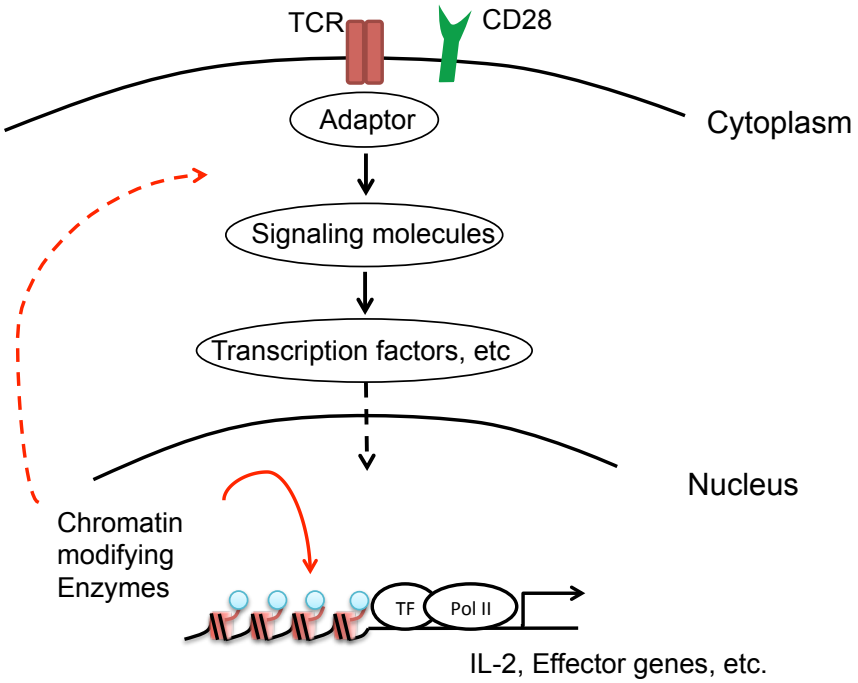

Figure 1.1. TCR-dependent signaling pathway TCR signaling cascades are initiated by ligation of TCR:pMHC along with CD28:B7. These receptor:ligand interactions recruit adaptor molecules to the cytoplasmic tails of the receptors. Post-translational modifying enzymes such as kinases are bound to adaptors, in turn and activate down stream signaling molecules. Eventually, this cascade activates transcription factors, which translocate into the nucleus to promotion transcription. Additionally, chromatin modifying enzymes regulate the transcription of genes.

1.2 Post-Translational modification and histone code hypothesis

Post-translational modifications (PTMs) are key regulators that transduce signals within a cell. The covalent modification of proteins by a phosphate group, a methyl group, an acetyl group, poly-ubiquitin and so on, can change their conformation, which exposes them to effector molecules or enable interactions with other proteins. These modifications are thought to be highly dynamic as both

facilitating enzymes and reverting enzymes already exist and their activities are often signal dependent.

In the past decade, post-translational modifications of histone proteins have garnered a lot of attention after Allis, Strahl and Jenuwein postulated the histone code hypothesis (Jenuwein and Allis, 2001; Strahl and Allis, 2000). Histones serve as scaffolds to package DNA into nucleosomes, which can be further folded into higher structures. According to the histone code hypothesis, specific covalent modifications of the N-terminal tails of histones can regulate transcriptional outcomes. For example, tri-methylation of histone 3 at lysine 27 (H3K27me3) is highly correlated with transcriptional silencing whereas tri-methylation of histone 3 at lysine 4 (H3K4me3) is associated with active transcription (Barski et al., 2007; Cao et al., 2002a; Strahl et al., 1999).

In general there are three classes of proteins described that establish and interact with the histone code. The first class is composed of "writers," which add covalent modifications to histone tails. These modifications include lysine/arginine methylation, lysine acetylation, lysine ubiquitination, serine/threonine phosphorylation and lysine sumoylation (Kouzarides, 2007). The second class is comprised of "erasers," which remove the covalent modifications on histone tails such as demethylases and phosphatases. The discovery of erasers indicated that histone modifications are not static but dynamic. However, how these processes are regulated is still under active investigation. The last class consists of "readers," which recognize specific PTMs on histones. Examples of such proteins are PHD finger containing proteins or chromo-domain containing proteins that bind to methyl-lysines and bromo-

domain containing proteins that interact with acetyl-lysines. Binding of "readers" controls transcriptional events such as heterochromatin formation as in the case of the chromo-domain protein HP-1α and transcriptional elongation mediated by the Brd4/p-TEFb complex (Eissenberg et al., 1992; Yang et al., 2005). The coordination of post-translational histone tail modifications and protein-protein interactions results in the regulation of gene transcription.

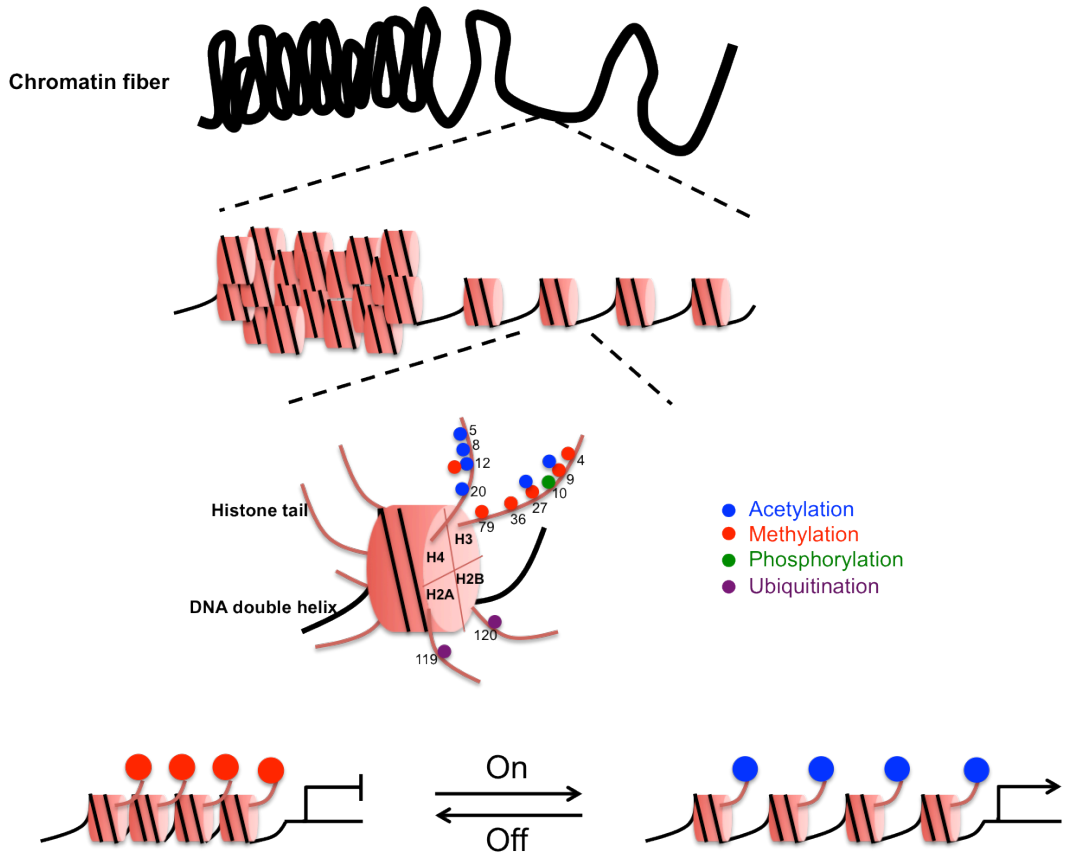

Figure 1.2. Histone code hypothesis Chromatin fibers are made of a bundle of nucleosomes, which consists of DNA wrapped around histone proteins (Kornberg, 1974). Histones serve as building blocks to make high order structures (Upper). Histone proteins contain an unstructured tails in its N-terminus, where various post-translational modifications can be added (Middle). Several lysine, arginine residues were identified to be methylated. Acetylation of lysine and serine/threonine phosphorylation also occurs. Additionally, H2A proteins were shown to be ubiquitinated. The histone code hypothesis proposes that certain modifications on specific amino acid residues of histone tails are associated with transcriptional activity by regulating structural features of chromatin (Bottom).

1.3 Lysine methylation and protein lysine methyltransferases (PKMT)

Lysine methylation has been extensively studied in the context of histone modifications. However, the initial discovery of lysine methylation was made in a

report describing the existence of the novel amino acid, ε-N-metyl-lysine, found in salmonella flagellar protein in 1959 (Ambler and Rees, 1959). The first observation on the methylation of lysines in histones was described five years later by Murray (Murray, 1964). Despite the fact that lysine methylation was initially discovered in a non-histone protein the biological relevance of lysine methylation has been extensively studied in the context of its function as an epigenetic mark. In recent years, the field of epigenetics has become an important area of intensive research that applies to many biological processes. Of particular interest is the role of epigenetic mechanisms in regulating cell identity by modulating the transcriptional output.

Recently, several studies have implicated that lysine methylation of non-histone substrates also plays a crucial role in transcription. The two best-known examples are lysine methylation of the NF-κB subunit RelA and p53. Lysine 310 of RelA (RelA K310me) can be methylated by SETD6 (Levy et al., 2011a) and this methylation enables GLP to bind to RelA; therefore, GLP-mediated H3K9me2 deposition results in gene silencing at NF-κB target loci. Interestingly, RelA K310me and S311 phosphorylation are mutually exclusive and signal-induced RelA phosphorylation displaces GLP from NF-κB targets. This methylation/phosphorylation switch is also found in H3K9me2/me3 and S10 phosphorylation (Fischle et al., 2005; Hirota et al., 2005), indicating that lysine methylation of non-histone substrates follows the principles observed in histone lysine methylation to some degree. There are several lysine residues on p53 that can be methylated. SET7/9-mediated p53 K372me1 increases promoter occupancy of p53 by enhancing the stability of p53 in the nucleus (Chuikov et al., 2004). An adjacent lysine

K372 was shown to be mono-methylated by Smyd2, which results in the abrogation of p53 transcriptional activity (Huang et al., 2006). Huang et al. showed that K372me1 inhibited K370me1, suggesting a possible crosstalk between two lysine methylations. One important aspect a p53 methylation is that it seems to be dynamically regulated. Lysine specific demethylase 1 (LSD1) was shown to remove a methyl group from p53 K372me2 that binds to its transcriptional co-activator 53BP1 (Huang et al., 2007). Upon demethylation of p53, binding to 53BP1 is lost and transcriptional activity diminished. Additional transcription factors were found to have methyl-lysines and the methylations of these residues are also involved in transcriptional regulation.

In addition to transcription, lysine methylation of non-histone substrates has recently been reported to be essential for signaling. Smyd3-mediated MAP3K2 methylation increases Erk1/2 phosphorylation in a Ras-driven cancer model (Mazur et al., 2014). The MAP3K2 K260 methylation prevents its binding to PP2A; therefore, the MAPK pathway was overactive in Smyd3 overexpressing cancer cells. In addition, VEGFR-2 methylation was shown to be required for tyrosine phosphorylation of VEGFR-2 (Hartsough et al., 2013). Although the studies mentioned above suggest that lysine methylation plays a role in signaling pathways, it is yet to be determined whether lysine methylation can be dynamically regulated in signal transduction and termination, as shown in phosphorylation-dependent signaling pathways.

The group of enzymes that mediate lysine methylation are called protein lysine methyltransferases (PKMTs). Since most methyltransferases were found to methylate histone proteins, they were designated as histone lysine methyltransferases (HKMTs). The human genome encodes more than 50 PKMTs. Most of them belong to the SET

(Su(var)3-9, Enhancer of zeste, Trithorax)-domain protein superfamily, with the exception of DOT1L, which is a non-SET domain lysine methyltransferase (Dillon et al., 2005). SET domains are comprised of around 130 amino acids and bind the universal methyl-donor and co-factor S-adenosyl methionine (SAM) which acts as a substrate for catalysis. These enzymes transfer one, two or three methyl groups donated from SAM to ε-N-lysine residues of their substrates. Many PKMTs were identified as "writers" of the histone code by genetic and biochemical approaches. As such, G9a, GLP, Suv39h1, Suv39h2 and ESET are responsible for the deposition of H3K9me3 marks and MLLs, SET1a, SET1b and SET7/9 were found to be responsible for the methylation of H3K4. In addition, NSD proteins were reported to be the enzymes for H3K36 methylation (Wagner and Carpenter, 2012). However, in the case of the H3K27me3 mark, there are only two enzymes capable of this modification, Ezh2 and its homolog Ezh1.

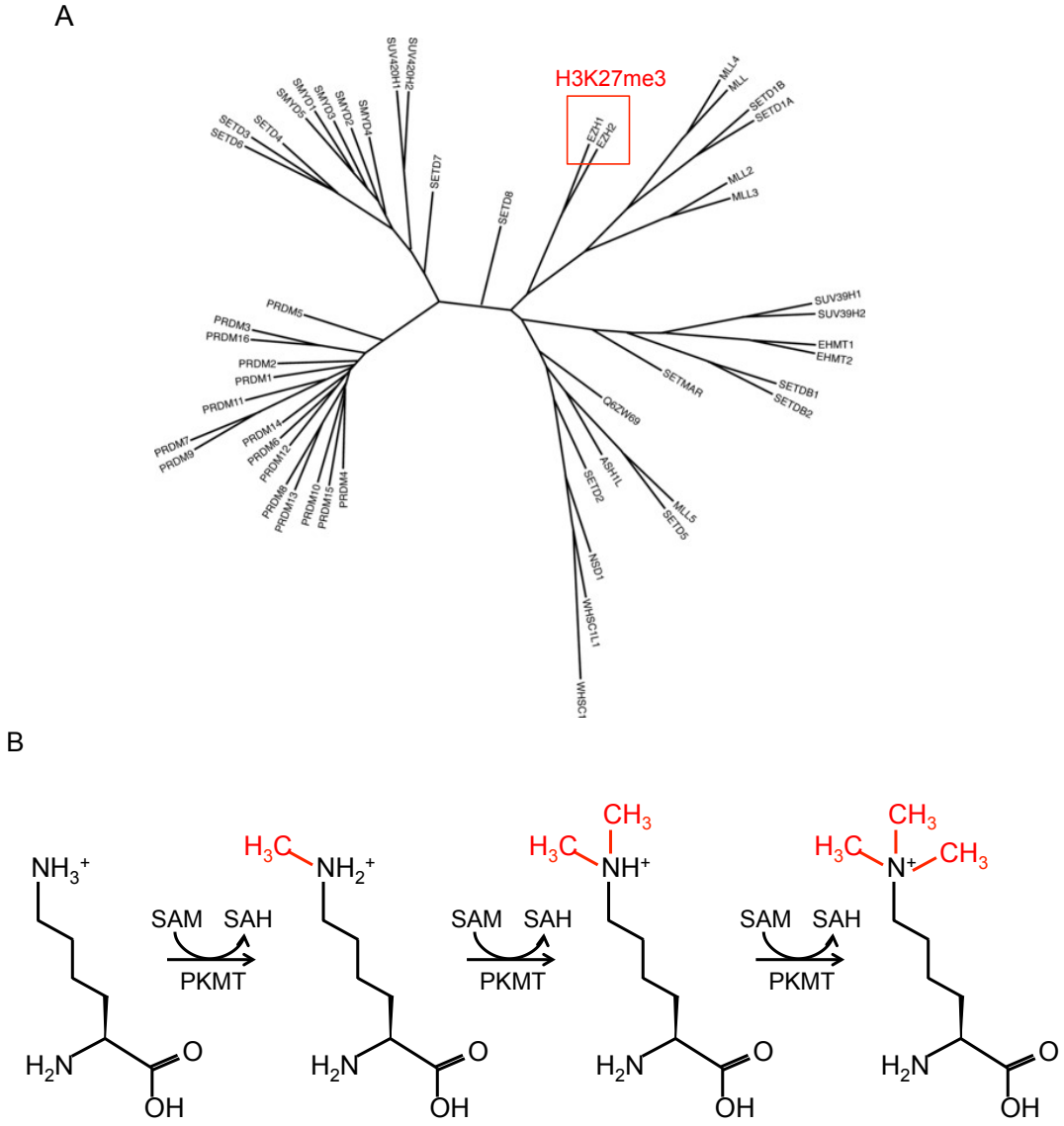

Figure 1.3. A phylogenetic tree of lysine methyltransferases and lysine methylation A. Phylogenetic tree of lysine methyltransferases encoded in the human genome. Ezh2 and its closely related homolog Ezh1 are the only known enzymes for H3K27me3 (Richon et al., 2011). **B.** Chemical reaction of lysine methylation. Up to three methyl groups donated by S-adenosyl methionine (SAM) can be added to ε-amino group lysine by protein lysine methyltransferase (PKMT). S-adenosyl homosystein (SAH) is made as byproduct.

1.4 Transcriptional Repression by Polycomb Repressive Complex 2

Ezh1 and Ezh2 are the enzymatic subunits of the polycomb repressive complex 2 (PRC2). PRC2 is a multi-protein complex which consists of at least 3 core components: Ezh1 or Ezh2, Eed and Suz12. These components are functionally necessary for PRC2 methyltransferase activity *in vivo* and *in vitro* (Faust et al., 1995; O'Carroll et al., 2001; Pasini et al., 2004). Initial purification of PRC2 from nuclear pellet fractions suggested that PRC2 has 5 components: Ezh2, Eed, Suz12, RbAp48 and AEBP2 (Cao et al., 2002a). The methyltransferase activity exclusively resides in Ezh1 and Ezh2, while Suz12 and Eed are essential for modulating the activity of the complex, AEBP2 is important for optimal histone methyltransferase activity towards H3K27me3 (Pasini et al., 2004) and the histone chaperone RbAp48 may promote histone binding of PRC2. More recently, Jarid2 was identified as an additional component of PRC2, which plays a role in recruitment of PRC2 to some target loci (Li et al., 2010).

Important insights into the function of PRC2 originated from developmental studies in *Drosophila melanogaster*. The Polycomb group (PcG) proteins were initially identified to play key roles in the regulation of *Drosophila Hox* genes (Lewis, 1978). During early *Drosophila* embryogenesis, PcGs function in maintaining the repression of *Hox* genes via chromatin remodeling, which can be mediated by the are three known PcG complexes in *Drosophila*: PRC1, PRC2 and PhoRC (Schuettengruber et al., 2007). PcGs are highly conserved in terms of function and the mammalian versions of these complexes have been purified biochemically and characterized by several laboratories. The main function of PRC2 is to repress gene

expression by the deposition of H3K27me3 mark (Figure 1.4). It has been shown that PRC2 is recruited to important developmental genes and the mode by which PRC2 functions in maintaining the repressive state of targets is by first establishing the initial H3K27me3 mark and propagation of the mark. Work from Reinberg and colleagues has shown that the Eed subunit of PRC2 uses an aromatic cage to recognize and bind the H3K27me3 mark, and thereby promotes the propagation of the histone modification by PRC2 to adjacent histones (Margueron et al., 2009). The PRC2-mediated H3K27me3 deposition also plays a role in the recruitment of PRC1. Briefly discussing the action of PRC1 in the chromatin remodeling, PRC1 binds to H3K27me3 via a chromo-domain of Cbx, one of PRC1 components. PRC1 generally consist of Bmi, RING1b, HPH and Cbx although PRC1 compositions are much more diverse between different complexes (Figure 1.4). RING1b is an ubiquitin E3 ligase that catalyzes H2AK119 ubiquitination (Wang et al., 2004). The H2AK119ub is thought to inhibit Pol II mediated transcriptional elongation; therefore, the target genes are not expressed. In addition to its role in H2AK119-dependent gene silencing, PRC1 also represses transcription by chromatin compaction (Eskeland et al., 2010). Collectively, PRC1 acts as an effector protein complex for PRC2-mediated gene silencing mechanisms (Figure 1.4). Although PRC1 was described as an effector of PRC2-mediated gene repression, PRC1 also can be recruited to target genomic loci in a PRC2-independent fashion (Tavares et al., 2012). Therefore, recent studies have shown that the precise mechanisms of PRC1-dependent transcription repression are more complex than they were thought to be; the details will not be discussed in this study.

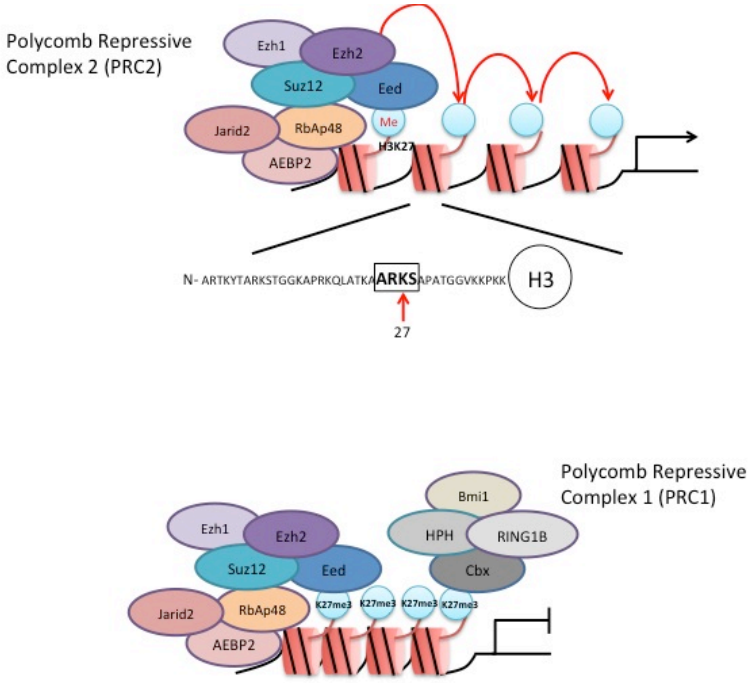

Figure 1.4. Polycomb Repressive Complex 2 and its function PRC2 methylates ARKS motif at H3K27. PRC2-mediated trimethylation of H3K27 results in recruitment of PRC1, which compacts chromatin and inhibits transcriptional elongation.

1.5 The role of PRC2-mediated gene silencing in T cell immunity

Chromatin modifications have an appreciable impact on the outcome of signaling pathways. Therefore, modulating chromatin structure determines the signal-induced transcriptional fate. In T cells, epigenetic mechanisms have been implicated in T helper lineage differentiation. Initial studies of PRC2 in T cell immunity focused on the role of PRC2 in Th1/Th2 differentiation. Although the first genetic study on PRC2 in T cells was from our laboratory (Su et al., 2005), it was unrelated to T cell effector

functions. By chromatin-IP (ChIP) analysis, *in vitro* Th2 differentiated cells were shown to lose H3K27me3 and Ezh2 binding at the IL-4/IL-13 locus, which can be found in naïve T cells (Koyanagi et al., 2005). Genetic studies have also shown that Ezh2 ablation leads to a gain of plasticity in Th1/Th2 differentiation (Tumes et al., 2013; Zhang et al., 2014). In addition to the Th1/Th2 paradigm, PRC2 has been implicated in the epigenetic regulation of regulatory T cell differentiation and function (Arvey et al., 2014; DuPage et al., 2015; Yang et al., 2015). Recently, our laboratory reported that Ezh2 controls invariant Nature Killer T (iNKT) cell development by controlling PLZF expression, the master transcription factor of iNKT cell development and function (Dobenecker et al., 2015).

In addition to studies on PRC2 function in T cell differentiation, the loss of Ezh2 in T cells results in reduced enrichment of H3K27me3 at the IFN-γ and Eomes loci in Th0 or iTreg cells *in vitro* (Zhang et al., 2014). Ezh2 was also shown to control survival-related gene expression such as Bcl2 in activated T cells (Zhang et al., 2014; Zhao et al., 2016). Along with these observations, Ezh2-deficient T cells have a defect in expansion *in vivo* or proliferation in a long-term culture *in vitro*.

The physiological role of PRC2 for T cell differentiation was demonstrated by several studies in animal models. Loss of Ezh2 in T cells exacerbated allergen-induced asthma by enhancing Th2 responses (Tumes et al., 2013). On the other hand, Th1 responses *in vivo* were also negatively affected by Ezh2 deficiency in pathogen infections such as *Toxoplasma gondii* and *Listeria monocytogenes* infections (Yang et al., 2015; Zhang et al., 2014). Furthermore, anti-tumor immunity required Ezh2

activity (Zhao et al., 2016). In summary, Ezh2 containing PRC2 governs T cell immunity; however, a clear mechanistic understanding is lacking.

1.6 Involvement of Ezh2 in TCR-signaling induced actin polymerization

Previous studies on PRC2 control of T cell immunity have attempted to explain PRC2-dependent T cell immunity by the transcriptional regulation through Ezh2. However, the early finding of Ezh2 as an interaction partner of the cytosolic protein Vav1 hints towards an additional mechanism of Ezh2 in the control of T cell activation, independent from its nuclear functions (Hobert et al., 1996). Vav proteins are important regulators for signal transduction, harboring GDP exchange factor (GEF) activities. Three isoforms, Vav1, Vav2 and Vav3, are expressed in mammalian cells (Bustelo, 2000). Among those, Vav1 expression is restricted to hematopoietic cells whereas Vav2 and Vav3 are expressed in a broad range of cell types. In T cells, Vav1 is a pleiotropic regulator for TCR signaling and absence of Vav1 impacts TCR-induced actin polymerization as well as calcium mobilization (Costello et al., 1999). Vav1 acts downstream of the TCR and its activity can be regulated by TCR-induced tyrosine phosphorylation. In detail, Vav1 has regulatory tyrosine residues on its acidic domain, which stabilize an auto-inhibitory conformation found in the steady state (Aghazadeh et al., 2000). Upon TCR-induced phosphorylation of those tyrosine resides, Vav1 changes its conformation into an active form, which exposes its GEF domain. Ezh2 was shown to bind to the N-terminal portion of Vav1 where the auto-inhibition takes place. Whether Ezh2 binding to Vav1 changes upon TCR stimulation and whether Ezh2 influences Vav1 conformation, are open questions.

Some known functions of Vav proteins in TCR-induced actin polymerization include a role as a GEF for RhoGTPases like Cdc42, Rac1 and RhoA (Bustelo, 2001; Turner and Billadeau, 2002). This effect is counteracted by GTPase activating proteins (GAPs), which induce the hydrolysis of GTP to GDP. GTP-loaded Cdc42 binds to WASP recruited to TCR signaling cluster by Nck. Cdc42 binding to WASP changes its conformation from a closed to an open conformation. This form of WASP exposes its C-terminal VCA domain and allows Arp2/3 to bind, thereby initiating the nucleation of actin for branched actin networks (Takenawa and Suetsugu, 2007). Alternatively, a Rac1-dependent pathway activates the WAVE2 complex in T cells to promote actin nucleation through Arps2/3 in a manner similar to WASP. Lastly, the RhoA pathway differs from Cdc42 and Rac1 in that it utilizes Dia for polymerization of linear actin filaments, rather than branched actin networks. Therefore, Vav1 acts upstream of Cdc42, Rac1 and RhoA in TCR-induced actin polymerization.

Along with the evidence of an interaction between Vav1 and Ezh2, our laboratory previously reported that Ezh2 plays an indispensable role for TCR-induced actin polymerization (Su et al., 2005). We have shown that Ezh2-deficient T cells do not accumulate F-actin content upon TCR crosslinking. This effect seems to be due to the impairment of the cytosolic function of Ezh2, as shown by rescue experiments in Ezh2-deficient MEFs with Ezh2 protein that lacks the nuclear localization signal (Ezh2ΔNLS). Rescue was not achieved with a SET domain mutant, indicating that the methyltransferase activity of Ezh2 is essential for actin polymerization. Moreover, deletion of Ezh2 in bone marrow results in failure of normal beta-selection due to a signaling defect during T cell development. These data provide us with crucial

evidence for the signaling requirement of Ezh2 in T cells. A more recent study supporting the cytosolic function of Ezh2 was conducted using other cell types. Genetic ablation of Ezh2 in dendritic cells results in a defect in integrin-dependent migration (Gunawan et al., 2015). The Ezh2-deficient dendritic cells did not display reduced H3K27me3 level. The prevalent hypothesis in the field is that PRC2 primarily functions through H3K27me3. Therefore, a precise mechanistic explanation is needed to clarify the role of PRC2 in signaling. Furthermore, to be able to judge the significance of the cytosolic function of PRC2 it is important to understand the composition of the complex and its cytosolic substrates.

1.7 Non-histone substrates of Ezh2

When discussing the cytosolic function of Ezh2, an outstanding question is whether Ezh2 can methylate non-histone proteins. Indeed, there are six proteins that have been identified as non-histone substrates of Ezh2: Rorα, STAT3, GATA4, Fra-2, Jarid2 and Talin-1. Rorα K38 mono-methylation by Ezh2 interacts with DCAF1, which leads to destabilization of Rorα by DCAF1-DDB-CUL4 E3 ligase-mediated ubiquitination (Lee et al., 2012). In this study, the chromo-like domain of DCAF1 was shown to recognize the methyl-lysine motif generated by Ezh2, suggesting that Ezh2-mediated lysine methylation of non-histone substrates can also function through "readers" as those found for histones. In addition, Ezh2 has been shown to methylate three transcription factors. First, STAT3 K49/K180 methylation by Ezh2 was reported (Dasgupta et al., 2015; Kim et al., 2013) to be required for an optimal level of STAT3 phosphorylation, which is crucial for its transcriptional activity. Second, GATA4 is

methylated by Ezh2 at K299 (He et al., 2012) and this methylation leads to repression of the transcriptional activity of GATA4 by antagonizing its acetylation. Lastly, Fra-2 K104me represses Fra-2 transcriptional activity in non-differentiated keratinocytes until differentiation is induced (Wurm et al., 2015). These examples showed that Ezh2-mediated lysine methylation impacted transcriptional activity and in the case of GATA-4 and STAT-3 Ezh2-mediated methylation affected the deposition of other post-translational modifications such as acetylation and phosphorylation. It was recently found that Ezh2 can tri-methylate Jarid2, a subunit of the PRC2 complex found in embryonic stem cells (ESCs), and this methylation creates a binding site for Eed (Sanulli et al., 2015) resulting in enhanced stimulation of PRC2 histone methyltransferase activity. While auto-phosphorylation is thought to be an excellent way of regulating enzyme activity, self-methylation may be also a conserved mechanism that provides an additional layer of fine-tuning of methyltransferase activity. Whereas all the substrates so far were implicated in regulating transcriptional events, Talin-1 was identified as a "true" cytosolic substrate of Ezh2 (Gunawan et al., 2015). As mentioned above, Ezh2 regulates cell migration in leukocytes through histone non-related functions. Talin-1 was proposed to be methylated by Ezh2 and its methylation controls adhesion turnover by dissociating Talin-1 from actin. Interestingly, actin and the actin binding protein EF1α1 were found to be methylated (Li et al., 2013; Vermillion et al., 2014), suggesting that lysine methylation has a significant contribution to actin cytoskeleton remodeling. Despite the identification of Talin-1 methylation, the previously observed function of Ezh2 in TCR-induced actin polymerization is yet to be clarified. One caveat of the reports described above is that

there is no information on the stoichiometric levels of methylation *in vivo*. Lysine methylation was shown by *in vitro* biochemical assays or mass spectrometric analysis of *in vitro* reactions. Even though these modifications were further validated by antibody-based approaches *in vivo*, it will be interesting to determine the levels of lysine methylation of non-histone substrates of Ezh2, although it may be technically difficult due to low levels found *in vivo*.

Non-histone substrates of PRC2 can be classified into two categories by comparing the similarity of their target sequences to the target sequence in histone H3. The first group of substrates contains a histone-like sequence. The "reader" proteins of modified histones do not recognize the whole protein but rather a short amino acid sequence (Li et al., 2007). This indicates that a short motif is sufficient to provide a methylation platform and its methylation can be recognized by conserved methyl-binding domains (Fischle et al., 2003). Our laboratory made the exciting discovery that such motifs can also be found in non-histone proteins. Self-methylation of G9a was identified at the histone-like sequence (K9-like sequence, ARKT) residing in the G9a protein (Sampath et al., 2007). This self-methylated lysine residue is recognized by the chromo-domain containing protein HP-1. Interestingly, Rorα methylation was identified by a bioinformatics screening for the histone-like sequence (RKS). The second class of substrates does not contain consensus sequences around methylation sites. Therefore, it is likely that Ezh2 methylates its target in a semi sequence-specific manner.

Table 1.1. List of identified substrates of Ezh2

Substrates	Lysine residue	Target sequence	Methylation state	Biochemical outcome	Biological function	
H3	K27	ARKSA	Di-, Tri-	Protein-protein interaction	Transcriptional repression	Histone-like sequence
RORα	K38	ARKSE	Mono-	Decreasing protein stability	Transcriptional activity	
STAT3	K49	ASKES	Di-	Unknown	Transcriptional activity	
	K180	YMKLH	Mono-	Promoting Other modification		No sequence consensus
GATA4	K299	TLKSQ	Mono-	Inhibiting Other modification	Transcriptional activity	
FRA2	K104	VIKTI	Mono-, Di-	Unknown	Transcriptional activity	
JARID2	K116	QRKFA	Mono-, Di- (*In vitro*) Di-, Tri- (*In vivo*)	Protein-protein interaction	Transcriptional repression	
Talin-1	K2454	AMKRL	Tri-	Protein cleavage	Adhesion turnover	

1.8 Biochemical functions of lysine methylation

Methyl-groups are relatively small and do not grossly change the chemical properties of proteins. While acetylation neutralizes the positive charge on lysine residues for example, methylation does not change the charge of the amino acid but plays a critical role in many biological processes (Figure 1.5).

First, lysine methylation can modulate post-translational modification of neighboring amino acids. A phosphorylation-methylation switch that was discussed above represents such a function. However, lysine methylation does not always inhibit the phosphorylation of neighboring residues. It can also promote the phosphorylation as shown in Rb methylation by Smyd2 as residue S811 of Rb is more phosphorylated upon K810 methylation (Cho et al., 2012). Also, methyl-lysine serves as a recruitment platform of other modifying enzymes and therefore facilitates additional modifications on other residues. One example is the recruitment of the acetyltransferase Tip-60 to p53, methylation of p53 by SET7/9 (Kurash et al., 2008), allows it to interact with Tip-60.

Another function of lysine methylation is to modulate protein stability. Since ubiquitination is also a posttranslational modification of lysines, prior lysine methylation can prevent proteins from being ubiquitinated. At the same time, as shown for Rorα methylation, lysine methylation can promote protein degradation through the recruitment of an E3 ligase (Lee et al., 2012). Therefore, lysine methylation can both increase and decrease protein stability.

As methyl-lysine binding proteins are being discovered, the main function of lysine methylation seems to serve as binding modules for those proteins. PHD finger, Tudor, MBT, chromo-domain, PWWP and WD-repeat are representative domains for methyl-lysine binding (Maurer-Stroh et al., 2003; Yap and Zhou, 2010). However, lysine methylation can not only promote but also hamper protein-protein interactions. Smyd3-mediated MAP3K2 methylation inhibits interaction between MAP3K2 and the phosphatase PP2A. Both promotion and inhibition of interactions by lysine

methylation strongly indicates that despite the small addition of "bulk" by the methyl-group to lysines, structural elements allow to clearly distinguish between methylated and non-methylated proteins.

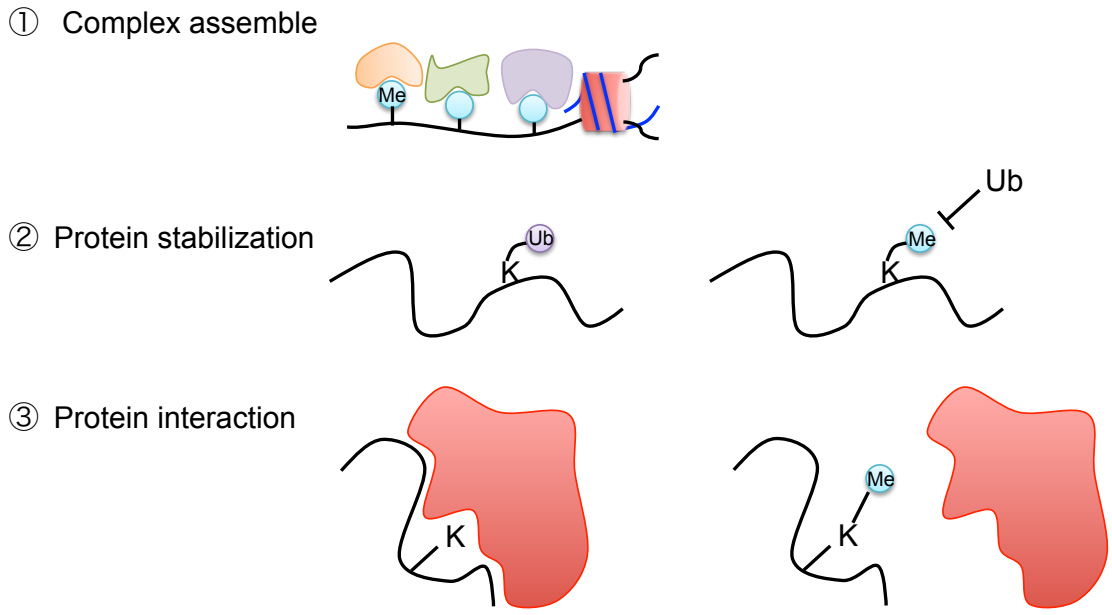

Figure 1.5. Biochemical functions of lysine methylation 1) Lysine methylation can provide docking sites for several proteins. Histone modification is a good example to demonstrate how lysine methylation can assemble an array of different "readers" 2) Since lysines can be target sites of E3 ligases, methylation can prevent ubiquitination-mediated protein degradation. 3) Lysine methylation can modulate protein interactions. This function includes both promotion and inhibition of interactions.

1.9 Aims of this study

In this study, we sought to understand the cytosolic functions of PRC2 in TCR-mediated T cell activation. We show that H3K27me3 levels are not altered in peripheral T cells of Ezh2$^{fl/fl}$; CD4-cre mice. Therefore, peripheral T cells from these

mice with wild-type surface-marker expression and wild-type gene expression pattern can be used as an excellent model for studying the nuclear and non-nuclear function of PRC2 in T cell activation and we will discuss the role of PRC2 in TCR-driven T cell expansion *in vivo* and *in vitro*.

Using the peripheral T cells with the genetic deletion of PRC2, we have found that TCR-mediated Erk phosphorylation was impaired in the absence of PRC2. Along with the previously described defect in TCR-induced actin polymerization pathway, we propose that PRC2 deficient T cells may have direct signaling defect in a fashion independent of histone modification. Signaling defects in PRC2-deficient mice could be indirect effects from some dysregulated gene that accumulated developmentally. Therefore, we will provide direct evidence of the cytosolic function of PRC2 for TCR signaling by three independent approaches. First, we examined the complex composition and properties in the cytosol. Understanding the components of cytosolic PRC2 (cPRC2) might also help us to understand why cPRC2 is essential for TCR signaling. Second, we will utilize pharmacological inhibition of PRC2. This approach will allow us to query the function of cPRC2, without having to worry about altered gene-expression, since we can utilize wild-type cells and short-term incubation with the inhibitor on ice, minimizing any nuclear changes. Also, it will allow us to distinguish between a possible adaptor function and the requirement of the methyltransferase activity of cPRC2 for TCR signaling. Finally, we identified Nck1 as cytosolic substrate of cPRC2. This allows us to determine where cPRC2 functions in the signaling cascade downstream of the TCR.

Lastly, we study the cPRC2-mediated lysine methylation dependent interaction partners of Nck1. This research has the potential to discover a formerly unappreciated mechanism that controls receptor-mediated signaling events.

1.10 Hypothesis

The fact that one of the key chromatin regulators, PRC2, directly controls TCR signaling is a very intriguing aspect of biology. This apparent moonlighting of a nuclear complex in the cytoplasm may act as a safeguard mechanism for cells to keep themselves from abnormal gene expression. H3K27me3 marks are very stable even in the absence of PRC2. H3K27me3 can be actively removed (Agger et al., 2007) or passively diluted in the absence of PRC2 by cell division and the necessity for new nucleosomes. Lack of H3K27me3 leads to altered gene-expression (Cao et al., 2002a). Therefore, maintaining sufficient amounts of PRC2 in dividing cells is crucial and indeed PRC2 expression drastically increases upon mitotic stimulation. Making PRC2 an integral and necessary component of the signaling cascade that can induce proliferation would ensure that only those cells divide that have sufficient enzyme complex in the cells. In addition, ensuring its enzymatic activity is important for proper gene regulation, therefore, such a safeguard mechanism should utilize common enzymatic properties in both signaling and epigenetic regulation to a certain degree. Therefore, *we hypothesize that PRC2 directly controls TCR-mediated T cell activation by methylating a cytosolic substrate*. This study reveals a novel signaling paradigm involving lysine methylation.

CHAPTER 2: MATERIALS AND METHODS

2.1 Mice

Previously generated $Ezh2^{fl/fl}$; CD4-Cre mice (Su et al., 2003; Su et al., 2005) were crossed with $Ezh1^{-/-}$ mice, which were generated by Dr. Donal O'Carroll (Thomas Jenuwein Lab), to give rise to $Ezh1^{-/-}$ $Ezh2^{fl/fl}$;CD4-Cre mice on B6/129 background. For testing single knockout for Ezh2, $Ezh2^{fl/fl}$; CD4-Cre mice on C57BL/6 background were used. $Eed^{fl/fl}$ mice on C57BL/6 background were kindly gifted from Dr. Meinrad Busslinger and crossed with CD4-Cre mice. To obtain a large number of cells, C57BL/6 mice were used for harvesting lymph nodes and spleens.

2.2 Infection

2 x 10^5 PFU per mouse of LCMV Armstrong was infected by intra-peritoneal injection. Peripheral Blood Mononuclear cells (PBMC) and serum were obtained from infected mice by retro-orbital bleeding on post-infection day 5, 8, 15 and 123. To analyze the virus-specific T cell responses, spleen and lymph nodes. Lung tissue was harvested to measure viral titer. Normal kinetics of virus-specific T cell responses is shown below. To examine the effector phase of immune response, the infected mice were sacrificed on post-infection day 8 and splenocytes were analyzed.

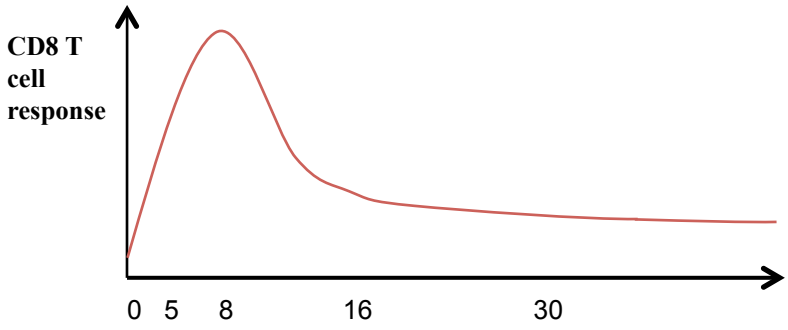

Figure 2.1. Kinetics of virus-specific T cell response Number of clonal T cells specific to virus is small at naïve T cell stage. Once virus evades, T cells that recognized the antigen expanded. Detection of virus-specific T cells can be done from 5 days after infection. Peak of CD8 T cell response is on day 8, followed by contraction phase where massive cell death of effector cells occurs. A significant number of virus-specific T cells remain even after the contraction phase, and they form memory T cell population.

2.3 Virus productions and plaque assays

LCMV Armstrong was produced in Baby Hamster Kidney (BHK) 21 cell lines. Monolayer of BHK21 cell line was infected with LCMV Armstrong at MOI of 0.3. Infection was done for 1 hr on rockers at 37°C. Pre-warmed DMEM media containing 10% FBS and 1% Penicillin/streptomycin were given to the infected cells. After 48 hrs, the media was harvested and spin down to get supernatant. The virus was titrated prior to use for *in vivo* experiments.

Virus titration was done by plaque assay. Serum was obtained by centrifugation of blood for 10min at 13000rpm. To isolate virus from tissues, tissues were homogenized in 1ml of media and spun down. Vero cells were grown for the plaque assay. Vero cells were infected with serum or harvested virus, which were diluted into proper range, for 1hr with shaking at 37°C. After infection, the infected

cells were incubated with 199 Media containing 10% FBS, 1% Penicillin/streptomycin, 1% L-glutamate and 0.5% agarose. After 4 days, the cells were stained overnight with 199 Media containing 0.5% neutral red with other supplements listed above. Plaques, which are seen as regions without cells, were counted and PFU was calculated according to dilution and the number of plaques.

2.4 Flow cytometry and detection of virus-specific T cells

Virus-specific T cells were detected using peptide-MHC class I tetramers. Monomers for LCMV GP_{33-41}, $GP_{276-286}$ and $NP_{396-404}$ were obtained from NIH tetramer core facility. Monomers were tetramerized with PE-conjugated streptavidin on ice for 1hr. Using flow cytometric analysis, frequency of virus-specific CD8 T cells and activation of T cells were examined. BD LSR II was used for flow cytometry and acquired data were analyzed with Flow Jo.

2.5 Restimulation of T cells for cytokine production

To measure virus-specific T cell response, cytokine production from T cells was examined. Splenocytes were stimulated with 0.2 μg/ml of GP_{33-41}, $GP_{276-286}$, $NP_{396-404}$ and GP_{61-80} for 5 hrs at 37°C in the presence of Golgi stop and Golgi plug (BD Biosciences). The stimulated cells were harvested and permeabilized with Foxp3 staining kit (eBioscience). Cells were stained for IFN-γ, TNF-α and IL-2, followed by acquisition by flow cytometry.

2.6 CFSE labeling and Stimulation of T cells

CD4 T cells were isolated from spleen and lymph nodes by MACS purification. Purified CD4 T cells were washed with PBS two times and labeled with CFSE at the final concentration of 2.5μM for 10min at room temperature. Labeling was stopped by FBS and washed with PBS three times. Labeled cells were stimulated on 96-well plates coated with 10 μg/ml of anti-CD3 and 2.5 μg/ml anti-CD28 antibodies or with 5 ng/ml of PMA plus 0.3 μg/ml of Ionomycin in a humidified 37°C, 5% CO_2 incubator. Cells were harvested after overnight and 3 days after stimulation.

2.7 Cell fractionation and Western blot

Purified CD4 T cells were lysed with 0.5% NP-40 containing TMSD lysis buffer (40mM Tris-HCl pH7.9, 5mM $MgCl_2$, 250mM Sucrose, 1mM dithiothreitol (DTT), 0.5% NP-40 (IGEPAL), protease cocktails (Sigma Aldrich), phosphatase cocktails (Millipore)) on ice for 15 min. The subcellular compartments were fractionated by centrifugation at 800xg for 10 min. Supernatant was further spun down to remove residual pellets, which supernatant was used as a cytosolic fraction. The pellets from centrifugation were washed twice with lysis buffer, then, incubated with high salt lysis buffer (50mM Tris-Hcl pH7.9, 420mM NaCl, 20mM NaF, 1mM EDTA, 1mM EGTA, 1.5mM $MgCl_2$, 10% glycerol, protease cocktails (Sigma Aldrich), phosphatase cocktails (Millipore)) for 10 min on ice. The extracts were sonicated for 10 cycles (30s per cycle), followed by centrifugation at 13000 rpm for 15 min, to obtain a nuclear extract. The concentrations of extracts were measured by standard BCA assay. The fractionated extracts or whole cell lysates were separated by

SDS-PAGE and transferred to a polyvinylidene difluoride membrane. The membrane was incubated with primary antibodies, followed by horseradish peroxidases conjugated secondary antibodies and developed with ECL systems according to manufacturer's instructions.

2.8 Erk phosphorylation assay

Purified CD4 T cells were incubated with 10 μg/ml of anti-CD3 antibody 2.5 μg/ml of anti-CD28 antibody on ice for 20 min, followed by cross-linking with 20 μg/ml of anti-Armenian Hamster IgG secondary antibody for 2 min or 10 min at 37°C. For PMA stimulation, cells were incubated with pre-warmed media containing 5ng/ml of PMA for 10min at 37°C. Cells were washed with cold BSS media, then, lysed with 0.5% of NP-40 lysis buffer (50mM Tris-Hcl pH7.9, 150mM NaCl, 20mM NaF, 1mM EDTA, 1mM EGTA, 1.5mM $MgCl_2$, 10% glycerol, 0.5% NP-40, protease cocktails (Sigma Aldrich), phosphatase cocktails (Millipore)) for 15min on ice. Lysates were obtained by centrifugation. The phosphorylated Erk1/2 were detected by western blot analysis using rabbit anti-phospho-Erk1/2 (T202/Y204) antibody (D13.14.4E, Cell Signaling Technologies) and mouse anti-Erk antibody (L34F12, Cell Signaling Technologies).

2.9 Immunoprecipitation

The fractionated lysates or lysates obtained by using ODG lysis buffer (2% of N-Octyl-β-D-Glucopyranoside, 50mM Tris-Hcl pH7.9, 150mM NaCl, 20mM NaF,

1mM EDTA, 1mM EGTA, 1.5mM $MgCl_2$, 10% glycerol, protease cocktails (Sigma Aldrich), phosphatase cocktails (Millipore)) were incubated with antibodies cross-linked to protein G dynabeads. The cross-linking of antibodies to beads was achieved by using BS3 cross-linker. Immunoprecipitates were washed with lysis buffer and eluted by boiling in sample loading buffer. Co-immunoprecipitates were detected by western blot analysis.

2.10 Streptavidin immunoprecipitaion for TCR

Purified CD4 T cells were incubated with anti-CD3/anti-CD28 antibodies, followed by biotinylated anti-Armenian Hamster IgG secondary antibodies for 2min at 37°C. For unstimulated cells, secondary antibodies reaction was done on ice for 15 min. Cell were lysed in ODG lysis buffer, followed by centrifugation. The supernatant were obtained and incubated with M-280 streptavidin beads for 2 hrs. Co-immunoprecipitates were analyzed by western blot analysis.

2.11 *In vitro* methyltransferase assay

In vitro methyltransferase assay was performed in methyltransferase assay buffer (50 mM Tris-HCl pH 8.5, 5 mM $MgCl_2$ and 1 mM DTT) with 0.69 μM of ^{3}H-SAM (Perkin Elmer) or 80 μM of SAM (NEB). 100 μM of peptides or 1 μg of proteins were used as substrates. 0.67 pmol of recombinant PRC2 containing Ezh2, Eed, Suz12, RbAp48 and AEBP2 (BPS Biosciences) was used for the methyltransferase reaction. The reaction was performed for 1hr 30min at 37°C and

stopped by adding sample loading buffer, followed by boiling. The reactants were loaded on SDS-PAGE gel, followed by incubating with Enhance solution (Perkin Elmer), and the methylation was probed by autoradiography.

2.12 Differential salt wash

Co-immunoprecipitates were incubated with Tris-HCl pH 7.9, 0.2mM EDTA, 5% Glycerol, 5mM DTT, differential concentration of NaCl (150mM to 600mM) for 30 min three times. Co-immunoprecipitates were further washed twice with 150mM NaCl buffer and eluted by boiling in sample loading buffer.

2.13 Human CD4 T cell and Jurkat cell stimulation

Human blood purchased from New York Blood Center for isolating CD4 T cells from PBMC. CD4 T cells were purified from human blood using RosetteSep^{TM} (Stem Cell Technologies). Purified T cells were pre-incubated with 10 μg/ml of mouse anti-human CD3 antibody (OKT3, eBioscience) for 15min on ice, followed by treatment of 20 μg/ml of F(ab')2 Goat anti-mouse IgG (H+L) secondary antibody (Thermo Scientific) for 2 min at 37°C. The stimulated cells were immediately washed with ice cold PBS and lysed with NP-40 lysis buffer. Phospho-Erk1/2 was measured by western blot analysis on human CD4 T cell lysates.

For Jurkat T cells, pre-warmed media containing 10 μg/ml of OKT3 was treated to the cells for 2 min at 37°C. Then, Jurkat cells were washed in cold PBS and lysed as described above. We also used J.Vav (Vav1-deficient Jurkat cell line) and

Nck1/2 knockdown Jurkat cells (ShRNA-mediated knockdown) (Cao et al., 2002b; Ngoenkam et al., 2014) for this experiment.

2.14 Antibodies

For Co-immunoprecipitation experiments, rabbit anti-Ezh2 antibody (D2C9, Cell Signaling Technologies), rabbit anti-Nck1/2 antibody (C-19, Santa Cruz Biotech), rabbit anti-Vav1 antibody (C-14, Santa Cruz Biotech) were used. For western blot analysis, mouse anti-Ezh2 antibody (Clone 11, BD biosciences), goat anti-Suz12 antibody (P-15, Santa Cruz Biotech), mouse anti-Vav1 antibody (05-219, Millipore), mouse anti-Nck antibody (Clone 108, BD biosciences), mouse anti-RbAp48 antibody (11G10, Abcam), rabbit anti-Jarid2 antibody (ab48137, Abcam). Anti-Eed rabbit and anti-Ezh1 antibodies were kindly provided by Danny Reinberg at NYU. For investigating TCR interaction with Ezh2, rat anti-CD3 antibody (CD3-12, Cell Signaling Technologies) was used. For measuring global levels of H3K27me3, rabbit anti-H3K27me3 antibody (07-449, Millipore) was used. For examining TCR-induced phosphorylation, mouse anti-PLCγ1 antibody (05-163, Millipore), rabbit anti-phospho-PLCγ1 (Y783) antibody (#2821, Cell Signaling Technologies), mouse anti-phospho-tyrosine antibody (4G10, Millipore), rabbit anti-phospho-Akt (T308) antibody (C31E5E, Cell Signaling Technologies), rabbit anti-phoshpo JNK (T183/Y185) antibody (#9251, Cell Signaling Technologies), goat anti-JNK antibody (C-17, Santa Cruz Biotech) and rabbit anti-phospho-Vav (Y174) antibody (sc-16408, Santa Cruz Biotech). For detection of methyl-lysines, rabbit anti-pan-methyl lysine antibody (#23366, Abcam) was used.

2.15 ChIP-Sequencing

Chromatin immunoprecipitation was performed as previously described (Lee et al., 2006). Purified CD4 T cells were cross-linked with 0.5% formaldehyde at RT for 10 min. Cells were lysed in RIPA lysis buffer containing 0.3M NaCl, followed by sonication. Sonicated extracts were incubated with antibodies bound to protein G overnight. Beads were washed with modified RIPA wash buffer containing 100mM LiCl and TE. De-crosslinking was done overnight at 65°C, followed by Rnase / Proteinase K treatement. ChIPed DNA and Input DNA were purified using Qiaquick PRC purification kit (Qiagen). ChIP was further validated by qPCR using SYBR Green PCR reagents and LightCycler 480. ChIPed DNA was generated into blunt-end DNA using DNA EndRepair kit (Epicenter Biotechnologies) according to the manufactuere's instructions. PCR purified end-repaired DNA was incubated with Klenow fragment (M0212, New England BioLabs) to add 'A' bases to the DNA. After PCP purification using MiniElute kit, the DNA fragments were ligated with Illumina/Solexa adaptors using T4 DNA ligase (New England BioLabds). With Illumina/Solexa primers 1.0 and 2.0, the DNA fragments were PCR amplified for 18 cycles. The ChIP-Seq library was further purified by MiniElute Kit, followed by sequencing on Illumina Hi-Seq 2000 for 50 cycles. The raw sequencing data were processed using CASAVA_v1.8.2 software to generate fastq files and aligned to the mouse genome (mm9) using Bowtie v0.12.7. Reads were filtered by alignment with more than 2 errors and more than 2 locations in the genome. For comparative analysis

of promoter regions, the number of aligned reads in the ±3 kb area from transcription start site of each gene was analyzed.

2.16 RNA-Sequencing

2μg of total RNA were used and ribosomal RNA was removed using Ribo-Zero Magnetic kit (Epicenter). RNA-Seq library was prepared with ScripSeq v2 RNA-Seq Library Preparation Kit (Epicenter) following the manufacturer's instructions. In brief, purified RNA was fragmented, followed by cDNA synthesis, adaptor ligation and pre-amplification. Samples were sequenced as described above with 100 cycles of amplification. Fastq reads were aligned to the mouse genome (mm9) using Tophat to account for splicing, alternative promoter usage, insertions and deletions. Also, differential gene expression, alternative promoter usage and splicing variant were analyzed using Cufflinks RNA-seq analysis tool.

2.17 Statistical analysis

Statistical analysis was performed in Prism (Graphpad) with the unpaired two-tailed Student's t-test. Data were present as mean ± standard deviation in most of figures.

CHAPTER 3: CONTROL OF TCR-MEIDATED T CELL ACTIVATION BY PRC2

3.1 Expression of Ezh1 and Ezh2

Ezh1 and Ezh2 are the catalytic subunits of PRC2 responsible for the methyltransferase activity of the complex. These enzymes are structurally very similar to each other and share 76% sequence identity. Particularly the SET domains, which are essential for the methyltransferase activity of Ezh1 and Ezh2 share a 96% sequence identity between them.

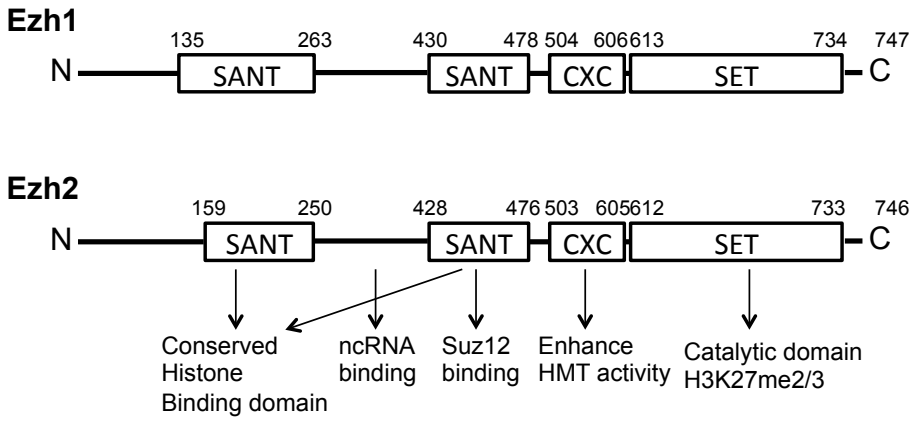

Figure 3.1. Domain structures of Ezh1 and Ezh2 Ezh1 and Ezh2 have the same domain structure with high sequence homology. Both of their enzymatic domains (SET) are located at the C-terminus and share 96% sequence identity.

However, the relative contribution of Ezh1 and Ezh2 for T cell immunity has not been addressed. Despite their structural similarity, Ezh1 and Ezh2 have quite

different expression patterns in T cells. Upon mitotic stimulation including TCR or PMA/Ionomycin, T cells up-regulat Ezh2 drastically whereas Ezh1 expression is relatively constant. This indicates that Ezh1 and Ezh2 may have differential contributions to T cell biology.

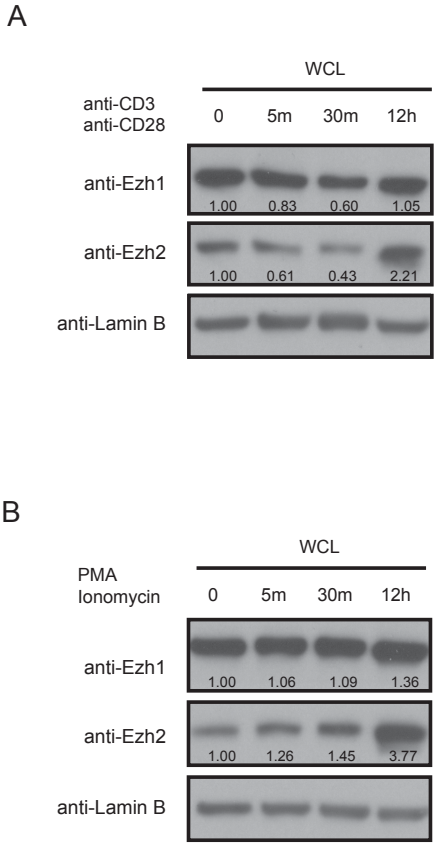

Figure 3.2. Selective upregulation of Ezh2 in activated T cells A. Ezh2 is up-regulated in CD4 T cells stimulated with anti-CD3 and anti-CD28 antibodies for 5 min, 30 min and 12hrs, compared to naïve T cells. Ezh1 expression is not up-regulated in activated T cells **B.** PMA and Ionomycin stimulation induces a significant increase in Ezh2 expression while Ezh1 expression is relatively stable.

3.2 Normal T cell development in the absence of PRC2 in T cells

To examine the role of PRC2 in TCR-mediated T cell activation, we developed animal models combining the Ezh2 conditional knockout ($Ezh2^{fl/fl}$) with CD4-cre in an Ezh1 null background ($Ezh1^{-/-}$). Additionally, we also targeted another component of the PRC2 complex, Eed by crossing $Eed^{fl/fl}$ mice with CD4-Cre mice to generate conditional knockout of Eed in T cells. In these mouse models, Ezh2 and Eed deletion occur in the double-positive thymocyte stage and allow the generation of Ezh2 and Eed deficient peripheral T cells. Since PRC2 is implicated in gene regulation during development, we examined whether our mouse models had developmental defects. We did not observe any gross defect in T cell development in these mice. $Ezh1^{-/-}$ $Ezh2^{fl/fl}$;CD4-Cre mice (PRC2 knockout mice), and $Eed^{fl/fl}$;CD4-Cre mice (Eed conditional knockout) were normal in terms of CD4 and CD8 ratio in peripheral lymphoid tissues and thymus (Figure 3.3 and Figure 3.4). Our laboratory reported that $Ezh2^{fl/fl}$;CD4-Cre mice (Ezh2 conditional knockout mice) have a bystander effect in activation of CD8 T cells due to the increased number of iNKT cells (Dobenecker et al., 2015). However, this phenotype disappeared when Ezh2 was ablated along in the Ezh1 null background (Figure 3.3A,B). In other words, there was no bystander effect in CD8 T cell activation and expansion was observed in lymphoid organs (Figure 3.3A,D). As reported for Ezh2 conditional knockout mice (Dobenecker et al., 2015; Su et al., 2005), PRC2 knockout mice also do not exhibit any obvious alterations in their $CD4^+$ T cell populations (Figure 3.3C). In accordance, CD8 and CD4 frequencies in thymus, spleen and lymph nodes of Eed conditional knockout mice were comparable

to wild-type controls (Figure 3.4A). Since Eed is essential for the assembly of the complex and subsequently, the enzymatic activities of both Ezh1 and Ezh2, we predicted that T cell phenotypes of Eed conditional knockout mice would phenocopy PRC2 conditional knockout mice and not Ezh2 conditional knockout mice. We found that Eed conditional knockout mice lack iNKT cells like the PRC2 conditional knockout mice (Figure 3.3B, 3.4B) and therefore did not display any bystander effect activation of the $CD8^+$ T cell population (Figure 3.4D). Activation markers of $CD4^+$ and $CD8^+$ T cells displayed similar patterns in terms of CD44 and CD122 expression, compared to wild-type control (Figure 3.4C,D). Also, the expression of CD62L, a lymphoid homing marker, was not changed upon Eed deletion, indicating that T cell homing to secondary lymphoid organs was intact (Figure 3.4C, D left panels). We previously observed that $Ezh1^{-/-}$ mice have no T cell phenotype, including iNKT cell development (data not shown).

Therefore, we conclude that PRC2 deficient mice do not have participate in $CD4^+$ or $CD8^+$ T cell development. This allowed us to use peripheral $CD4^+$ T cells from Ezh1 knockout, Ezh2 conditional knockout and PRC2 knockout mice to investigate the role of PRC2 in T cell activation.

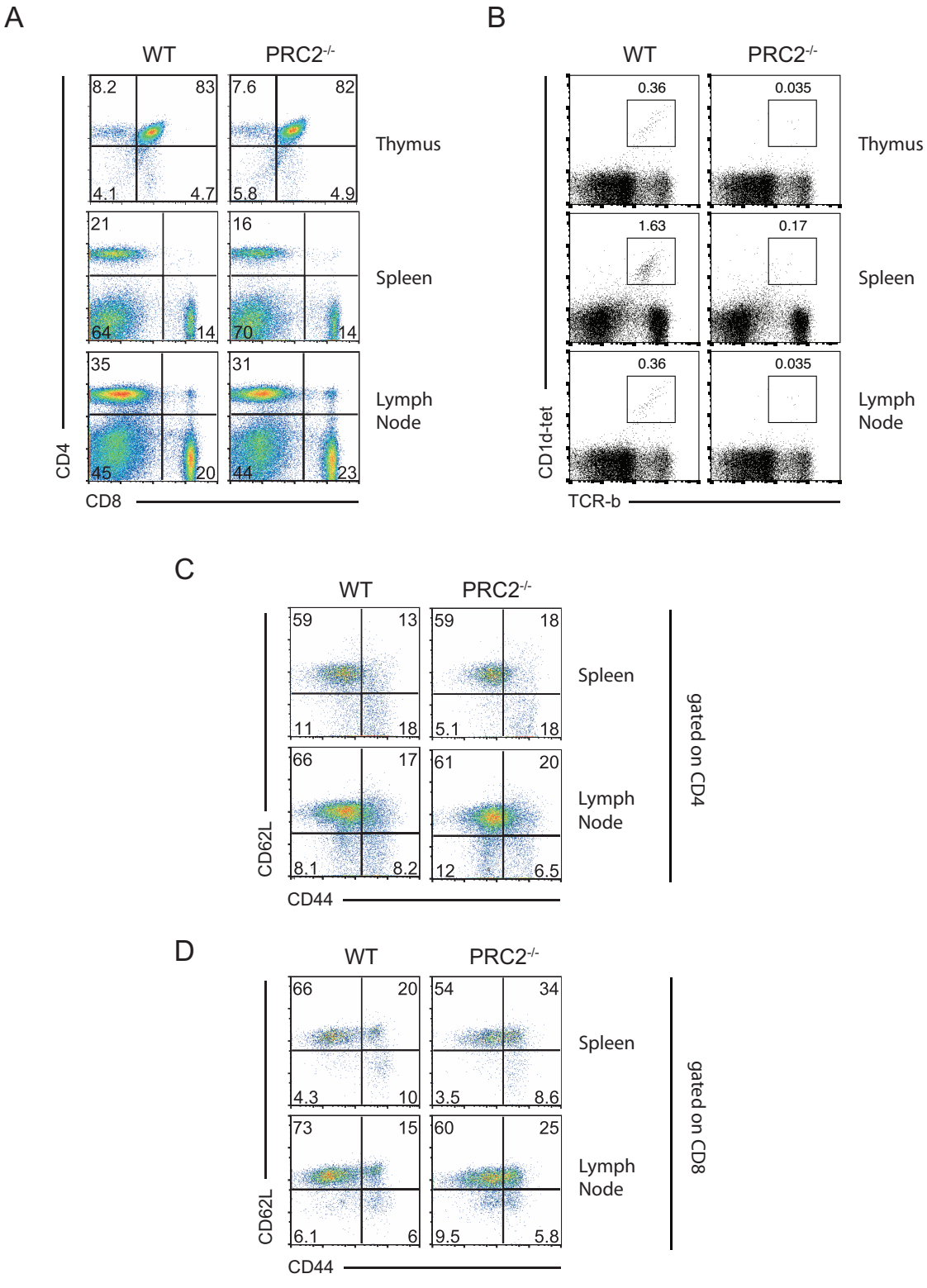
A
WT
PRC2-/-
8.2
83
4.1
4.7
7.6
82
5.8
4.9
Thymus
21
64
14
16
70
14
Spleen
35
45
20
31
44
23
Lymph Node
CD4
CD8
B
WT
PRC2-/-
0.36
0.035
Thymus
1.63
0.17
Spleen
0.36
0.035
Lymph Node
CD1d-tet
TCR-b
C
WT
PRC2-/-
59
13
11
18
59
18
5.1
18
Spleen
66
17
8.1
8.2
61
20
12
6.5
Lymph Node
gated on CD4
CD62L
CD44
D
WT
PRC2-/-
66
20
4.3
10
54
34
3.5
8.6
Spleen
73
15
6.1
6
60
25
9.5
5.8
Lymph Node
gated on CD8
CD62L
CD44

Figure 3.3. Phenotype of peripheral $CD4^+$ and $CD8^+$ T cells is unaffected by T cell specific deletion of Ezh1/2. A. The ratio of $CD4^+$ and $CD8^+$ T cells was examined in thymus, spleen and lymph nodes by flow cytometry. **B.** Cells were stained for CD1d tetramer and TCR-β to define iNKT population. **C, D.** Activation phenotype of splenic and lymph node $CD4^+$ T cells (**C**) and $CD8^+$ T cells (**D**). Cells were stained for CD44 and CD62L. (WT: $Ezh2^{f/f}$, $PRC2^{-/-}$: $Ezh1^{-/-}Ezh2^{f/f}$;CD4-Cre)

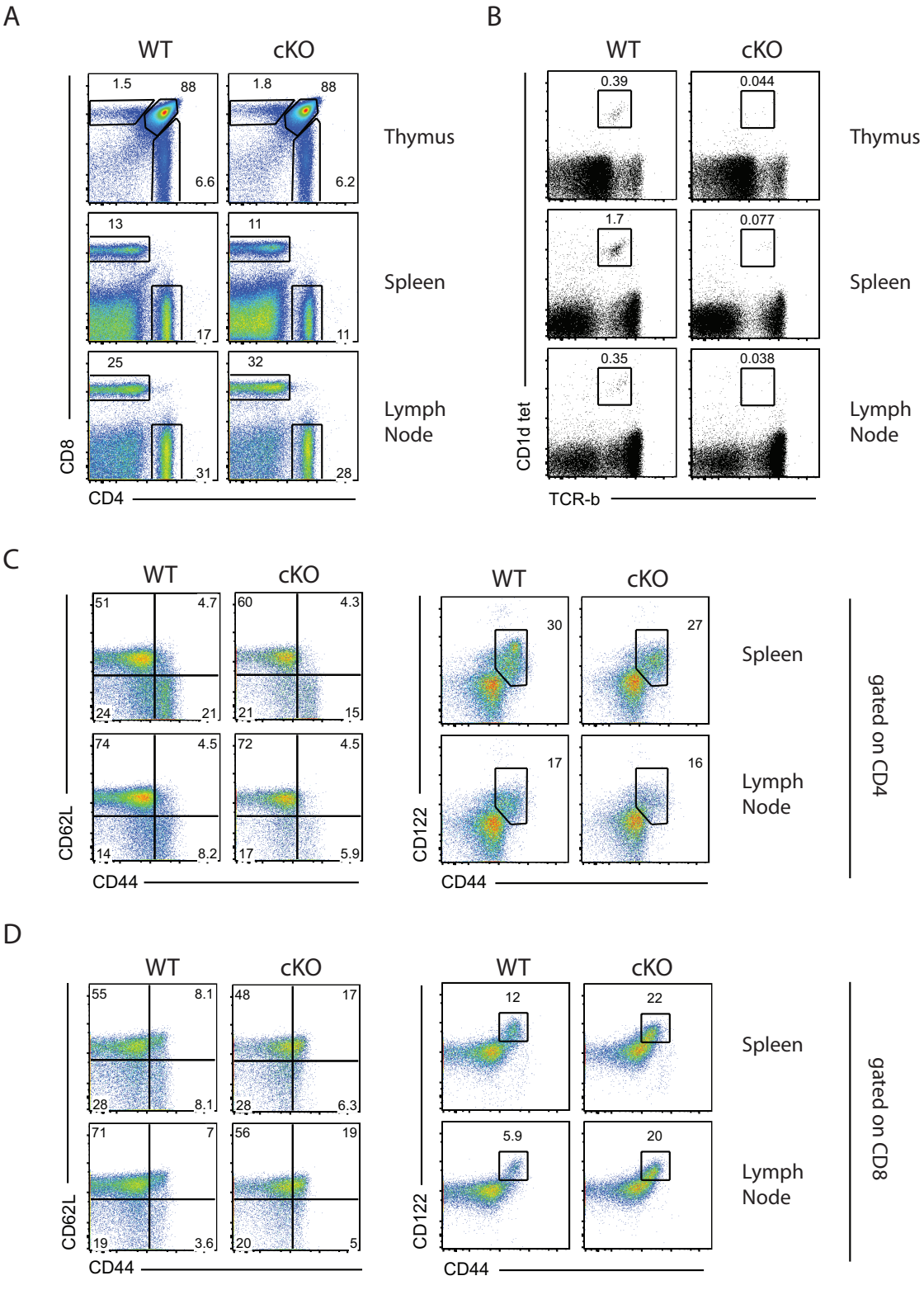
A
WT
cKO
1.5
88
6.6
1.8
88
6.2
Thymus
13
17
11
Spleen
25
31
32
28
Lymph Node
CD8
CD4
B
WT
cKO
0.39
0.044
Thymus
1.7
0.077
Spleen
0.35
0.038
Lymph Node
CD1d tet
TCR-b
C
WT
cKO
51
4.7
24
21
60
4.3
21
15
74
4.5
14
8.2
72
4.5
17
5.9
CD62L
CD44
WT
cKO
30
27
17
16
CD122
CD44
Spleen
Lymph Node
gated on CD4
D
WT
cKO
55
8.1
28
8.1
48
17
28
6.3
71
7
19
3.6
56
19
20
5
CD62L
CD44
WT
cKO
12
22
5.9
20
CD122
CD44
Spleen
Lymph Node
gated on CD8

Figure 3.4. Normal CD4/CD8 T cell development in Eed conditional knockout mice. A. Distribution of $CD4^+$ and $CD8^+$ T cells in thymus (upper), spleen (middle) and lymph nodes (bottom) was analyzed by flow cytometry. **B.** Cells from thymus, spleen and lymph nodes were stained for CD1d tetramer and TCR-β to define iNKT population. **C.** Expression of activation marker CD44 and homing marker CD62L in $CD4^+$ T cells (left). CD44 and IL15-receptor CD122 (right). **D.** Expression of activation markers in $CD8^+$ T cells. (WT: $Eed^{f/f}$, cKO: $Eed^{f/f}$;CD4-Cre)

3.3 Unaltered H3K27me3 and gene expression in naïve PRC2-deficient T cells

Since the nuclear function of PRC2 in histone modification is well known we addressed the epigenetic state and gene expression pattern in PRC2 deficient peripheral T cells. We approached the problem in three different ways. First, we performed western blot analysis on lysates from naïve CD4 T cells purified from wild-type, Ezh1$^{-/-}$, Ezh2$^{fl/fl}$;CD4-Cre and Ezh1$^{-/-}$ Ezh2$^{f/f}$;CD4-Cre mice (PRC2$^{-/-}$). We also purified the cells from Eed$^{fl/fl}$ mice and Eed$^{f/lfl}$;CD4-Cre mice. Global levels of H3K27me3 in naïve CD4 T cells were not affected by deletion of Ezh1, Ezh2 and Eed in T cells (Figure 3.5A,B). Next, we also examined the levels of H3K27me3 in PRC2 deficient T cells at a single cell level using flow cytometry. Ezh2$^{-/-}$ or PRC2$^{-/-}$ T cells exhibited similar levels of H3K27me3 in comparison to wild-type T cells (Figure 3.5C). PRC2 deficient naïve CD8^{+} T cells also showed the same levels of H3K27me3 to wild-type CD8^{+} T cells (Figure3.5C, right). In addition, to examine the impact of PRC2 on local levels of H3K27me3, we have performed a genome-wide analysis on H3K27me3 by ChIP-Seq. Compared to wild-type T cells, Ezh1$^{-/-}$, Ezh2$^{-/-}$ and PRC2$^{-/-}$ T cells have comparable levels of H3K27me3 in a genome-wide scale (Figure 3.5D). Additionally, RNA-seq data show that all the mutants have very few changes in gene expression, compared to wild-type cells (Figure 3.5E). Collectively, PRC2 deficient naïve T cells show wild-type like patterns of H3K27me3 and gene expression. These data imply that H3K27me3 is highly stable in undividing cells like naïve T cells.

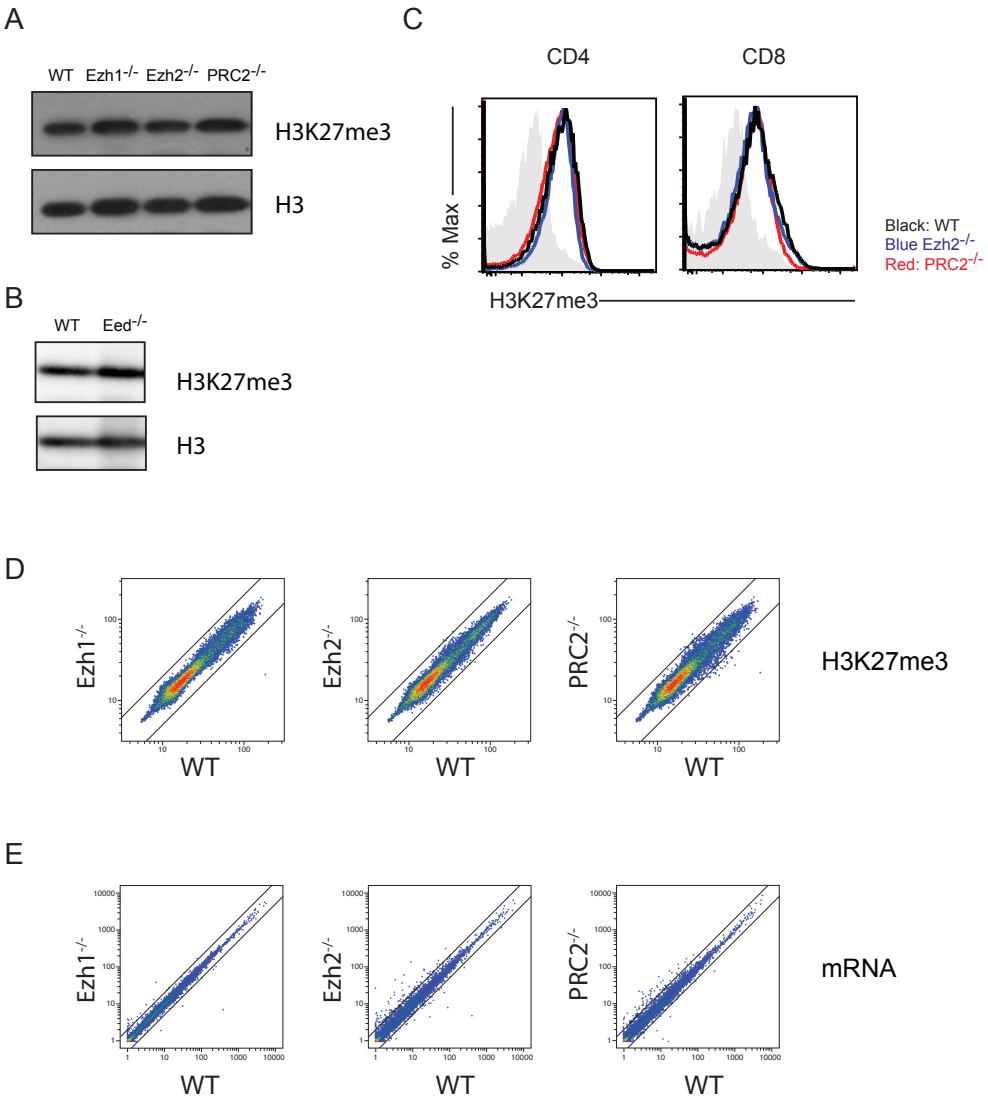

Figure 3.5. PRC2 deficiency exhibits wild-type pattern of H3K27me3 and gene expression in naïve T cells A, B. Western blot analysis on cell lysates for H3K27me3 and H3. **C.** Flow cytometric analysis of H3K27me3 levels in $CD4^+$ (left) and $CD8^+$ (right) T cells. Each genotype of mutants is indicated by different colors. Solid Grey area represents negative control for H3K27me3 staining (non-permeabilized cells) **D.** Genome-wide H3K27me3 association with individual genes in naïve wild-type and mutant T cells, determined by ChIP-Seq analysis for H3K27me3. Diagonal lines indicate 2-fold changes between wild-type and mutants. **E.** Gene expression levels were determined by RNA-Seq. Levels of mRNA of each gene in wild-type and mutant cells were plotted. Diagonal lines indicate 2-fold changes between wild-type and mutants. $PRC2^{-/-}$ represents T cells from $Ezh1^{-/-}Ezh2^{f/f}$;CD4-Cre mice.

3.4 Selective role of PRC2 in TCR-mediated T cell proliferation *in vitro*

Our genetic models provide us with an excellent tool for understanding the role of PRC2 in TCR-mediated T cell activation. First, T cells from conditional knockout mice, as discussed above, do not have developmental defects. Second, our models do not to have abnormal gene expression, which could directly impact TCR signaling. Therefore, by utilizing these animal models we can investigate the role of PRC2 in T cell activation by measuring the proliferation capacity of PRC2 deficient T cells upon TCR stimulation. To induce proliferation by TCR stimulation, we stimulated CFSE-labeled T cells on plate-bound with anti-CD3 antibody. Whereas wild-type T cells divided at least five times upon anti-CD3 stimulation, PRC2-deficient T cells failed to proliferate (Figure 3.6A). Ezh1 deficiency did not have any effect on TCR-induced T cell proliferation. $Ezh2^{-/-}$ T cells displayed only a minor defect in proliferation, however, we observed some variation between experiments. Although we reported before that $Ezh2^{-/-}$ T cells have a defect in TCR-induced proliferation (Su et al., 2005), $Ezh2^{-/-}$ T cells proliferated quite normally in our hands. This discrepancy may be due to the two different experimental methods used. In the previous publication proliferation was measured by ^{3}H incorporation, while this set of data determined proliferation by CFSE dilution. If cells massively died right after stimulation, ^{3}H incorporation assay will show the major defect. However, this seems to be not the case since we observed no difference in survival one day after stimulation (Data not shown). Therefore, it is likely that other factors such as genetic background or age might be involved in these diverging experimental outcomes. Along with deficiency in Ezh1 and Ezh2, Eed deletion caused a dramatic defect in TCR-induced cell

proliferation (Figure 3.6B). Since Eed is essential for Ezh1 and Ezh2 enzymatic activity, this result suggests that Ezh1 and Ezh2 in the context of a complex with Eed are important for TCR-mediated T cell proliferation. The data also confirm that Eed knockout is equivalent to Ezh1 and Ezh2 double knockout. Co-stimulation of anti-CD28 antibody only partially rescued the phenotype (Figure 3.6A,B) and IL-2 failed to rescue the defect (Data not shown). On the other hand, PRC2 deficient T cells and Eed knockout T cells proliferated normally when they were treated with PMA/Ionomycin, which bypass the proximal signaling (Figure 3.6A,B). These data indicate, that PRC2 deficient T cells are capable of proliferating in principle but they cannot proliferate in response to TCR stimulation, due to a defect in signaling. In other words, PRC2 is required for receptor proximal signaling events, but dispensable for gene regulation in resting naïve T cells.

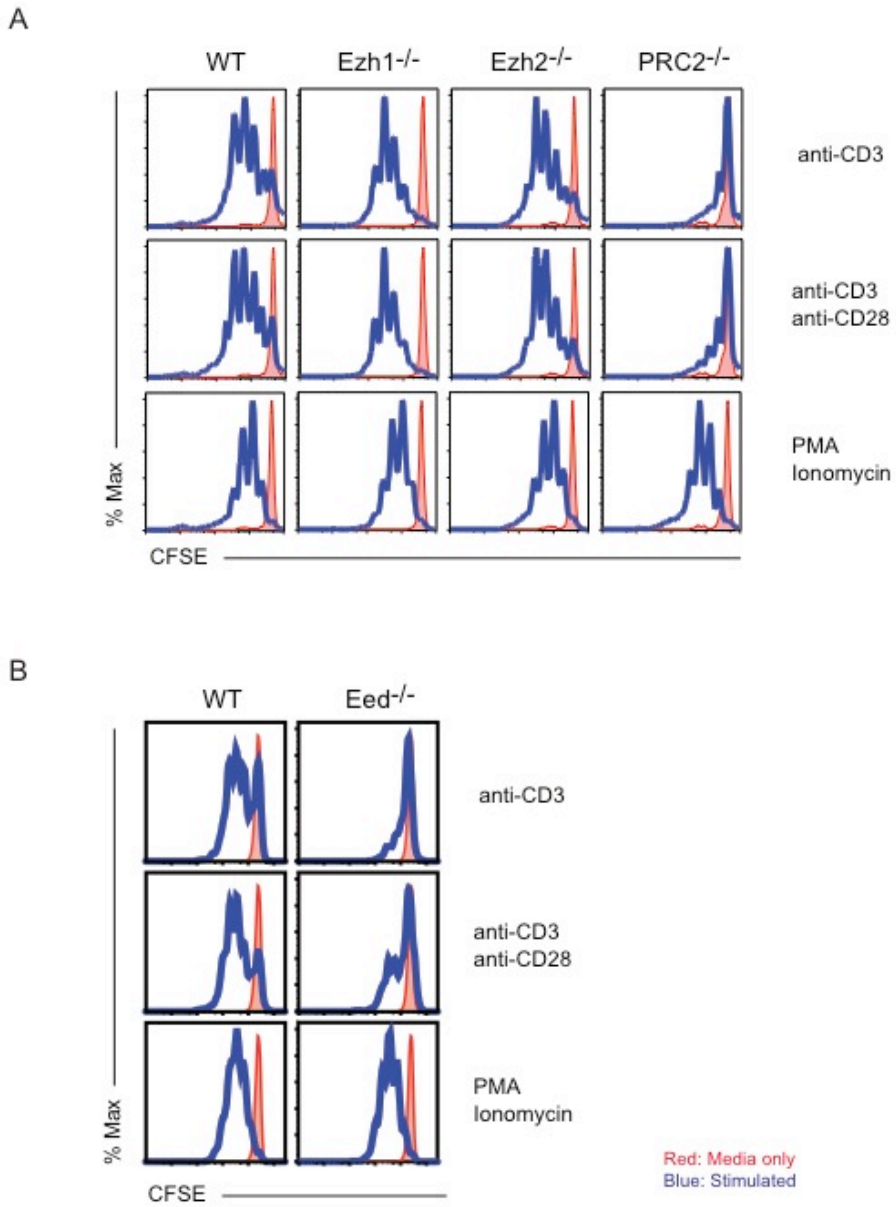

Figure 3.6. PRC2 deficient T cells fail to proliferate upon TCR stimulation A. CFSE labeled wild-type and indicated mutant $CD4^+$ T cells were stimulated with anti-CD3 antibody (upper), anti-CD3/anti-CD28 antibodies (middle) and PMA/Ionomycin (bottom) for 3 days. Cell division was assessed by CFSE dilution. **B.** $Eed^{-/-}$ T cells and littermate controls were stimulated as described above. Red solid graph represents cells cultured in media alone for 3 days. Data are representatives of at least two independent experiments with two or three biological replicates in each experiment.

3.5 PRC2 controls TCR-mediated Erk phosphorylation

To explore how PRC2 controls TCR induced proliferation, we examined the TCR signaling cascade in PRC2 deficient T cells. Tyrosine phosphorylation of multiple substrates including Zap70, Vav and PLCγ1 initiate TCR signaling. We found no defect in the phosphorylation of these proteins upon TCR stimulation (Figure 3.7A). As discussed earlier, TCR engagement activates several signaling pathways including the MAPK pathway and the PI3K pathway. While we did not see defective phosphorylation of JNK and Akt, we found a significant reduction (nearly 70% at 2 min after stimulation) in phosphorylation of Erk1/2 in Ezh2 deficient and PRC2 deficient T cells, compared to wild-type controls (Figure 3.7A). The MAPK pathway is known to control TCR induced proliferation (Alberola-Ila et al., 1995; Pages et al., 1999), which is why the defect in Erk activation might explain the lack of proliferation. To test, if the defect is truly a signaling defect and not a general defect in the MAPK pathway, we stimulated Ezh2 and PRC2 deficient T cells with PMA/Ionomycin and analyzed Erk phosphorylation. Neither Ezh2 nor PRC2 deficient T cells showed a defect in PMA/Ionomycin induced Erk phosphorylation (Data not shown), confirming that the defect observed after TCR stimulation is most likely a signaling defect and does not reflect a general inability of these cells to activate the MAPK pathway. As an additional control we induced robust Erk phosphorylation in PMA/Inonmycin expanded, rested and then restimulated T cells. For restimulation T cells were treated with anti-CD3/anti-CD28 antibodies. As compared to wild-type controls, Ezh2 deficient T cells displayed a 66.7% reduction in the level of phospho-Erk1/2 two minutes after stimulation, (Figure 3.7B). Contrary to Erk phosphorylation,

Ezh2 deficiency did not lead to a defect in Akt phosphorylation (Figure 3.7B). Therefore, Ezh2 controls TCR-induced Erk phosphorylation in naïve as well as activated T cells.

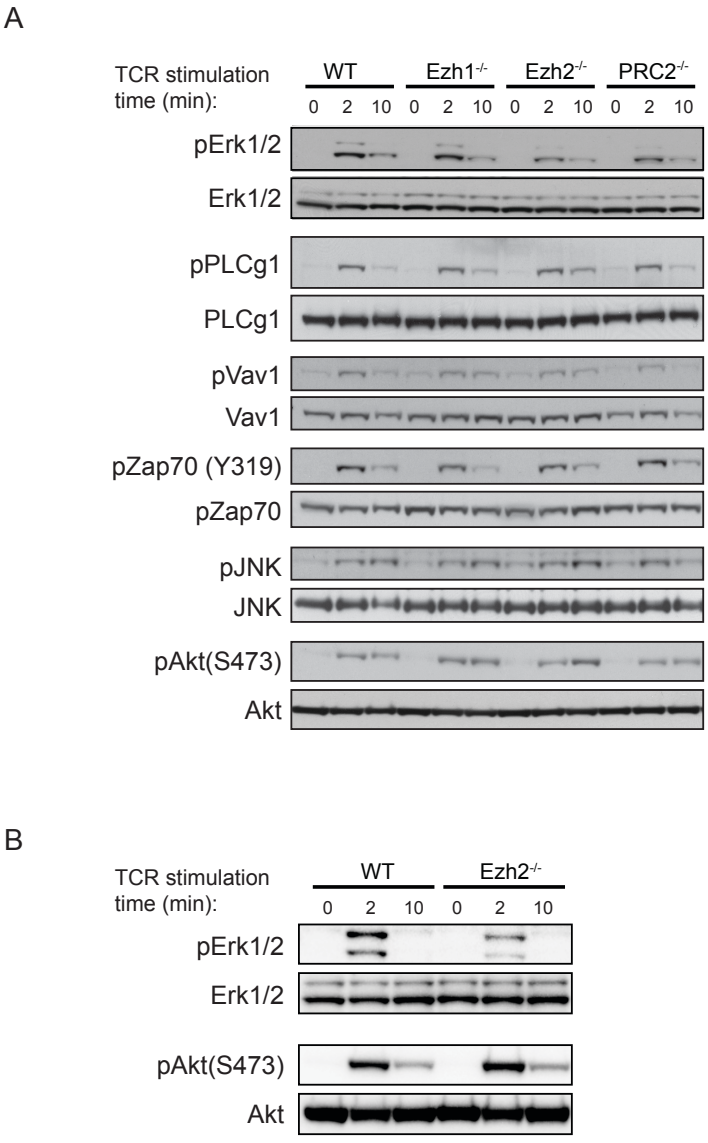

Figure 3.7. TCR-induced Erk phoshporylation is impaired in the absence of Ezh2. A. TCR-induced phosphorylation of key signaling molecules were examined by Western blot analysis. Naïve CD4 T cells of indicated mutants were stimulated with anti-CD3/anti-CD28 antibodies, followed by cross-linking with secondary antibody. Ezh2$^{-/-}$ and PRC2$^{-/-}$ T cells showed reduced induction of Erk phosphorylation upon TCR stimulation. B. CD4 T cells from Ezh2 conditional knockout (CD4-Cre) mice and littermate controls were stimulated with PMA/Ionomycin for 2 days. The cells were rested one day, then, subjected to Erk phosphorylation assay, as described above.

3.6 PRC2 inhibitors suppress TCR-induced Erk phosphorylation

The defect in TCR-induced Erk phosphorylation is likely not due to changes in gene expression, since we observed no changes in H3K27me3 and only minor changes in our RNA-seq; additionally the duration of the stimulation itself is too short to induce gene expression changes that could explain the defect. However, it could be argued that several minor changes, which were not detected with our genome-wide analysis, could play a role and the observed Erk defect reflects the indirect effects of such alterations. To address this issue, we utilized pharmacological inhibition of PRC2. We used GSK503, a selective and potent inhibitor of Ezh2. GSK503 is about 200 fold selective over Ezh1 (K_i^{app}: 3nM for Ezh2 and 638nM for Ezh1, IC_{50} value: 8nM for Ezh2 and 633nM for Ezh1) (Beguelin et al., 2013). GSK503 has favorable pharmacological kinetics in mice and therefore utilized for the *in vivo* experiments.

To identify the best strategy for efficient inhibitor accumulation in T cells we compared several different pre-incubation and stimulation schemes and measured the intracellular concentration of GSK503 by mass spectrometry (Figure 3.8A). We confirmed that pre-incubation of cells on ice with GSK503 was as efficient as pre-incubation at 37°C (Figure 3.8B). Pre-incubation increased the amount of intracellular GSK503 as compared to no pre-incubation plus inhibitor during the stimulation at 37°C. Therefore, treatment of GSK503 on ice for 1hr was chosen to test the direct involvement of Ezh2 in TCR-induced Erk phosphorylation. We predicted that the pre-incubation step on ice would minimize the possibility of transcriptional alterations during this period. We also measured the intracellular concentration after incubation of cells with 0 μM, 2 μM, 10 μM and 50 μM of GSK503 on ice for 1hr. We saw

similar levels of inhibitor influx for 2 and 10 μM GSK503, but drastically increased influx after incubation with 50 μM GDK503 (Figure 3.8C,D).

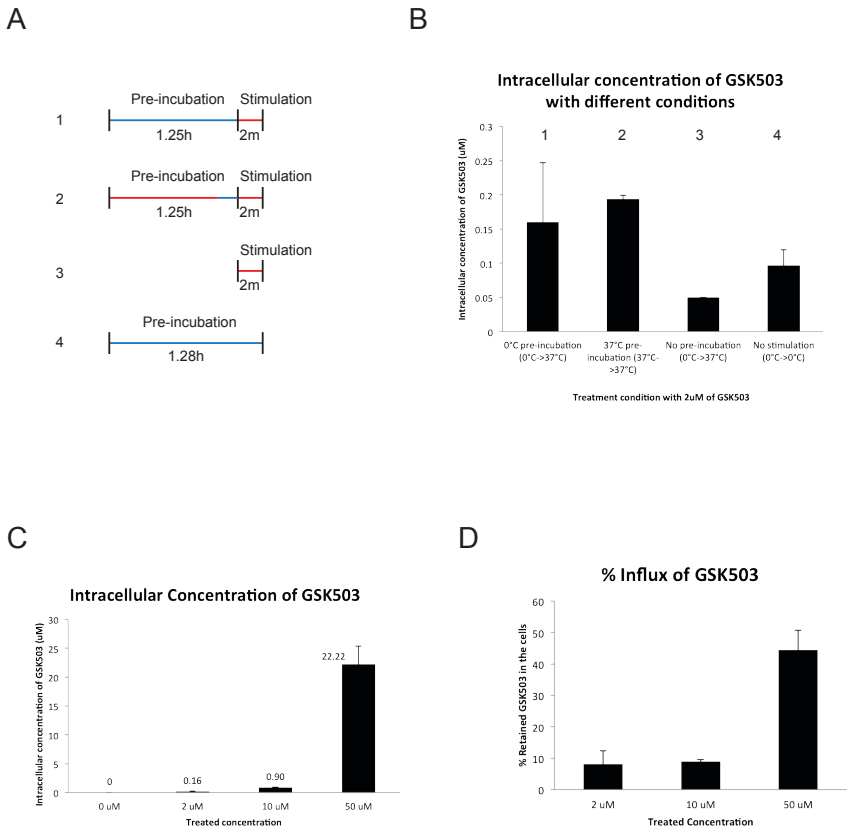

Figure 3.8. Intracellular concentration of GSK503 A. Experimental schemes for GSK503 treatment of $CD4^+$ T cells. Colors indicate temperatures during incubation (Blue: 0°C, Red: 37°C). Condition 1: cells were pre-incubated with 2 μM of GSK503 on ice for 1.25hr, followed by stimulating by TCR cross-linking at 37°C for 2 min. Condition 2: cells were pre-incubated and stimulated at 37°C. Condition 3: Cells were stimulated at 37°C for 2 min without pre-incubation. Condition 4: Cells were pre-incubated on ice, but were not stimulated. **B.** Intracellular concentrations of GSK503 after pre-incubation according to schemes described in **A** were measured by Mass spectrometry. **C.** Intracellular concentrations of GSK503 in the cells treated with 0 to 50 μM of the inhibitors. **D.** Intracellular concentration of GSK503 is displayed as percent of the treatment concentration. Data represent mean ± standard deviation from three biological replicates (n=3).

Next, to test the hypothesis that Ezh2 directly controls TCR signaling, we assessed TCR-induced Erk phosphorylation in the presence of GSK503. While TCR engagement induces robust Erk phosphorylation in DMSO treated T cells, GSK503 suppressed Erk phosphorylation in a dose dependent manner (Figure 3.9A). GSK600A, an inactive control compound for GSK503, did not exhibit the same effect, ensuring the specificity of GSK503 action on PRC2 in the inhibition of Erk phosphorylation (Figure 3.10). On the other hand, GSK503 treatment did not affect Erk phosphorylation induced by PMA, which directly activates PKC and RasGRP to activate Erk, circumventing proximal TCR signaling (Figure 3.9B). These results are in agreement with the finding that T cells do not require PRC2 for PMA/Ionomycin induced proliferation.

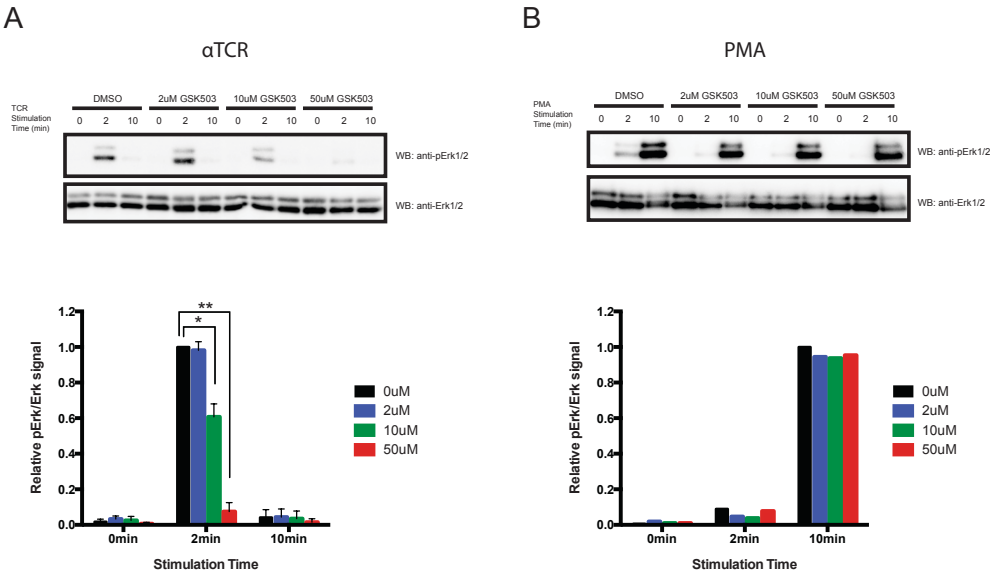

Figure 3.9. GSK503 suppresses TCR-induced Erk phosphorylation Purified CD4 T cells were pre-incubated with 0, 2, 10 and 50 μM of GSK503 for 1hr on ice. Cells were stimulated by TCR cross-linking (**A**) or PMA (**B**) for 2 min and 10 min. Phospho-Erk1/2 (T202/Y204) and total Erk1/2 were detected by Western blot analysis. Relative level of Erk phosphorylation was quantified by comparing phospho-Erk1/2 signal normalized to total Erk1/2 signal. Data are shown as mean ± standard deviation and is representative of at least three independent experiments. Student's t-test, *$p<0.05$, **$p<0.01$.

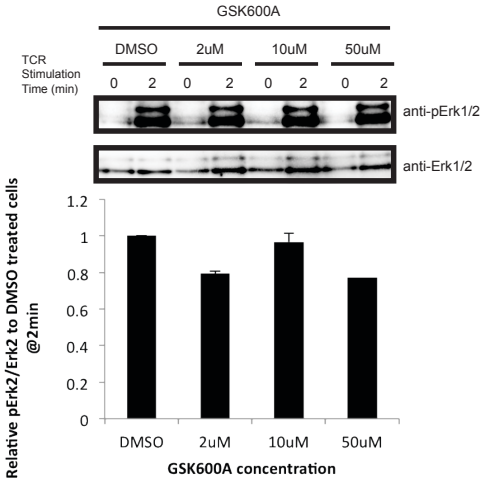

Figure 3.10. GSK600A does not inhibit TCR-induced Erk phosphorylation GSK600A, an inactive control compound for GSK503, was used to treat $CD4^+$ T cells at 0 to 50 μM concentrations. Cells were stimulated by TCR cross-linking and Erk phosphorylation was examined. Data are shown mean ± standard deviation and representative of two independent experiments.

We additionally confirmed the requirement of Ezh2 for TCR-mediated Erk activation with UNC1999, an independently developed inhibitor. UNC1999 inhibits both Ezh1 and Ezh2 and thereby we could achieve a clearer pharmacological inhibition of PRC2 (Konze et al., 2013). UNC1999 effectively abolishes TCR-induced Erk phosphorylation even at lower concentrations (Figure 3.11A). Treatment of UNC2400, an inactive control compound for UNC1999 showed no effect on Erk phosphorylation, confirming that PRC2 inhibition suppresses TCR-induced Erk phosphorylation (Figure 3.11B). Although we did not find an additive effect of

combined deficiency in Ezh1 and Ezh2 with respect to Erk phosphorylation, our data on TCR-induced proliferation strongly suggest that inhibition of both enzymes has a stronger impact on TCR signaling than Ezh2 deficiency alone. The fact that UNC1999 was more effective, although we did not measure the intracellular concentration of UNC1999, and the fact that GSK503 completely inhibited Erk phosphorylation at a concentration that could also inhibit Ezh1, suggests that the same is also true for Erk activation.

Collectively, these data provide direct evidence of control of TCR signaling by PRC2 independent of its role in histone modification. Pharmacological inhibition also indicates that the methyltransferase activity of Ezh2 is required for TCR-mediated Erk phosphorylation.

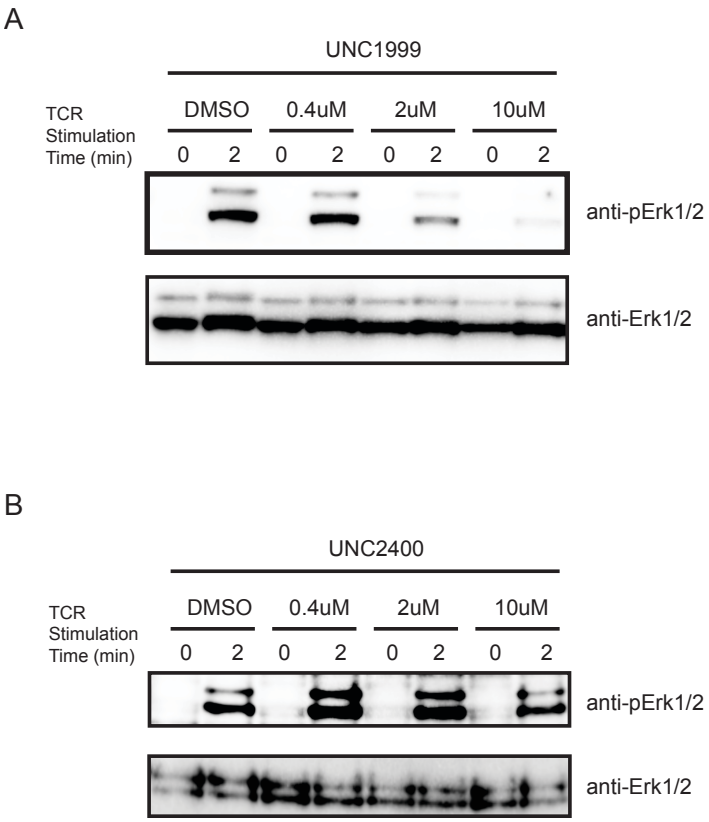

Figure 3.11. UNC1999, an independent Ezh2 inhibitor, efficiently blocks TCR-induced Erk phosphorylation A. $CD4^+$ T cells were treated with 0 to 10 μM of UNC1999, followed by TCR cross-linking. Levels of Erk phosphorylation were measured by Western blot analysis. Data are representative of two independent experiments. **B.** Cells were treated with 0 to 10 μM of UNC2400, a control compound for UNC1999, and TCR-induced Erk phosphorylation was measured. Data are representative of two independent experiments.

3.7 Inhibition of PRC2 does not affect TCR-induced tyrosine phosphorylation

Activation of the TCR leads to a cascade of posttranslational modifications independent from Erk phosphorylation. We showed that Ezh2 ablation only had a

specific effect on Erk and not on any other induced modifications (Fig 3.7). To ensure that the defect in Erk phosphorylation after treatment with GSK503 is specific and not due to a general defect in the TCR induced signaling cascade we tested other TCR-induced tyrosine phosphorylations. First we checked the overall pattern of tyrosine phosphorylation by Western blot analysis using a pan-anti-phospho-tyrosine antibody. There was no qualitative difference between DMSO treated cells and GSK503 treated cells (Figure 3.12A). This was even true at extremely high concentration of GSK503 (100 μM). One of the key signaling proteins for TCR signal transduction is PLCγ1. DAG produced by PLCγ1 is a critical signaling intermediate for the Erk signaling pathway. Activation of PLCγ1 is regulated by tyrosine phosphorylation by Itk. Therefore, we checked if phosphorylation of PLCγ1 is affected by GSK503 treatment. Similar to genetic deletion of Ezh2, the pharmacological inhibition of Ezh2 by GSK503 did not influence the tyrosine phosphorylation of PLCγ1 (Figure 3.12B). In summary, Ezh2 inhibition does not alter TCR-induced tyrosine phosphorylation in general. Also, we conclude that GSK503 does not block the entire TCR signaling cascade, rather, it specifically regulates Erk phosphorylation.

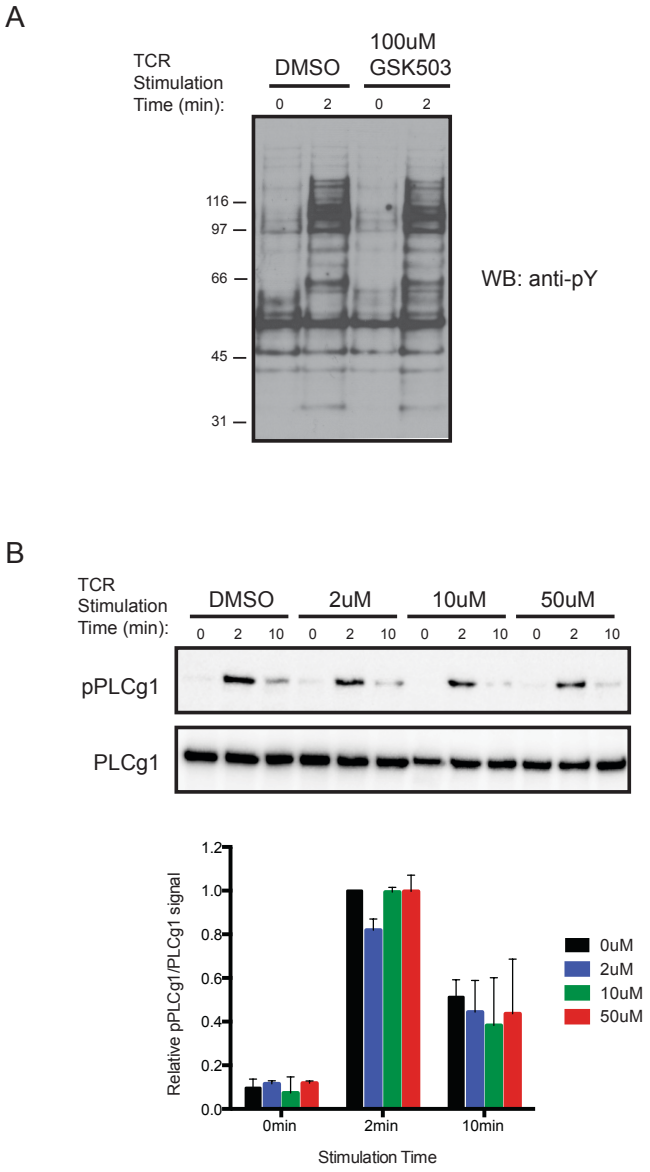

Figure 3.12. GSK503 does not alter TCR-induced tyrosine phosphorylation. A. Purified CD4 T cells were pre-incubated with DMSO or a high concentration of GSK503, followed by TCR stimulation. Overall tyrosine phosphorylation events were examined by phospho-tyrosine Western blot. **B.** TCR-induced phospho-PLCγ1 levels in CD4 T cells treated with 0 to 50 μM of GSK503 were measured. Relative PLCγ1 phosphorylation levels were obtained by normalizing phospho-PLCγ1 signal to total PLCγ1 signal. Data are shown mean ± standard deviation and representative of three (**A**) or two independent experiments (**B**).

3.8 Ezh2 controls TCR-mediated Erk phosphorylation in human T cells

To address if the role of Ezh2 in signaling is conserved between human and mouse, we investigated the function of Ezh2 in TCR-induced Erk phosphorylation in human T cells. CD4 T cells were isolated from human blood and incubated with anti-CD3 antibody (OKT3), followed by cross-linking. Compared to DMSO treated human CD4 T cells, GSK503 treated human CD4 T cells showed a reduced induction of Erk phosphorylation in a dose dependent manner (Figure 3.13A). Interestingly, this effect could be achieved even without pre-incubation with the inhibitor (Figure 3.13B). Although a direct comparison between GSK503 treatment in human and mouse T cells is difficult due to the difference in the source of the cells, it seems that human T cells are highly sensitive to GSK503. As seen in mouse T cells, human T cells could induce robust Erk phosphorylation upon PMA stimulation, which was not affected by GSK503 treatment (Figure 3.13C). Therefore, there is a common pathway between mouse and human for Ezh2 dependent TCR signaling. However, we observed almost no effect of the Ezh2 inhibitor in Jurkat cells (Data not shown). This suggests that perhaps a compensatory signaling pathway may exist in this leukemic cell line that bypasses the requirement of Ezh2 for TCR-induced Erk phosphorylation. In conclusion, Ezh2 methyltransferase activity is required for TCR-mediated Erk activation in human T cells.

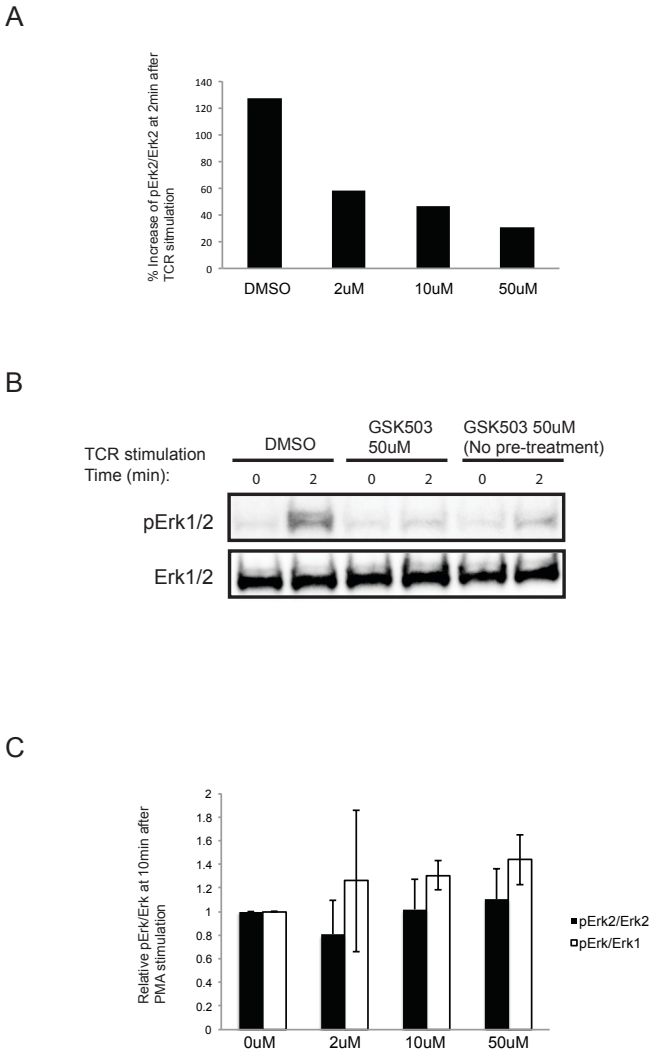

Figure 3.13. GSK503 inhibits TCR-induced Erk phosphorylation in human T cells A. CD4 T cells were purified from human blood and pre-incubated with indicated concentration of GSK503 for 1 hr on ice. The cells were treated with mouse anti-human CD3 antibody (OKT3) for 15 min on ice, followed by cross-linking with secondary antibody at 37°C for 2 min. Phosphorylation of Erk was measured by Western blot and quantified for Erk induction. Phospho-Erk signal was normalized to total Erk signal and the fold-increase from 0 min to 2 min was calculated. **B.** Erk phosphorylation was examined with pre-incubation of 50 μM of GSK503 or without (50 μM of GSK503 was only present during stimulation). **C.** Human CD4 T cells were pre-incubated with GSK503 for 1 hr on ice, then, stimulated with PMA. PMA-induced Erk phosphorylation in the presence of indicated concentration of GSK503 was quantified. Data are shown mean ± standard deviation and representative of two independent experiments.

3.9 PRC2 controls antigen-specific T cell expansion *in vivo*

We have shown that PRC2 directly regulates TCR signaling, particularly the TCR-induced Erk signaling pathway. Accordingly, TCR-mediated proliferation *in vitro* was impaired in the absence of PRC2. Therefore, we addressed the relevance of PRC2 function in *in vivo* T cell immunity. We first investigated the role of PRC2 in *in vivo* T cell activation by using the Lymphocytic choriomeningitis virus (LCMV) infection model. LCMV was first isolated from an infected monkey brain by Charles Armstrong. Later, Michael Oldstone and Rafi Ahmed obtained a variant of LCMV Armstrong from mouse spleen (Ahmed et al., 1984), called clone 13. Although they have the same immune-dominant epitopes such as GP_{33-41}, $GP_{276-286}$, $NP_{396-404}$, and NP_{61-80}, the two different strains bring about very different outcomes in terms of anti-viral immune response in mice. LCMV Armstrong acutely infects mice and is cleared by $CD8^+$ T cell mediated immune response. Clone 13 persistently infects mice and impairs $CD8^+$ T cell functions. Therefore, this virus infection system can monitor the function of the same clonal population in a different infection setting. For this reason, the LCMV infection model has been extensively used for studying anti-viral T cell immunity and tolerance. The clearance of this virus is largely $CD8^+$ T cell dependent. In addition to robust $CD8^+$ T cell response, LCMV Armstrong also induces Th1 responses. The peak of response is normally seen 8 days after infection. The kinetics of immune response is relatively consistent, clear and well characterized, making it an excellent tool to trace virus-specific T cells. Especially the immune response against the Armstrong strain infection exhibits the classical dynamics of a T cell response.

Therefore, we used the LCMV Armstrong acute infection model to understand the *in vivo* function of PRC2.

We infected wild-type ($Ezh2^{fl/fl}$, WT), Ezh1 knockout ($Ezh1^{-/-}$, Ezh1 KO), Ezh2 conditional knockout ($Ezh2^{fl/fl}$; CD4-Cre, Ezh2 cKO), and PRC2 knockout ($Ezh1^{-/-}Ezh2^{f/f}$;CD4-Cre, Ezh1/2 dKO) mice with LCMV Armstrong and utilized peptide-MHC class I tetramers to measure the number of virus-specific T cells. As expected, wild-type and Ezh1 knockout mice had a robust GP33-specific $CD8^+$ T cell expansion at the effector phase (Figure 3.14A). Strikingly, this expansion was greatly diminished in Ezh2 conditional knockout and PRC2 knockout mice (Figure 3.14A). Not only $CD8^+$ T cell that recognize GP33 epitope were impaired but also the GP276 and NP396 specific T cells did not expand in the Ezh2 conditional knockout mice (Figure 3.14B). To check if Eed also plays an essential role in anti-viral immunity, we infected Eed conditional knockout ($Eed^{fl/fl}$;CD4-Cre) mice with LCMV Armstrong. Indeed, Eed conditional knockout mice also fail to induce $CD8^+$ T cell expansion (Figure 3.14C). These results were confirmed by examination of cytokine production of virus-specific T cells. The hallmark of the anti-viral $CD8^+$ T cell response is the production of effector cytokines such as IFN-γ, TNF-α and IL-2 and Granzyme B. The production of these cytokines was severely hampered in *ex vivo* isolated $CD8^+$ T cells from Ezh2 and Eed deficient mice (Figure 3.14D, E). The lack effector cytokine production is probably due to the lack of antigen-specific T cells. Additionally, Granzyme B expression was significantly reduced in Ezh2 and Eed deficient $CD8^+$ T cells during infection (Data not shown). We also assessed $CD4^+$ responses in terms of IFN-γ, TNF-α and IL-2 production. While $CD4^+$ T cells from wild-type control mice

expressed these cytokines, Ezh2 and Eed deficient $CD4^+$ T cells failed to produce them, indicating that antigen-specific $CD4^+$ T cell expansion is also impaired in the absence of PRC2 (Figure 3.14F,G). These sets of data strongly indicate that PRC2 plays an essential role in TCR-mediated T cell expansion *in vivo*.

These results raised the question of at which stage of the immune response PRC2 is required for T cell expansion. Since PRC2 has been reported to play a role in the regulation of cell senescence (Kamminga et al., 2006), the greatly reduced number of antigen-specific T cells might be due to rapid cell death after an initial expansion in the early phase of the immune response. To check if PRC2 plays a role in early phase T cell expansion, we examined antigen-specific T cell frequencies at day 5 post-infection, the earliest time point where we can detect a significant number of antigen specific viral tetramer positive cells. Interestingly, the numbers of tetramer positive T cells in Ezh2 conditional knockout mice and Eed conditional knockout mice were significantly lower than their wild-type control mice (Figure 3.15A,B). This suggests that the antigen-specific T cells never expanded. Moreover, the percentage of Ki-67 positive cells among $CD8^+$ T cell in Ezh2 conditional knockout mice was lower than in the wild-type mice (Figure 3.15C). These data show that PRC2 deficiency leads to a failure of TCR-mediated T cell proliferation *in vivo*. Next, we asked whether T cell proliferation is delayed or T cells are permanently unresponsive. We analyzed PBMC from wild-type and Ezh2 or Eed conditional knockout mice at day 5, 8 and 15 after infection. We measured the frequencies of GP33 specific T cells from individual mice at these time points. Until Day 8, compared to wild-type, Ezh2 conditional knockout mice exhibited much slower kinetics of GP33 specific T cell expansion, although both

groups show a similar pattern (Figure 3.15D). By day 15 wild-type T cells started to contract while Ezh2 deficient mice had large variations between them. In other words, some Ezh2 conditional knockout mice kept increasing in the frequency of GP33 specific T cells while some of them showed contraction. Eed conditional knockout mice also had the similar phenotype (Figure 3.15E). However, the absolute number of antigen specific T cells in lymphoid organs and their functionality should be further addressed to pinpoint the real kinetics in immune responses. In conclusion, PRC2 deficiency in T cells causes an early proliferation defect *in vivo*.

Lastly, to confirm that the impaired immune response in the absence of PRC2 correlates with failed virus clearance, we measured the virus titers from serum, spleen and lung of infected mice. Since we observed a failed induction of the anti-viral $CD8^+$ T cell response, we speculated that the LCMV Armstrong infection would become a persistent infection in PRC2 deficient mice. In wild-type mice LCMV Armstrong is cleared by the immune system by day 8, and the virus titers are close to the detection limit. This was also the case for Ezh1 knockout mice (Figure 13.16A-D). In contrast, Ezh2 conditional knockout, Ezh1/2 double knockout mice, and Eed conditional knockout mice still had much higher titers in the serum and in several organs (Figure 13.16A-D). Moreover, the virus was not cleared even 123 days after infection (Figure 13.16E-F). Therefore, PRC2 deficient mice are incapable of clearing the normally acute LCMV Armstrong virus, resulting in a persistent infection. Collectively, PRC2 is essential for anti-viral T cell immunity.

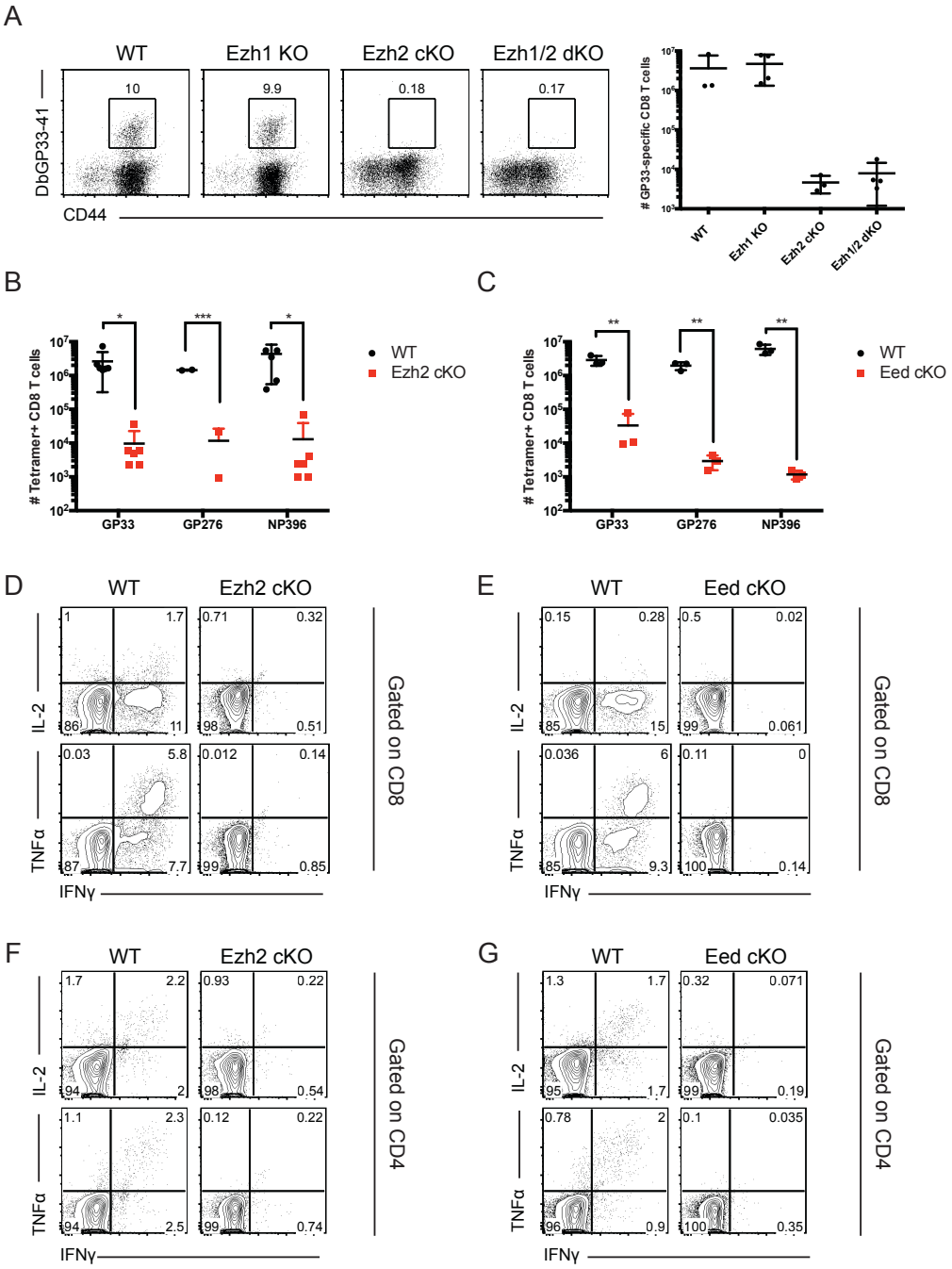
A
WT
Ezh1 KO
Ezh2 cKO
Ezh1/2 dKO
DbGP33-41
CD44
10
9.9
0.18
0.17
GP33-specific CD8 T cells
B
Tetramer+ CD8 T cells
GP33
GP276
NP396
WT
Ezh2 cKO
C
Eed cKO
D
IL-2
TNFα
IFNγ
Gated on CD8
E
F
Gated on CD4
G

Figure 3.14. PRC2 plays an indispensable role in antigen-specific T cell expansion. A. $DbGP_{33-41}$ positive T cells among splenic $CD8^+$ T cells were stained with tetramer. The splenocytes were obtained from LCMV infected mice on the post-infection day 8. The plots are gated on $CD8^+$ T cells (left). The absolute numbers of GP33 specific $CD8^+$ T cells from wild-type and indicated mutants were graphed (right). Data are shown as mean ± standard deviation and n=3-4 mice in each group **B.** The absolute number of GP33, GP276, and NP396 specific $CD8^+$ T cells in spleens from wild-type mice and Ezh2 cKO mice on the post-infection day 8. N=5-6 mice in each group. Data are shown as mean ± standard deviation and representative of two independent experiments. **C.** The absolute numbers of splenic tetramer positive $CD8^+$ T cells in Eed cKO and its wild-type control mice. N=3 mice in each group Data are shown as mean ± standard deviation and representative of three independent experiments. **D-G.** Flow cytometric analysis of cytokine production in $CD4^+$ and $CD8^+$ T cells. Splenocytes from wild-type control, Ezh2 cKO (D,F) and Eed cKO (E,G) mice on the post-infection day 8 were stimulated with GP_{33-41} peptides (D,E) and GP_{61-80} peptides (F,G) for 5hrs *ex vivo*. The stimulated cells were analyzed for IFN-γ, TNF-α and IL-2 by intracellular staining. The flow plots are gated on $CD8^+$ (D,E) and $CD4^+$ (F,G) and are representatives of three individual mice showing similar results. WT: $Ezh2^{fl/fl}$ or $Eed^{fl/fl}$, Ezh1 KO: $Ezh1^{-/-}$, Ezh2 cKO: $Ezh2^{fl/fl}$; CD4-Cre, Ezh1/2 dKO: $Ezh1^{-/-}$ $Ezh2^{fl/fl}$; CD4-Cre. Student's t-test, *$p<0.05$, **$p<0.01$, ***$p<0.001$

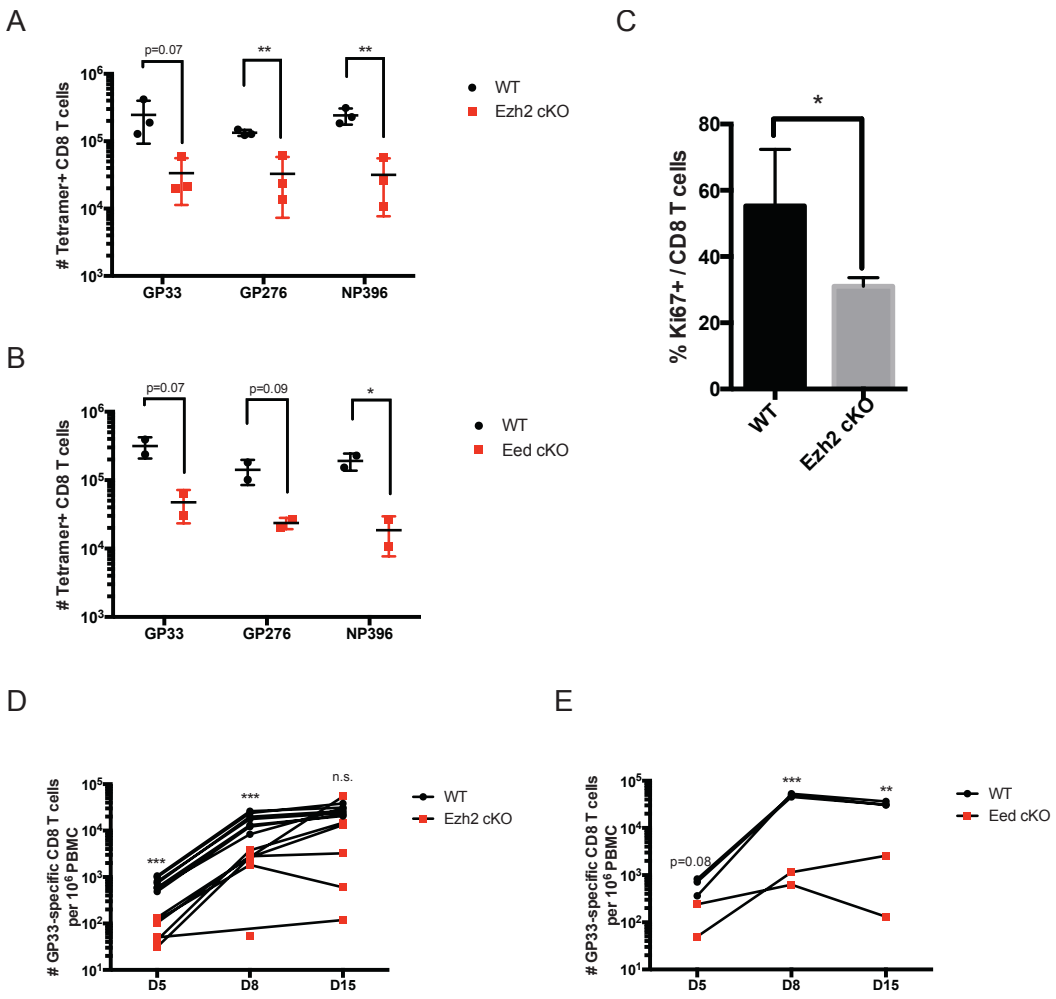

Figure 3.15. PRC2 deficient T cells fail to proliferate at early stage of immune response. A,B. The numbers of tetramer positive T cells in spleens from wild-type and Ezh2 cKO mice (**A**) and Eed cKO (**B**) on post-infection day 5. N=3 or 2 mice per each group **C.** Percentage of Ki-67+ cells among splenic $CD8^+$ T cells from wild-type and Ezh2 cKO mice on post-infection day 5. **D,E**. Kinetics of GP33 specific T cell frequency in PBMC of wild-type and Ezh2 cKO (**D**) or Eed cKO (**E**). Data from the same individual mice at different time points are connected with lines. Data are shown as mean ± standard deviation. Student's t-test, *p<0.05, **p<0.01, ***p<0.001

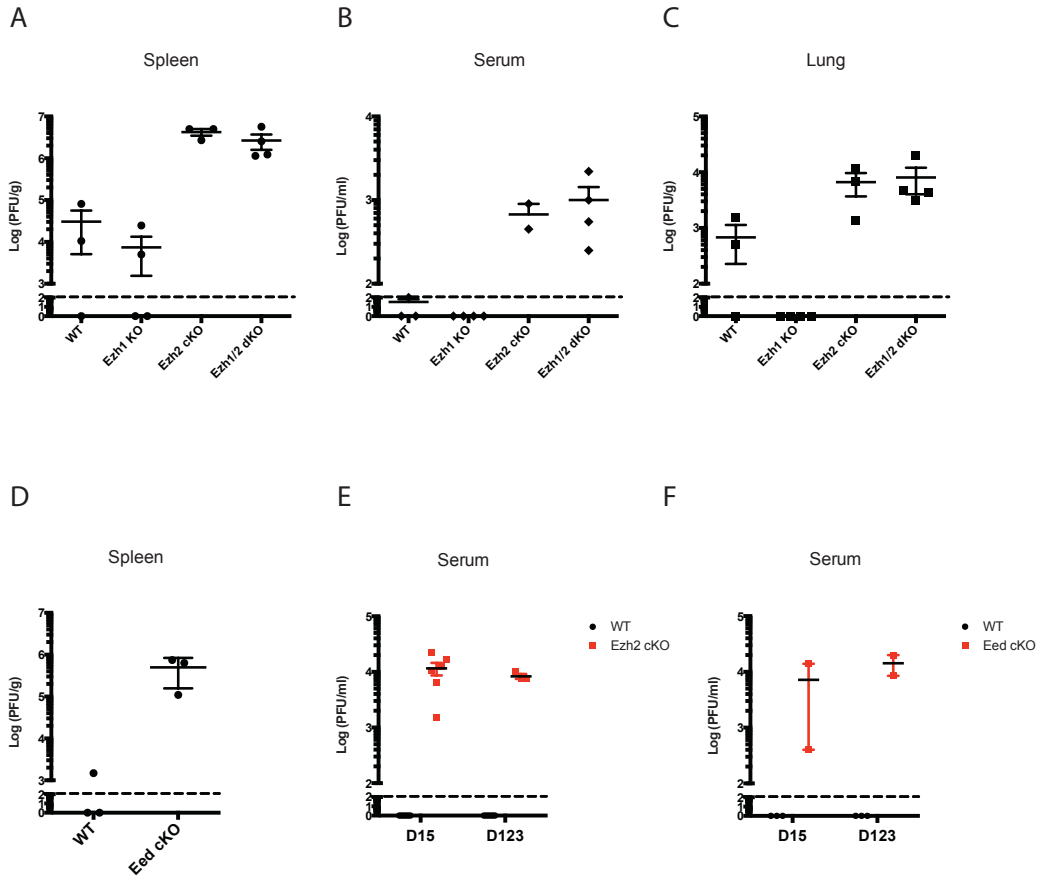

Figure 3.16. PRC2 deficiency leads to persistent infection. (A-C). Virus titers on the post-infection day 8 were measured from spleen, serum, and lung. Spleen, serum, and lung were harvested from wild-type and indicated PRC2 mutants and homogenized to obtain virus, followed by performing plaque assay. The virus quantity was calculated by normalizing PFU to volume of serum or weight of organs. Log 10 values of the normalized PFU/g or PFU/ml were plotted. N=3-4 mice per each group **D.** Virus titers in spleens of wild-type and Eed cKO mice on post-infection day 8. N=3 per each group **E,F.** Serum virus titers of wild-type and Ezh2 cKO (**E**) and Eed cKO (**F**) was measured on post-infection day 15 and 123. N=7 or n=2 The crossline in each plot represents the detection limit of the plaque assay. Data are shown as mean ± standard error.

3.10 Suppression of T cell immunity by PRC2 inhibition

Since we have shown that pharmacological inhibition of PRC2 prevented TCR-mediated Erk phosphorylation, we then attempted to use the inhibitor to modulate T cell immunity *in vivo*. We administrated 150 mg per kg of GSK503 compound to C57BL/6 mice intra-peritoneally everyday starting on the day of the LCMV infection. On day 8-post infection, we sacrificed the mice to examine the frequencies antigen-specific T cells in the spleen. As predicted, virus infection induced splenomegaly in solvent treated group, and the number of $CD4^+$ and $CD8^+$ T cells as well as B cells were increased, compared to uninfected controls (Figure 3.17A). However in GSK503 treated mice the number of T and B cells did not increase (Figure 3.17A). Importantly, there was no change in the number of B and T cells between solvent and GSK503 treated mice without infection, ruling out any possibility that toxicity of the inhibitor might have caused the decrease in cell numbers. When we analyzed the activation phenotypes in terms of CD44 and CD62L, the frequency and number of activated ($CD44^{hi}$; $CD62L^{lo}$) $CD8^+$ T cells were significantly reduced upon GSK503 treatment during infection (Figure 3.17B). The percentage of activated cells among the $CD4^+$ T cell population was only slightly reduced but the total number of activated $CD4^+$ T cells was clearly decreased (Figure 3.17B). Therefore, overall T cell activation was diminished by GSK503 treatment. Importantly, the number of virus-specific T cells were also significantly diminished, despite a large degree of variation in the GSK503 treated group (Figure 3.17C). The decreased number of virus-specific T cells and activated T cells correlated with increased virus titers in the GSK503

treated group (Figure 3.17D-F). In conclusion, pharmacological PRC2 inhibition suppresses antigen-specific T cell expansion *in vivo*.

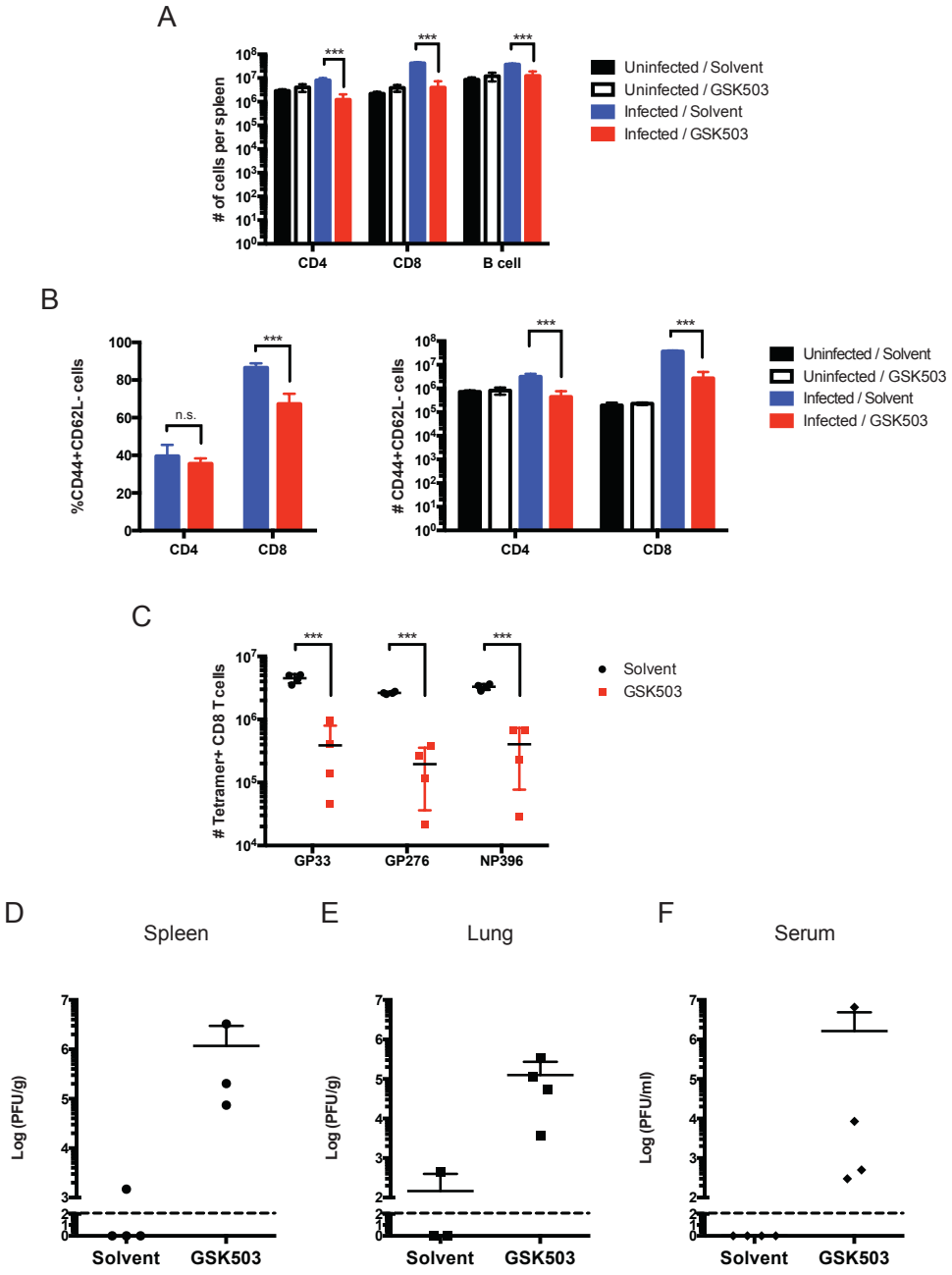
A
# of cells per spleen
CD4
CD8
B cell
***
Uninfected / Solvent
Uninfected / GSK503
Infected / Solvent
Infected / GSK503
B
%CD44+CD62L- cells
n.s.
CD44+CD62L- cells
C
Tetramer+ CD8 T cells
GP33
GP276
NP396
Solvent
GSK503
D
Spleen
E
Lung
F
Serum
Log (PFU/g)
Log (PFU/ml)

Figure 3.17. GSK503 inhibits T cell mediated anti-viral immunity. GSK503 and its solvent control were daily treated to C57BL/6 mice after LCMV Armstrong infection **A.** The number of splenic $CD4^+$, $CD8^+$ T and $CD19^+$ B cells of GSK503 and its solvent control treated mice on the post-infection day 8 were plotted. **B.** The frequency (left) and the number (right) of $CD44^+CD62L^-$ cells among $CD4^+$ and $CD8^+$ T cells are graphed. **C.** The number of $DbGP_{33\text{-}41}$ tetramer positive CD8 T cells from spleens of GSK503 and solvent treated mice. N=4 mice per each group Data were shown as mean ± standard deviation **D-F.** Virus titers in spleen (**D**), lung (**E**) and serum (**F**) were measured by plaque assay. N=4 mice per each group Data were shown as mean ± standard error. Student's t-test, *$p<0.05$, **$p<0.01$, ***$p<0.001$

3.11 Conclusion

In this chapter, we discuss the role of PRC2 in TCR-mediated T cell activation by directly controlling TCR signaling. Using genetic models, which eliminate PRC2 in peripheral T cells without having any gross developmental defect, we have shown the critical role of PRC2 for TCR-induced Erk phosphorylation and T cell proliferation. T cell proliferation was not affected by PRC2 deficiency when cells were stimulated with PMA/Ionomycin, which bypass the proximal signaling pathway. Importantly, the signaling defect we have seen in PRC2 deficient naïve T cells does not seem to be related to the nuclear function of PRC2. This conclusion is supported by the unaltered H3K27me3 level and gene expression in the absence of PRC2. However, arguments against using genetic model to prove the direct involvement of PRC2 in signaling are that PRC2 deficient T cell may have unknown developmental defects, or an accumulation of subtle gene expression changes that would not be detected in our statistical analysis. We addressed this issue by utilizing pharmacological inhibition of PRC2, providing direct proof for the direct contribution of PRC2-mediated lysine methylation to signal transduction. Indeed, Ezh2 inhibitors could suppress TCR-induced Erk phosphorylation. The inhibitor did not suppress PMA-induced Erk phosphorylation, consistent with our earlier finding that PMA-induced T cell proliferation does not require PRC2. Also, control compounds and unaffected general tyrosine phosphorylation downstream of the TCR support the specificity of PRC2 inhibitors in TCR-induced Erk phosphorylation. Finally, we show the relevance of PRC2 in T cell activation *in vivo*. Using acute an infection model, PRC2 deficiency and inhibition severely compromised T cell immunity.

CHAPTER 4: IDENTIFICATION OF A CYTOSOLIC SUBSTRATE OF EZH2 AND THE FUNCTION OF EZH2-MEDIATED LYSINE METHYLATION

4.1 The PRC2 complex exists in the cytosol

The suppression of TCR-induced Erk phosphorylation by inhibition of PRC2 in wild-type T cells strongly indicates a function of PRC2 in cytosolic signaling. Therefore, in this chapter, we hypothesize that PRC2 exists in the cytosol, contains the core components essential for methyltransferase activity and cytosol-specific components, which integrate PRC2 into TCR signaling. We primarily investigate the cytosolic PRC2 (cPRC2) with regard to its cytosolic interaction partners and complex composition. We performed nuclear and cytosolic fractionations of T cells and performed Western blot analysis for known PRC2 components. Previous studies have shown that nuclear PRC2 consists of at least four core components including Ezh2 (or Ezh1), Eed, Suz12 and RbAp48. AEBP2 was also identified in the initial complex purification from the Yi Zhang lab, and Jarid2 was later discovered as an additional component of PRC2. Our Western blot analysis shows that the nuclear PRC2 components, Ezh1, Ezh2, Suz12, Eed and RbAp48 are also expressed in cytosol of both naïve and activated T cells (Figure 4.1A). Jarid2 expression is upregulated in activated T cells as previously reported (Pereira et al., 2014) and it was readily detected in the cytosol of activated T cells. The amounts of Ezh2, Jarid2 and Suz12 also significantly increased while the expression of Ezh1, Eed and RbAp48 were unchanged or only moderately increased in the cytosol (Figure 4.1A). Although we did not directly quantify the amounts of Ezh1 and Ezh2 in the cytosol, given the strong

upregulation of Ezh2 after activation, it is plausible that in activated T cells most cPRC2s contains Ezh2 as its methyltransferase subunit. Additionally although the PRC2 complex is often described as a nuclear complex it is important to consider the following information. The Western blot data presented here were generated by loading equal amounts of total protein lysate from each fraction (Figure 4.1A). Cytosolic fractions from activated T cells have approximately three times more protein than cytosolic fractions from naïve T cells. Therefore, taking into account the increase of cellular contents in the cytosol of activated T cell, the absolute amount of cytosolic Ezh2 is higher than nuclear Ezh2. Next, we tested whether these components form a complex in the cytosol by performing Ezh2 co-immunoprecipitations. Indeed, all known core components including Suz12, Eed, Jarid2, and RbAp48 could be co-immunoprecipitated with Ezh2 from cytoslic fractions (Figure 4.1B,C). Interestingly we also found Ezh1 was interacting with Ezh2. The classical view is that individual PRC2 complexes contain either Ezh1 or Ezh2. Our data suggest that Ezh1-PRC2 and Ezh2-PRC2 interact or a novel PRC2 complex might be envisioned that contains both enzymes. In addition, our data confirm the previously published data that cPRC2 has enzymatic activity like the nuclear complex since all the components necessary for histone methyltransferase activity are present (Su et al., 2005).

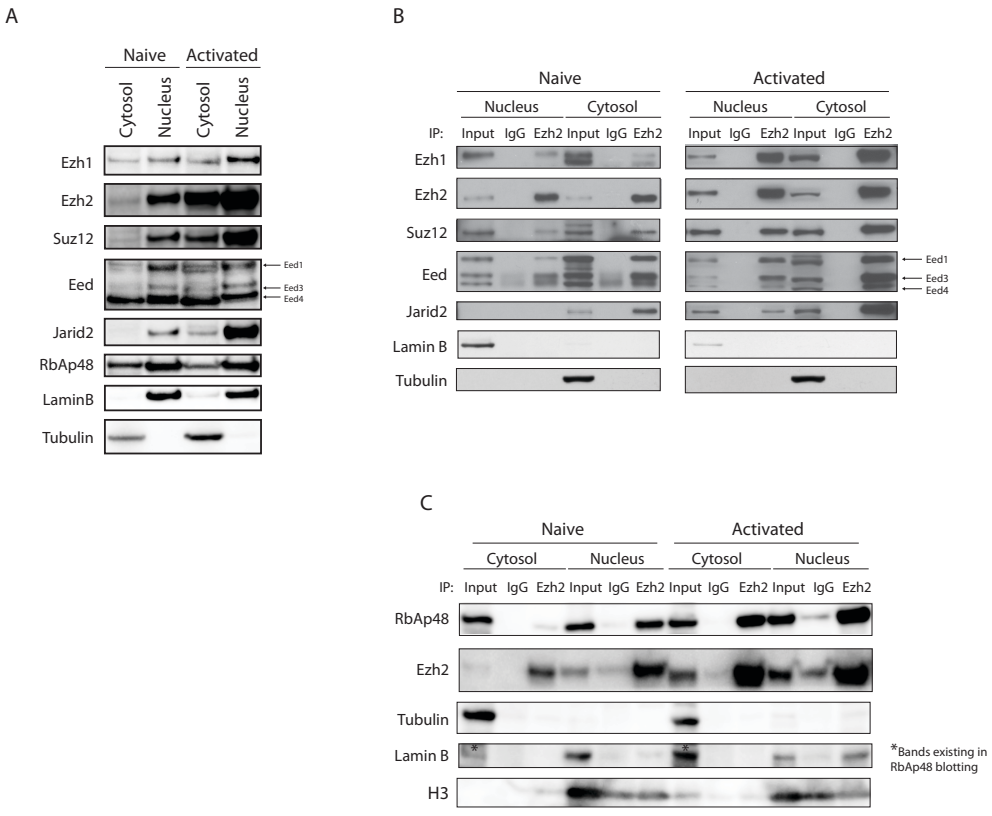

Figure 4.1. PRC2 is present in the cytosol. A. Western blot analysis for Ezh1, Ezh2, Suz12, Eed, Jarid2 and RbAp48 of cytosolic/nuclear fractions of naïve and activated T cells. To obtain activated T cells, purified $CD4^+$ T cells were stimulated on plate-bound anti-CD3/anti-CD28 antibodies for 3 days. Lamin B and Tubulin were used as fractionation and loading controls. **B,C.** Co-immunoprecipitation assay with Ezh2. Ezh2 was immunoprecipitated from cytosolic/nuclear fractions of naïve and activated T cells and analyzed for co-immunoprecipitation of Ezh1, Ezh2, Eed, Suz12, Jarid2 and RbAp48. Tubulin, Lamin B and H3 were used as fractionation controls.

4.2 Vav, Nck, and Ezh2 form a stable complex in the cytosol

cPRC2 controls TCR induced Erk phosphorylation. To address if this is through a direct interaction with components of the signaling cascade, we focused on

cytosolic interaction partners of Ezh2. As described earlier, Ezh2 was discovered in mammals as an interaction partner of Vav1 (Hobert et al., 1996). In addition to Vav1, we also studied the possible interaction between Nck proteins and Ezh2. Nck1 and its homolog Nck2, hereafter referred to as Nck since our analysis does not distinguish between Nck1 and Nck2 in Western blot, are signaling adaptor molecules that have more than 60 interaction partners (Lettau et al., 2010). Nck deficiency phenocopies Ezh2 deficiency in TCR-induced Erk phosphorylation and actin polymerization in MEFs and T cells (Roy et al., 2010). Interestingly, Nck deficient T cells have a selective defect in Erk signaling pathway but intact JNK and Akt activation, something we also observed in Ezh2 deficient T cells. Therefore, we hypothesize that Nck is a possible link between cPRC2 and the TCR signaling cascade. To test this hypothesis, we immunoprecipitated Nck from the cytosol of cells that received TCR stimulation for 0 to 30 min, followed by Western blot analysis for Vav1 and Ezh2. As our hypothesis predicted, Nck was constitutively associated with Ezh2 and Vav1 (Figure 4.2A). We also detected Suz12 in Nck immunoprecipitates, indicating that the interaction is with cPRC2 and not free Ezh2 (Data not shown). To test the quality of the interaction between Ezh2, Nck and Vav1, we performed washes of the IPed material with increasing amounts of salt. Ezh2, Nck and Vav1 form a stable complex, resistant to even 600mM NaCl (Figure 4.2B,C). These data support two arguments: 1) cPRC2 is physically coupled to the TCR signaling cascade via interaction with Vav1 and Nck and 2) cPRC2 may be functionally relevant for TCR signaling. Therefore, it would be interesting to investigate the functional outcome of the disruption of this complex.

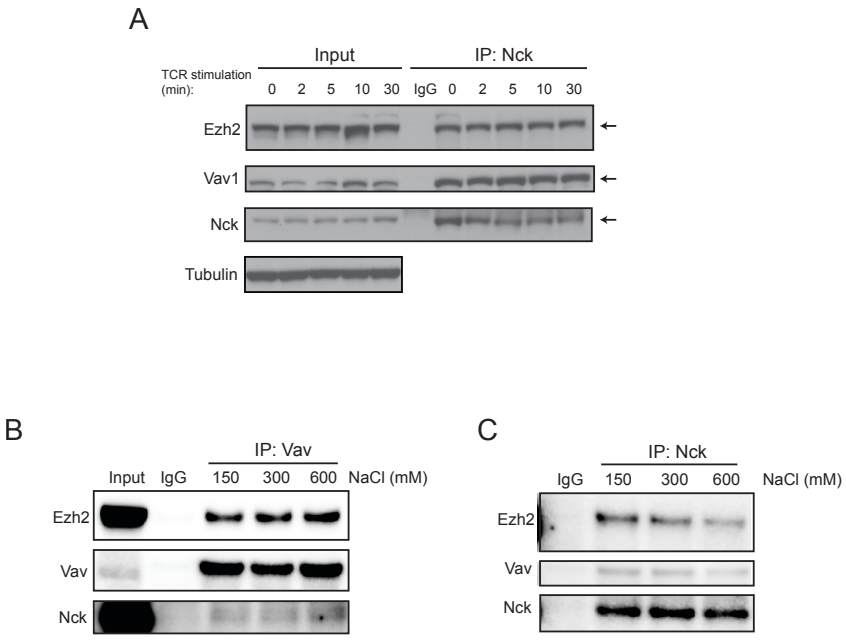

Figure 4.2. Vav1, Nck and Ezh2 form a stable complex in the cytosol. A. Nck co-immunoprecipitation in unstimulated/stimulated Jurkat cell lysates. Duration of stimulation with anti-human CD3 antibody (OKT3) is indicated. The co-immunoprecipitates were analyzed for Ezh2, Vav1 and Nck. **B.** Vav1 was immunoprecipitated from purified murine $CD4^+$ T cells. The co-immunoprecipitates were incubated with 150, 300 and 600 mM of NaCl containing wash buffer to remove weak interactions. The co-immunoprecipitates were analyzed for Ezh2, Vav1 and Nck. **C.** Nck co-immunoprecipitates from purified murine $CD4^+$ T cells were incubated with 150, 300 and 600 mM of NaCl containing wash buffer, followed by Western blot analysis for Ezh2, Vav1 and Nck.

4.3 Nck is required for Vav1/Ezh2 association

Next, we closely examined the Nck/Vav1/Ezh2 complex. We wanted to address the contribution of Nck to the interaction between Vav1 and Ezh2. Therefore we immunoprecipitated Vav1 from an Nck1/2 knockdown Jurkat cell line and probed

by Western blot for the presence of Ezh2. The ShRNA knockdown resulted in ~70% reduction in protein levels of Nck1/2. Surprisingly, shRNA-mediated knockdown of Nck led to reduced interaction between Ezh2 and Vav1 (Figure 4.3). Therefore, Nck is important for Vav1/Ezh2 association. The interaction between Ezh2 and Vav1 seems to be constitutive and independent of TCR engagement confirming the previous published observation (Su et al., 2005). TCR stimulation did not increase or decrease the reduction in interaction between Vav1 and Ezh2. Therefore, Nck contribution to the interaction between Ezh2 and Vav1 was not increased or decreased upon TCR stimulation (Figure 4.3), indicating that TCR stimulation does not facilitate or diminish this interaction.

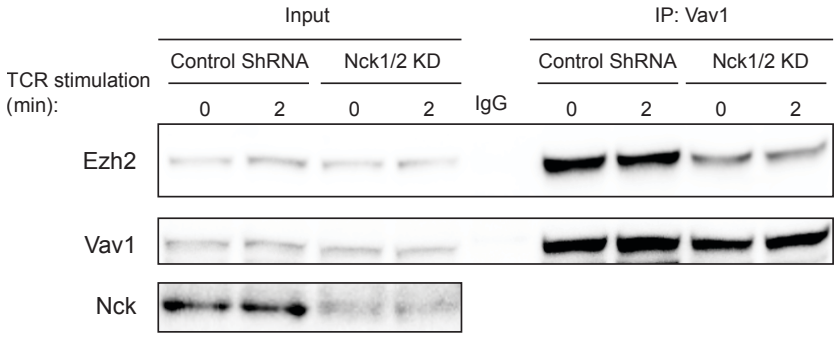

Figure 4.3. Nck is required for Vav1/Ezh2 association. Wild-type Jurkat cells and shRNA-mediated Nck1/2 knockdown cells were stimulated with anti-human CD3 antibody (OKT3). Vav1 was immunoprecipitated from cytosolic cell lysates and the co-immunoprecipitates were analyzed for Ezh2 by Western blot. Nck Western blot was done to show the knockdown. Data are representative of two independent experiments.

4.4 Ezh2 is associated with the TCR

We have explored the composition of cPRC2 and found that two critical components of TCR signaling pathway are associated with Ezh2, Vav1 and Nck. Vav1 is a known interaction partner of Zap70 (Katzav et al., 1994), a kinase that binds to phosphorylated ITAM motifs in the cytoplasmic tails of the TCR. Nck also directly interacts with the TCR, namely with the proline rich region of CD3ε (Gil et al., 2002). Therefore, we hypothesized that Ezh2 may be associated with TCR. To test this hypothesis, we to pulled down the TCR and associated proteins by two different methods. First, we pulled down the TCR complex by first incubating the cells with anti-CD3/anti-CD28 antibodies, crosslinking of the TCR with biotin-conjugated secondary antibody and ultimately pulling down the bound complexes with streptavidin coated magnetic beads. As a control, we performed the same pull downs from unstimulated cells but with a minor modification. We incubated the cells with the same antibodies as for the stimulated cells, however, we incubated the cells for a longer period on ice and instead of allowing the secondary antibodies to bind to the primary antibodies at 37°C, which would induce the TCR signaling cascade, we also incubated with the secondary antibody on ice. Interestingly, the TCR pull down from unstimulated and stimulated cells both contained Ezh2 (Figure 4.4A). When we normalized the amount of proteins pulled down to amount of CD3ε pull down, we found that the association between Ezh2 and TCR was increased by 1.57 fold upon TCR stimulation. Also, Vav1 inducibly associated with TCR (2.54 fold increase after stimulation). Ezh2 was not found in unbiotinylated secondary antibody treated cells, meaning that Ezh2 was specifically pulled down with TCR bound to biotin-conjugated

antibody (Figure 4.4A). As stimulation control, we confirmed that Erk phosphorylation was induced in stimulated cells. For the interaction of Nck with TCR, the result looks somewhat complicated since we did not observe any induction upon stimulation (1.04 fold increased after stimulation). The incubation with secondary antibody on ice might still trigger conformational changes of the TCR and expose Nck binding sites although this treatment prevents TCR-induced phosphorylation events. In support of this hypothesis is a report that showed that the interaction between Nck and CD3ε was increased upon TCR engagement even in the presence of the Src-kinase inhibitor PP2 (Paensuwan et al., 2016). The second method we employed to test the interaction between Ezh2 and TCR was reciprocal immunoprecipitation of Ezh2 and CD3ε, followed by western blot detection of Ezh2 and CD3ε. We confirmed the association of Ezh2 and CD3ε in both unstimulated and stimulated T cells (Figure 4.4B). The interaction seems to be increased upon stimulation. These data show that the cPRC2 complex directly interacts with CD3ε and is well localized to influence the TCR signaling pathway.

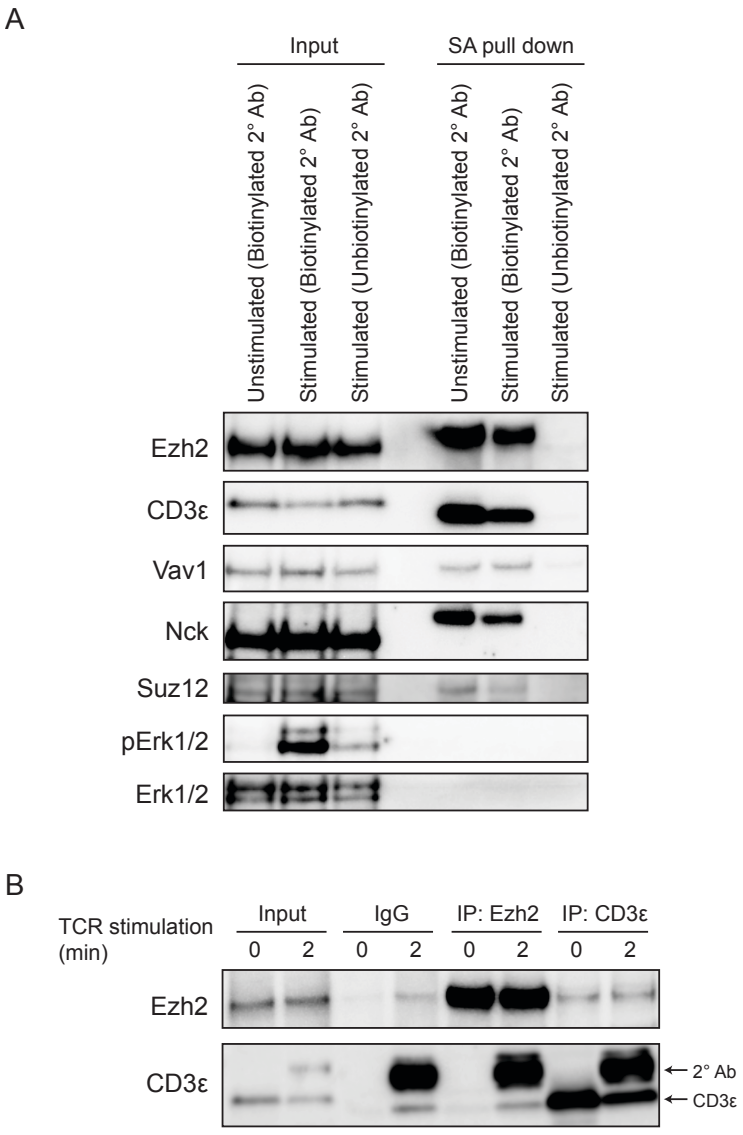

Figure 4.4. Ezh2 is associated with TCR. A. Streptavidin pull-down of biotinylated secondary antibody bound to anti-CD3/anti-CD28 antibodies. Purified $CD4^+$ T cells were treated with anti-CD3/anti-CD28 antibodies for 15 min on ice, followed by incubation with biotinylated or unbiotinylated secondary antibodies on ice for 15 min (unstimulated) or at 37°C for 2 min (stimulated). The pull-down was analyzed for Ezh2, CD3ε, Vav1, Nck and Suz12 by Western blot. Phospho-Erk and total Erk was blotted as TCR stimulation control. **B.** Co-immunoprecipitation of Ezh2 and CD3ε from unstimulated and TCR-stimulated T cells. Co-immunoprecipitates were immunoblotted for Ezh2 and CD3ε.

4.5 Conclusion

Here we showed that the PRC2 complex is present in the cytosol of human and mouse T cells and that it is associated with Nck and Vav1. These cytosol specific components seem to connect cPRC2 directly to the TCR. Moreover, Ezh2 indirectly or directly is associated with the TCR. This finding implies three things. The fact that cPRC2 contains the core components of the nuclear PRC2 suggests it has methyltransferase activity. Indeed, we already found evidence that the methyltransferase activity of cPRC2 is necessary to allow full Erk phosphorylation after TCR crosslinking in the previous chapter, provided by the PRC2 inhibitor experiments. Second, cPRC2 is constitutively associated with its cytosolic interaction partners. These interactions might retain cPRC2 in the cytoplasm, which otherwise might be translocated to nucleus due to its NLS sequence. In agreement with this observation, the dramatic increase in the amount of cPRC2 in the cytosol of activated T cells could be explained by the increased expression of Vav1 in stimulated cells. The larger cytosolic proportion of the PRC2 complex might also be important for proper gene regulation, since an overabundance of PRC2 in the nucleus could lead to an overly repressive epigenetic environment. Lastly, the interaction between Ezh2 and CD3ε of the TCR explains why PRC2 deficiency specifically disrupts proximal TCR signaling. In summary, we show that a cytosolic PRC2 complex exists and that it interacts with central components of TCR signaling.

CHAPTER 5: IDENTIFICATION OF AN EZH2 SUBSTRATE AND THE FUNCTION OF EZH2-MEDIATED LYSINE METHYLATION

5.1 Identification of histone-like sequences in Vav1 interaction partners

To ascertain the importance of cPRC2 for signaling, it became necessary to understand the precise mechanisms. In the previous chapters we identified strong evidence that cPRC2 methyltransferase activity is required for TCR-induced Erk phosphorylation and that cPRC2 contains the essential components for this activity. Therefore, it is likely that Ezh2-mediated lysine methylation governs the function of cPRC2. In this chapter, we attempt to identify cytosolic substrates of Ezh2.

To identify cytosolic substrates of Ezh2, we utilized an *in silico* screen for target consensus sequences among Vav1 interacting proteins. As mentioned above, a histone-like sequence can help to identify protein sequences that can be methylated by histone methyltransferases. Our laboratory was successful before in identifying non-histone substrates of G9a/GLP with this approach (Sampath et al., 2007). Here we tried to identify sequences encompassing the target lysine residues that can be methylated by Ezh2. Vav1 is a functional and direct interaction partner of Ezh2 with a known role as adapter protein therefore we tried to find the Ezh2-target sequence among Vav1 interacting proteins (Figure 5.1A). We identified a histone-like sequence in the linker region between the first and second SH3 domain of Nck1 (Figure 5.1B). As shown in the figure, the amino acid sequence surrounding lysine 64 of Nck1 is highly similar to the sequences of histone 3 lysine 27, which is the methylation site for Ezh2.

Nck exists as two homologs, Nck1 and Nck2, which have 76% sequence homology. The proteins contain three SH3 domains, which can bind to proline rich region and one SH2 domain that can recognize phosphorylated tyrosines (Pawson, 1994; Pawson and Gish, 1992). Most sequence variation between Nck1 and Nck2 reside in the linker regions, whose function is not well studied. These structural features enable the Nck proteins to serve as signaling adaptor molecules by linking tyrosine phosphorylation on one protein to various downstream proteins containing proline rich regions. In particular, Nck is required for TCR-induced Erk phosphorylation, although the exact mechanism is not known (Roy et al., 2010). A well-known function of Nck is the recruitment of actin polymerizing protein WASP to TCR signaling cluster (Zeng et al., 2003). In MEFs, PDGF-induced actin polymerization is also dependent on Nck proteins (Bladt et al., 2003). Since Nck controls Erk signaling pathway in T cells and actin polymerization pathway in MEFs, and the same pathways are affected in Ezh2 deficient T cells and MEFs, respectively (Ref), it is conceivable that Ezh2 and Nck function in the same pathway. Therefore, we hypothesize that Nck1 is a cytosolic substrate of Ezh2.

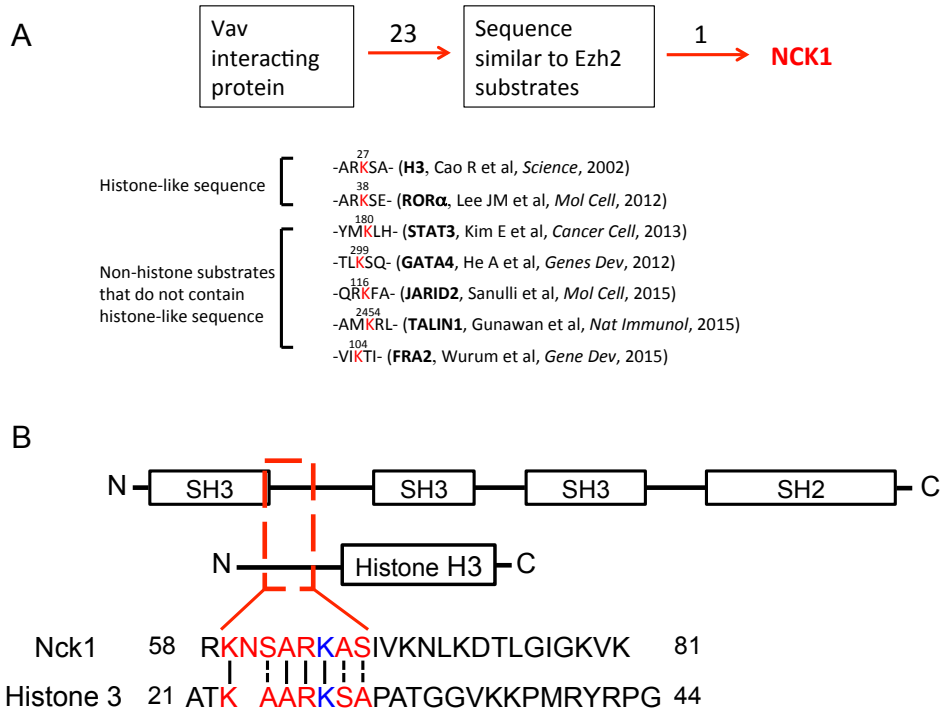

Figure 5.1. Nck1 contains a histone-like sequence. A. *In silico* search for Ezh2 target consensus sequences among Vav1 interacting proteins. Seven sequences from known targets of Ezh2 were aligned to Vav interacting proteins. Nck1 was identified to have a histone-like sequence. **B.** Histone-like sequence in Nck1. Nck1 has a histone-like sequence in a linker region between the first and second SH3 domain. Sequence similarity to the histone 3 sequence was labeled with red and the lysine residue that can be methylated by Ezh2 was colored in blue.

5.2 Nck1 is methylated by Ezh2

To directly test whether Ezh2 methylates the cytosolic protein Nck1, we performed *in vitro* methyltransferase assays with recombinant PRC2. In this assay, we used His tagged Nck1 as a substrate and recombinant PRC2 containing Ezh2, Eed, Suz12, RbAp48 and AEBP2. We traced the methylation by using ^{3}H-SAM as methyl-donor and detected the methylated proteins by auto-radiography. Our results show that

PRC2 can directly methylate Nck1 protein *in vitro* (Figure 5.2A). We also confirmed by Mass Spectrometry that *in vitro* methylated Nck1 contains methyl-lysine residues (Figure 5.2B). Indeed, the methylation site was the site we had predicted in our *in silico* target screen.

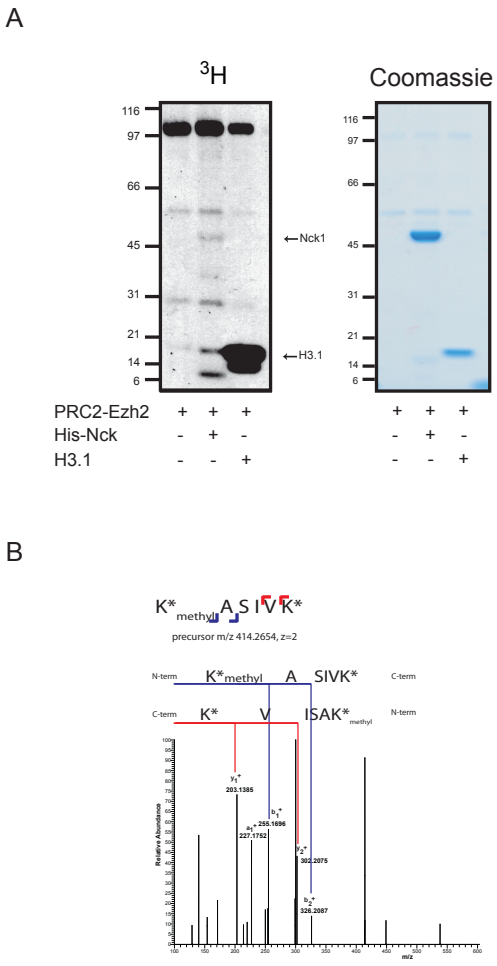

Figure 5.2. Ezh2 methylates Nck1 A. *In vitro* methyltransferase assay was performed using ^{3}H-SAM. Recombinant PRC2 was incubated with recombinant his-tagged Nck1 for 1.5 hr at 30°C. Histone 3.1 was used as positive control. Autoradiography (left) and coomassie staining (right) are shown. **B.** Nck1 protein from *in vitro* methyltransferase assay was subjected to mass spectrometric analysis. LC-MS/MS spectra of Nck1 is displayed.

Next, we sought to confirm that the methylation also occurs *in vivo*. We immunoprecipitated Nck1 from cytosolic lysates of unstimulated and TCR-stimulated Jurkats, followed by probing for lysine methylation using an anti-pan methyl lysine antibody. The ability of antibody to detect methylated Nck was confirmed by Western blot of *in vitro* methylated Nck (Figure 5.3A). As shown, PRC2 mediated methylation of Nck1 was detected by the pan-methyl lysine antibody. Furthermore, we detected the methylation in Nck pulled down from Jurkat cell lysates, suggesting that Ezh2-medated Nck methylation is present in Jurkat cells, independent of activation of the cells (Figure 5.3B).

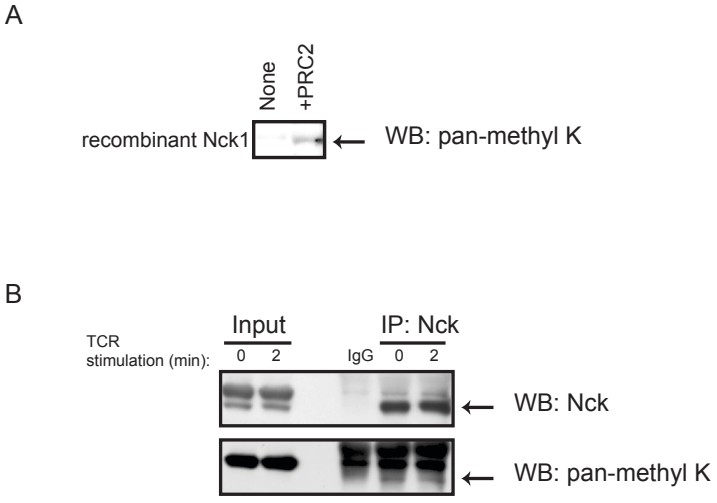

Figure 5.3. Nck is methylated in T cells. A. Westernblot analysis on recombinant Nck1 protein methylated *in vitro* using a pan-methyl lysine antibody. **B.** Lysates from unstimulated Jurkat cells or cells stimulated with anti-human CD3 antibody (OKT3) for 2 min was used for Nck immunoprecipitation. The immunoprecipitates were probed for Nck and pan-methyl-lysine.

5.3 Ezh2 methylates a lysine residue in a histone-like sequence

To confirm the identified methylation site, we performed methyltransferase assays with $Nck1_{58-81}$ peptides containing amino acid substitutions. We designed Nck1 peptides aligned to the histone-like sequence. Then, we also designed K-to-R or K-to-A substituted peptides to test the contribution of each lysine to the methylation signal. As predicted, substitution of lysine 64 to either arginine or alanine substantially abolished the methylation signal (Figure 5.4). We also observed methylation on lysine 59, although the degree of methylation was lower than for lysine 64. By comparing the substitutions of K-to-R and K-to-A substitutions of lysine 59 indicated that structural factors might regulate the methylation of lysine 64. In other words, while K-to-R substitution of lysine 59 did not affect the methylation of lysine 64, the K-to-A substitution reduced the methylation of lysine 64. When we introduce substitution to both lysines, we could completely remove the methylation signal, indicatinging that PRC2 methylation is specific towards lysine residues and not arginine. Also, no other lysines in the region could be methylated *in vitro*. Therefore, these data strongly support our hypothesis that Ezh2 methylates the histone-like sequence of Nck1.

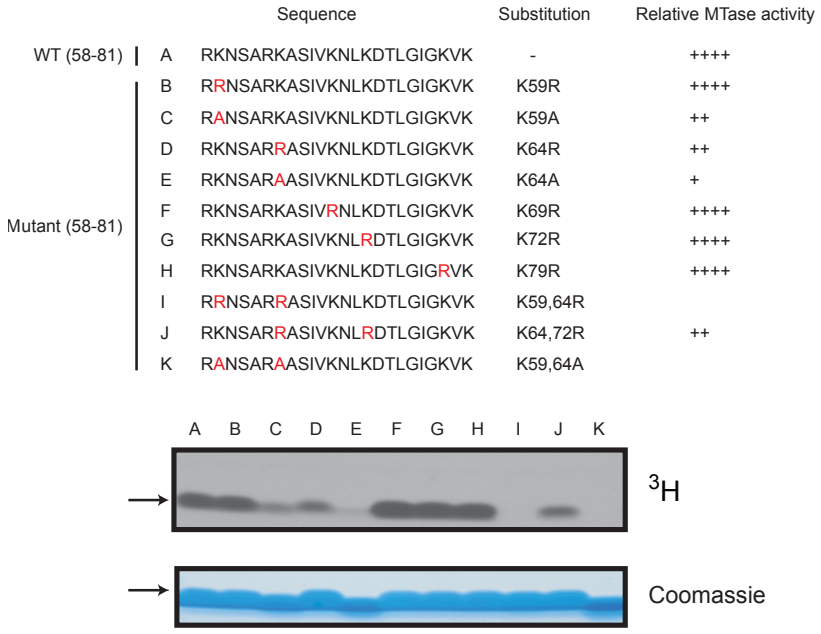

Figure 5.4. Lysine 64 of Nck1 is methylated by Ezh2 *In vitro* methyltransferase assay was performed with $Nck1_{58-81}$ peptides. Nck1 peptides were designed as shown. Amino acid substitutions are depicted in red and indicated in the column substitutions. Band intensities from autoradiography were quantified and displayed in the right column. Relative values were indicated (+ < 0.25, ++ < 0.5, +++ < 0.75, ++++ >0.75 to wild-type peptide).

5.4 Nck1-interacting proteins contain methyltransferase activity for H3 and Nck1

In the previous section, we showed that recombinant PRC2 complex is able to methylate Nck1, however, cPRC2 *in vivo* may contain additional components necessary to facilitate the methylation of its substrates. Therefore, we decided to use the Nck1-PRC2 complex identified in the previous section to address the possible

methylation of Nck1 by cPRC2. We hypothesized that the Nck containing PRC2 complex has methyltransferase activity and can methylate Nck. To test this hypothesis, first, we examined if Nck interacting proteins have methyltransferase activity on histones. We immunoprecipitated Nck and used the co-immunoprecipitating cPRC2 complex as enzyme in an *in vitro* histone methyltransferase assay. As positive control, we immunoprecipitated Ezh2 from the cytoplasm and used it as enzyme for the reaction. Our data show that co-immunoprecipitates of Nck and Ezh2 can methylate Nck1 (Figure 5.5). Therefore, Nck interacts with a histone methyltransferases, presumably Ezh2.

We next asked if Nck interacting proteins could methylate Nck1. For this, we used the same experimental scheme as in Figure 5.5 but utilized recombinant His-tagged Nck1 protein as a substrate instead of H3.1. Interestingly, we found that co-immunoprecipitates of Nck could methylate Nck1 itself, suggesting that Nck can be methylated by its interaction partners (Figure 5.6). We could also detect co-immunoprecipitation of Ezh2 with Nck. Therefore, these data show that a Nck containing methyltransferase complex can methylate Nck1 and that the cPRC2 complex co-immunoprecipitates with Nck. But these data cannot exclude the presence of an additional methyltransferase. Therefore we performed the methyltransferase assay in the presence of the Ezh2 inhibitor GSK343. The methylation signal was significantly reduced, but not completely abolished (Data not shown). This indicates either the presence of an additional enzyme capable to methylate Nck1 or the incomplete inhibition of Ezh2. We have not attempted to control for the second possibility since we are unsure about the affinity of the PRC2 complex to different

substrates. We have preliminary data that an Ezh1 containing PRC2 complex can also methylate Nck peptide. Therefore, the incomplete blockade of Nck1 methylation by GSK343 may be due the lower activity of this inhibitor towards Ezh1, which is another component of cPRC2 (Figure 4.1B).

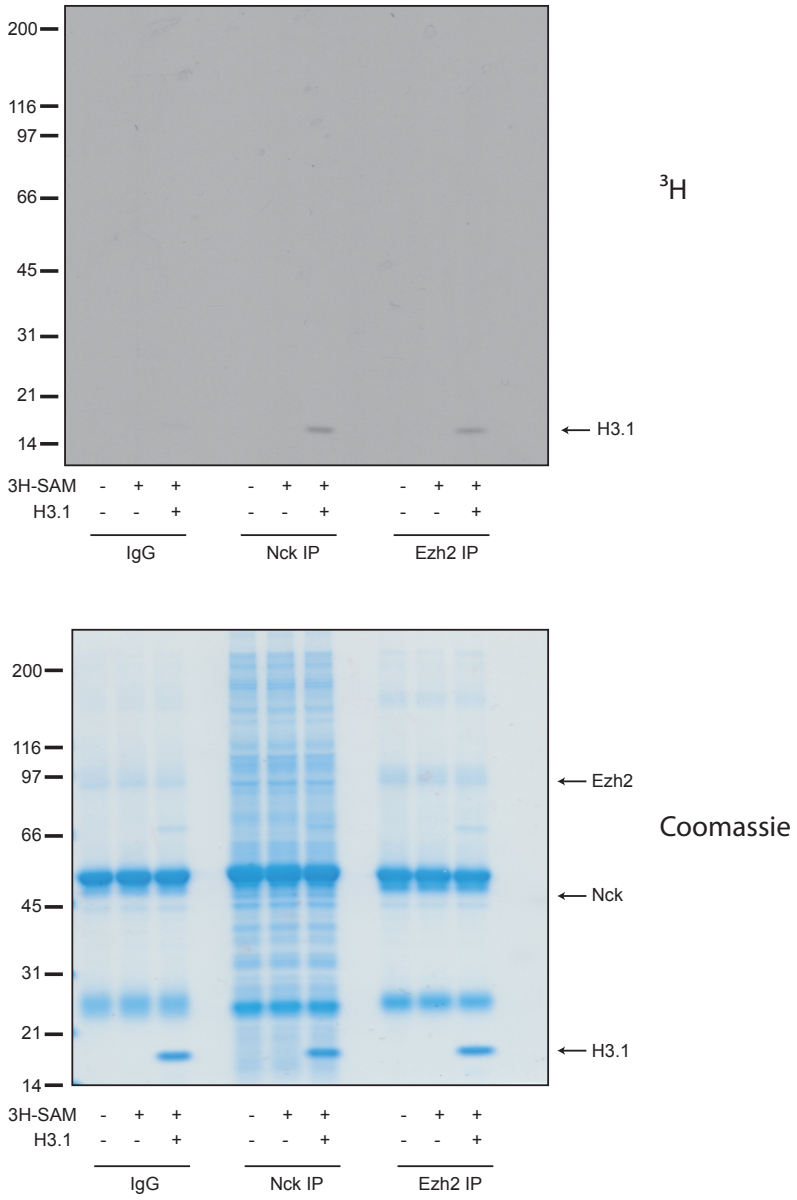

Figure 5.5. Nck interacting proteins contain histone methyltransferase activity. Jurkat cell lysates were incubated with rabbit IgG, anti-Nck antibody, or anti-Ezh2 antibody for co-immunoprecipitations. The co-immunoprecipitates were used for *in vitro* methyltransferase assay with H3.1 and ^{3}H-SAM.

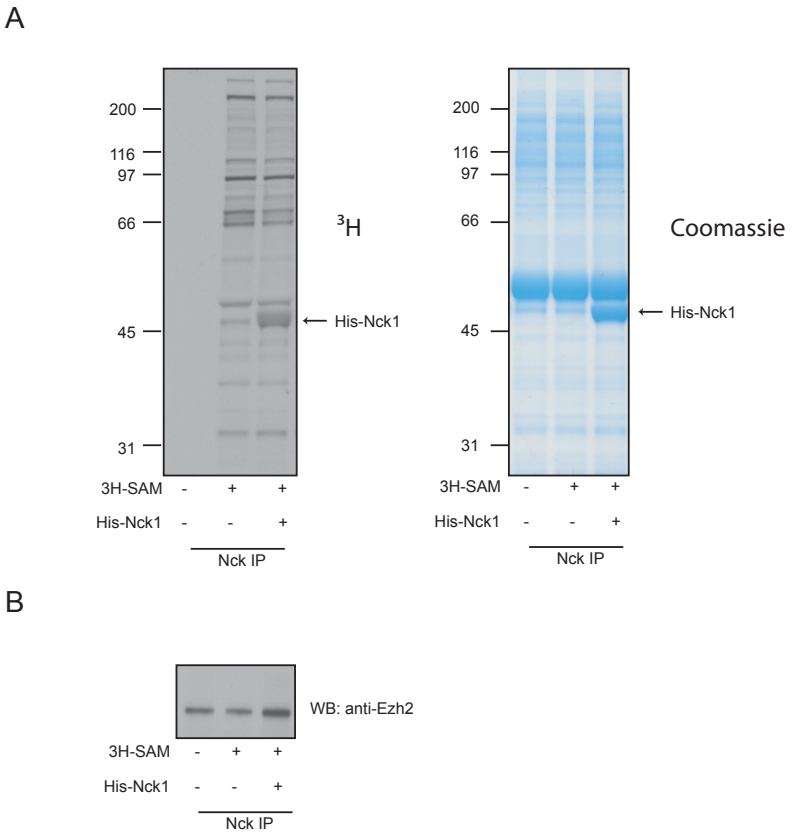

Figure 5.6. Nck interacting proteins methylate Nck1. A. Nck1 was immunoprecipitated from Jurkat cell lysates, followed by *in vitro* methyltransferase assay with the co-immunoprecipitated product, recombinant His-Nck1 protein and ^{3}H-SAM. His-Nck1 is indicated on the autoradiography (left) and the coomassie staining (right). **B.** Co-immunoprecipitation of Ezh2 with Nck.

5.5 Self-methylation of Ezh2

One consistent observation we made in the methyltransferase assays was the Ezh2 self-methylation (Figure 5.2B). The band corresponding to Ezh2 was heavily methylated in the reaction. This led us to investigate the self-methylation of Ezh2 since Ezh2 itself is another cytosolic substrate. For a cleaner system of Ezh2 self-methylation, we performed *in vitro* methyltransferase assays in the absence of other substrates, followed by mass spectrometric analysis. We observed that Ezh2 is methylated after an *in vitro* reaction (Figure 5.7A). When this reaction product was subjected to mass spectrometric analysis, we found that lysine 735 was mono-methylated (Figure 5.7B). This lysine is located at C-terminal region of Ezh2, right next to SET domain (Figure 5.7C). To exclude an *in vitro* artifact we decided to check for Ezh2 self-methylation *in vivo*. When we pulled down Ezh2 from stimulated T cells and analyzed it by mass spectrometry, we found the same site was methylated *in vivo*, suggesting that Ezh2 methylation may be physiologically important. Whether the methylation is stimulus-dependent or not is worthwhile to be further investigated.

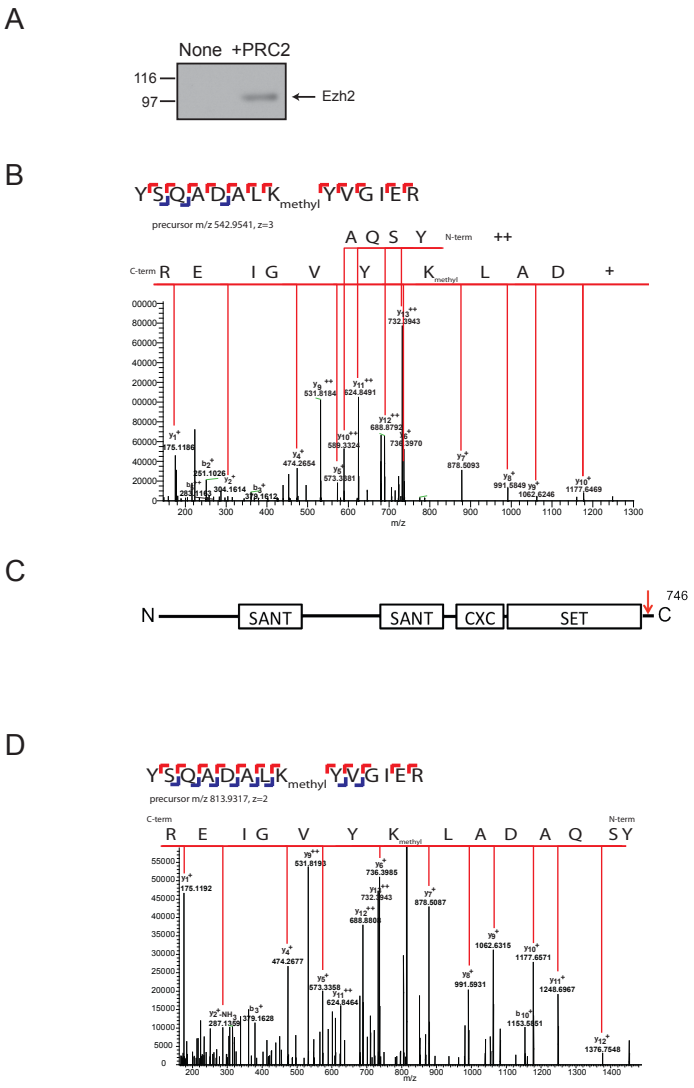

Figure 5.7. Ezh2 is self-methylated. A. Autoradiography of *in vitro* methyltransferase assay on Ezh2. **B.** Mass spectrometric analysis of *in vitro* methylated Ezh2. **C.** Domain structure of Ezh2 and methylation site. Lysine 735 (indicated with red arrow) at the C-terminal region of Ezh2 was methylated. **D.** $CD4^+$ T cells were stimulated with anti-CD3/CD28 antibodies. The lysates were incubated with anti-Ezh2 antibody to pull down Ezh2 and the immunoprecipitated Ezh2 were subjected to mass spectrometric analysis.

5.6 PRC2-mediated lysine methylation modulates protein-protein interaction

The final question in this study is to determine the function of Ezh2-mediated methylation. In this study, we identified two substrates of Ezh2. Interestingly, Jarid2, another PRC2 component, is also methylated by Ezh2 (Sanulli et al., 2015). Therefore, there are three proteins associated with cPRC2 that are targets of Ezh2. Given that methylation can play a role in the modulation of protein-protein interactions, these methylation targets might potentially serve as docking sites for other proteins. If this is the case, Ezh2-mediated methylation would contribute to the formation of a large signaling complex. Our hypothesis is that PRC2-mediated methylation of its components and other cytosolic substrates facilitates protein recruitment. To validate this hypothesis, we examined the interactome of Nck and Ezh2 in the presence/absence of Ezh2-mediated methylation. For this approach we utilized proteomic analysis of immunoprecipitated material from untreated or Ezh2 inhibitor treated cells.

We treated murine CD4 T cells with GSK503 following the previous experimental scheme, which inhibits TCR-induced Erk phosphorylation. We immunoprecipitated Nck or Ezh2 from the TCR-stimulated cells, followed by identification of co-immunoprecipitated proteins. Then, we identified the proteins that were less enriched in Nck-IP upon GSK503 treatment. We found that 71 proteins were specifically enriched after Nck-IP over control IgG-IP. The co-immunoprecipitation with Nck of 6 proteins was lost after GSK503 treatment and are therefore most likely dependent on Ezh2-mediated methylation (Figure 5.8). On the other hand the co-immunoprecipitation of 2 proteins increased in the GSK503 treated samples,

indicating that the recruitment of some proteins is inhibited by Ezh2-mediated methylation.

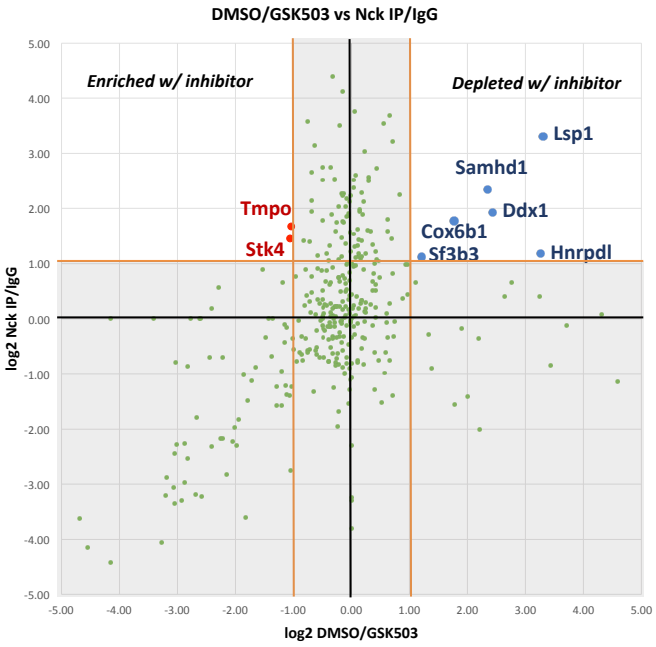

Figure 5.8. Interactome of Nck changes upon GSK503 treatment Purified murine CD4$^+$ T cells were pre-incubated with DMSO or GSK503 for 1hr on ice, followed by TCR cross-linking for 2 min at 37°C. Nck co-immunoprecipitation was performed and eluted samples were subjected to mass spectrometry. Each dot represents the normalized log2 value of peptide abundance in Nck-IP/IgG-IP from DMSO treated cells (y-axis) and Nck-IP from DMSO treated cells/Nck IP from GSK503 treated cells (x-axis). Bright area indicates proteins enriched in Nck IP. Ribosomal proteins and keratins were removed from the list.

Additionally, we performed the same analysis on the Ezh2 interactome. In this analysis, we included unstimulated CD4$^+$ T cells to see if any interactions are TCR-inducible and can be modulated by Ezh2 inhibition. As reported by others, Ezh2 co-

immunoprecipitation contained Ezh1, Ezh2, Suz12, Eed, RbAp46/48, AEBP2, Jarid2, and MTF2 (Figure 5.9). The abundance of these proteins in the Ezh2 immunoprecipitation was not altered, neither upon stimulation nor GSK503 treatment. Therefore, Ezh2-mediated lysine methylation does not modulate the core complex composition.

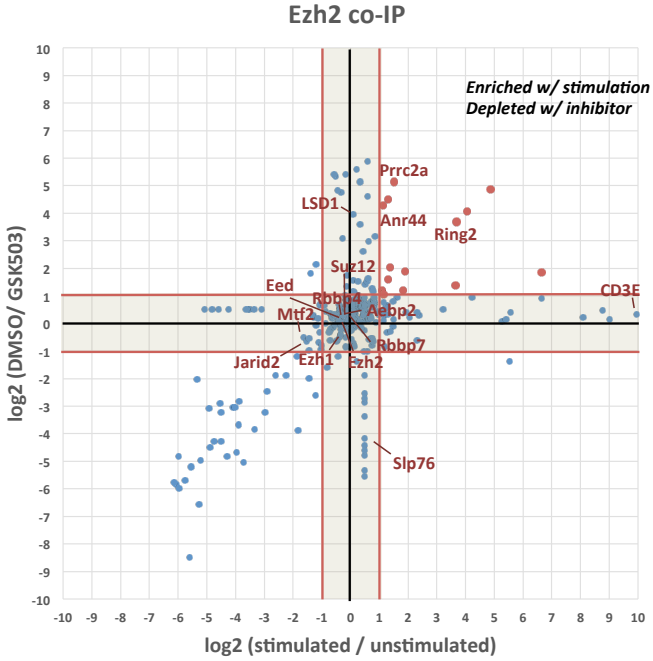

Figure 5.9. Ezh2 interactome in T cells modulated by Ezh2 inhibition. Mass spectrometric analysis of Ezh2 interaction partners in unstimulated and stimulated T cells in the presence/absence of GSK503. GSK503 or DMSO treated cells were stimulated with TCR for 2 min. Co-immunoprecipitation of Ezh2 was analyzed. The protein list was filtered by IgG immunoprecipitation control, followed by removal of ribosomal proteins and keratins. Each dot represents the normalized log2 value of peptide abundance in Ezh2 IP from DMSO treated stimulated cells/GSK503 treated stimulated cells (y-axis) and Ezh2 IP from DMSO treated stimulated cells/DMSO treated unstimulated cells (x-axis).

Table 5.1. List of proteins that interact with Ezh2 upon TCR stimulation but lose interaction in the presence of GSK503

Description	stim/unstim	stim/pre Inhib
ATP synthase subunit f, mitochondrial OS=Mus musculus GN=Atp5j2 PE=4 SV=1 - [F8WHP8_MOUSE]	3.55	3.55
E3 ubiquitin-protein ligase RING2 OS=Mus musculus GN=Rnf2 PE=1 SV=1 - [RING2_MOUSE]	3.19	3.19
Elongation factor 2 OS=Mus musculus GN=Eef2 PE=1 SV=2 - [EF2_MOUSE]	1.40	1.40
Fructose-bisphosphate aldolase (Fragment) OS=Mus musculus GN=Aldoa PE=3 SV=1 - [D3YWI1_MOUSE]	4.37	4.37
Protein PRRC2A OS=Mus musculus GN=Prrc2a PE=4 SV=1 - [G3UX48_MOUSE]	1.02	4.62
Tubulin alpha-4A chain OS=Mus musculus GN=Tuba4a PE=1 SV=1 - [TBA4A_MOUSE]	6.14	1.36
Leydig cell tumor 10 kDa protein homolog OS=Mus musculus GN=D8Ertd738e PE=2 SV=1 - [L10K_MOUSE]	1.33	0.70
Protein Znf512b OS=Mus musculus GN=Znf512b PE=4 SV=1 - [B7ZCR6_MOUSE]	3.14	0.87
Probable ATP-dependent RNA helicase DDX17 OS=Mus musculus GN=Ddx17 PE=2 SV=1 - [DDX17_MOUSE]	0.87	1.55
Ribonuclease P protein subunit p38 OS=Mus musculus GN=Rpp38 PE=4 SV=1 - [A2AJG0_MOUSE]	0.59	0.68
Ribosome biogenesis regulatory protein homolog OS=Mus musculus GN=Rrs1 PE=2 SV=1 - [RRS1_MOUSE]	0.79	4.00
Serine/threonine-protein phosphatase 6 regulatory ankyrin repeat subunit B OS=Mus musculus GN=Ankrd44 PE=2 SV=1 - [ANR44_MOUSE]	0.62	3.78
Sphingosine-1-phosphate phosphatase 1 OS=Mus musculus GN=Sgpp1 PE=1 SV=1 - [SGPP1_MOUSE]	0.81	1.10
T-complex protein 1 subunit alpha OS=Mus musculus GN=Tcp1 PE=1 SV=3 - [TCPA_MOUSE]	0.65	0.56

Interestingly, CD3 and LCP2 (Slp76) were associated with Ezh2 in T cells, confirming our previous finding that Ezh2 is associated with the TCR complex. Our analysis identified 46 proteins that had increased interaction with Ezh2 after stimulation and 14 out of 46 proteins had decreased interaction in the presence of GSK503 (Figure 5.9 and Table 5.1). Collectively, these data suggest that Ezh2-mediated lysine methylation modulates TCR-dependent interaction with cPRC2. Also, together with Nck methylation, multiple methylation sites render cPRC2 into a signaling scaffold to assemble a macromolecular complex (Figure 5.10). Once GSK503 inhibits methylation, the complex is no longer properly assembled and signaling is defective.

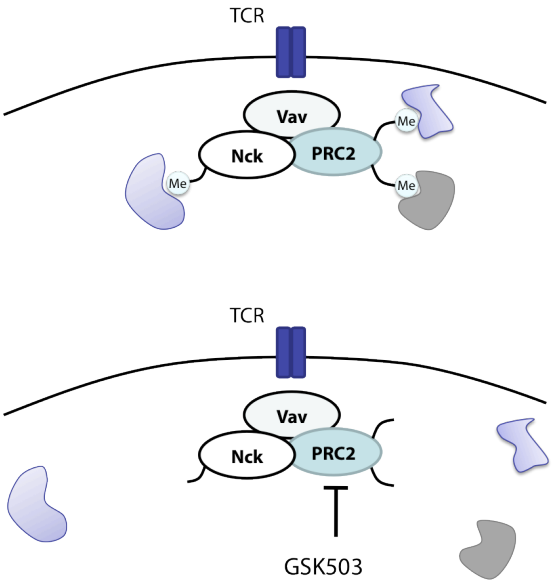

Figure 5.10. Model of the function of cPRC2 in protein complex formation cPRC2 contains multiple lysine residues, including Nck K64, Ezh2 K735 and Jarid2 K116, which can undergo methylation. Ezh2-mediated methylation is important for the recruitment of multiple biding partners to assemble signaling complex. Ezh2 inhibition blocks the generation of docking sites, thereby, impairs the complex formation.

Lastly, we also attempted to address the contribution of Vav1 to the Ezh2 interactome upon TCR stimulation. Interaction between Vav1 and Ezh2 has implicated for its functional importance in Talin1 methylation in dendritic cells (Gunawan et al., 2015). The proposed mechanism of methylation states that Vav1 recruits Ezh2 to its substrates. Therefore, for some substrates, Vav1 deficiency would lead to the loss of methylation, mimicking Ezh2 inhibition, resulting in the loss of interaction with cPRC2. We hypothesized that Vav1 deficiency may alter the Ezh2 interactome after TCR stimulation. To examine the Ezh2 interactome in Vav1 deficient T cells, we used the J.Vav Jurkat cell line, which lacks Vav1. First, we confirm that the cPRC2 complex in Jurkat cells contains all the previously identified components including

Ezh1, Ezh2, Suz12, Eed, RbAp46/48, AEBP2, Jarid2, and MTF2 (Figure 5.11). In Jurkat cells, we could identify two more complex components, are PHF1 and PHF19. 247 proteins were enriched in Nck-IP from unstimulated cells. Among those, 28 proteins had increased interactions with Ezh2 and 27 proteins had reduced interactions. When we analyzed the whole list, 44 proteins interact with Ezh2 upon stimulation in wild-type Jurkat cells. By comparing proteins that increase their association with Ezh2 after TCR stimulation in wild-type Jurkat cells but not Vav1 deficient Jurkat we were able to identify proteins whose interaction is TCR-induced and controlled by Vav1. 28 proteins met these criteria (Table 5.2). This list includes several cytoskeleton-related proteins such CKAP2L and tropomyosin, confirming that Ezh2 is involved in cytoskeleton remodeling in the context of interaction with Vav1. Notably, one of the key cell death molecules, BID was associated with Ezh2 upon stimulation only in wild-type cell. This may explain how Ezh2 regulates cell survival in tumor cells. Also, interaction with the important TCR signaling molecule calreticulin with Ezh2 is increased upon stimulation in wild-type Jurkat while the interaction was not induced in Vav1 KO cells. In summary, these data show that the TCR dependent Ezh2 interactome is regulated by Vav1.

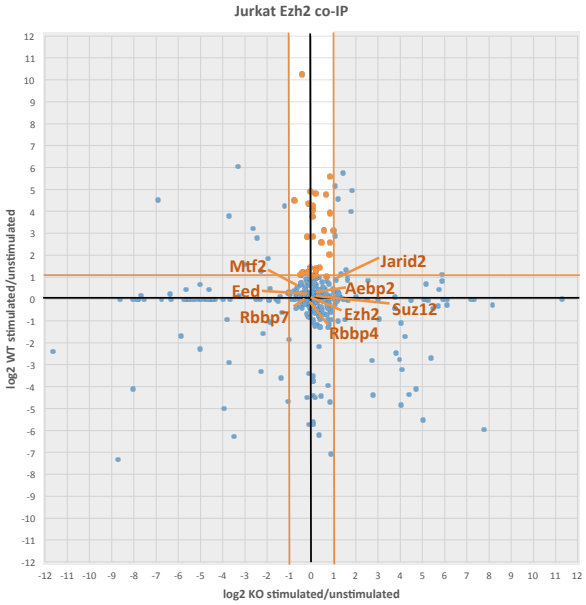

Figure 5.11. The Ezh2 interactome is modulated by Vav1 deficiency upon TCR stimulation Ezh2 was pulled down from wild-type Jurkat cells (WT) and the Vav1 deficient Jurkat cell line J.vav (KO), followed by mass spectrometric analysis of interaction partners. Each dot represents the normalized log2 value of the peptide abundance in Ezh2 IP from stimulated wild-type Jurkat cells/unstimulated wild-type Jurkat cells (y-axis) and Ezh2 IP from stimulated J.Vav cells/unstimulated J.Vav cells (x-axis). The bright area indicates proteins increased in wild-type cells after stimulation but unchanged in J.Vav cells upon stimulation. IgG IP was used for filtering parameter and ribosomal proteins and keratins were removed from the list.

One of the striking things we found here was that Ezh2 IP from any of the Jurkat samples contained Ezh1 whereas all the samples for primary CD4 T cells did have Ezh1 in the list of proteins interacting with Ezh2. Perhaps, this observation implies that there is a different function of Ezh1-PRC2 in Jurkat cells than in primary T cells. For example, in primary T cells, Ezh1-PRC2 and Ezh2-PRC2 may exist in a dimer while Jurkat cells have separate Ezh1-PRC2 and Ezh2-PRC2 complexes. The functional difference of these complexes will be worthwhile studying.

Table 5.2. List of proteins with increased interaction with Ezh2 in wild-type cells after TCR stimulation but unchanged interaction with Ezh2 in J.Vav cells

Description	stim/unstim J.Vav	stim/unstim WT
Calreticulin OS=Homo sapiens GN=CALR PE=1 SV=1 - [CALR_HUMAN]	0.94	3.14
Myosin regulatory light chain 12A OS=Homo sapiens GN=MYL12A PE=1 SV=2 - [ML12A_HUMAN]	0.65	1.05
Isoform Short of 14-3-3 protein beta/alpha OS=Homo sapiens GN=YWHAB - [1433B_HUMAN]	0.14	1.11
Isoform 2 of Heterogeneous nuclear ribonucleoprotein A1 OS=Homo sapiens GN=HNRNPA1 - [ROA1_HUMAN]	-0.03	1.09
Probable ATP-dependent RNA helicase DDX46 OS=Homo sapiens GN=DDX46 PE=1 SV=2 - [DDX46_HUMAN]	0.79	3.94
Tetratricopeptide repeat protein 1 OS=Homo sapiens GN=TTC1 PE=1 SV=1 - [TTC1_HUMAN]	-0.52	1.12
Tropomyosin 3 OS=Homo sapiens GN=TPM3 PE=2 SV=1 - [Q5VU59_HUMAN]	-0.44	1.25
Tropomyosin alpha-4 chain OS=Homo sapiens GN=TPM4 PE=1 SV=3 - [TPM4_HUMAN]	-0.11	1.47
Myosin light chain 6B OS=Homo sapiens GN=MYL6B PE=1 SV=1 - [MYL6B_HUMAN]	0.39	2.62
Isoform 2 of Uncharacterized protein C19orf47 OS=Homo sapiens GN=C19orf47 - [CS047_HUMAN]	-0.24	1.25
Importin subunit alpha-2 OS=Homo sapiens GN=KPNA2 PE=1 SV=1 - [IMA2_HUMAN]	0.14	1.40
Alanine--tRNA ligase, cytoplasmic OS=Homo sapiens GN=AARS PE=1 SV=2 - [SYAC_HUMAN]	0.00	2.86
Set1/Ash2 histone methyltransferase complex subunit ASH2 OS=Homo sapiens GN=ASH2L PE=4 SV=1 - [F5H8F7_HUMAN]	0.00	3.78
Isoform B of SWI/SNF-related matrix-associated actin-dependent regulator of chromatin subfamily B member 1 OS=Homo sapiens GN=SMARCB1 - [SNF5_HUMAN]	0.00	4.09
BH3-interacting domain death agonist OS=Homo sapiens GN=BID PE=1 SV=1 - [BID_HUMAN]	0.00	4.27
Myosin phosphatase Rho-interacting protein (Fragment) OS=Homo sapiens GN=MPRIP PE=4 SV=3 - [H0Y2S9_HUMAN]	-0.17	4.35
THO complex subunit 7 homolog OS=Homo sapiens GN=THOC7 PE=1 SV=3 - [THOC7_HUMAN]	0.80	2.59
Ran GTPase-activating protein 1 OS=Homo sapiens GN=RANGAP1 PE=1 SV=1 - [RAGP1_HUMAN]	0.51	3.17
Isoform 2 of Supervillin OS=Homo sapiens GN=SVIL - [SVIL_HUMAN]	0.00	1.07
RNA-binding protein with serine-rich domain 1 OS=Homo sapiens GN=RNPS1 PE=4 SV=1 - [H3BV80_HUMAN]	0.16	1.32
Dolichol-phosphate mannosyltransferase OS=Homo sapiens GN=DPM1 PE=1 SV=1 - [DPM1_HUMAN]	0.14	4.84
Cytoskeleton-associated protein 2-like OS=Homo sapiens GN=CKAP2L PE=1 SV=4 - [CKP2L_HUMAN]	-0.10	4.92
Mitotic spindle-associated MMXD complex subunit MIP18 OS=Homo sapiens GN=FAM96B PE=1 SV=1 - [MIP18_HUMAN]	0.79	5.61
Isoform 2 of ATP-citrate synthase OS=Homo sapiens GN=ACLY - [ACLY_HUMAN]	-0.47	10.28
Vacuolar protein sorting-associated protein 26B OS=Homo sapiens GN=VPS26B PE=4 SV=1 - [E9PRT4_HUMAN]	-0.82	4.54
Protein FRG1 OS=Homo sapiens GN=FRG1 PE=1 SV=1 - [FRG1_HUMAN]	0.60	4.80
Hematopoietic lineage cell-specific protein OS=Homo sapiens GN=HCLS1 PE=4 SV=1 - [E7EVW7_HUMAN]	-0.26	2.86
Isoform 10 of Serine/threonine-protein kinase MARK2 OS=Homo sapiens GN=MARK2 - [MARK2_HUMAN]	0.76	2.05

Lastly, we found that both unstimulated and stimulated Vav1 deficient cells lacked the association between Ezh2 and CD3ε. These data strongly suggest that Vav1 regulates the association of Ezh2 with the TCR.

5.7 Conclusions

In this chapter, we mainly discussed the mechanistic perspectives of cPRC2 in T cells. We identified two novel substrates, Nck1 and Ezh2, and their methylation sites. In addition, we showed that Nck interacting proteins contain methyltransferase activity. Our proteomic analysis suggests that Ezh2-mediated lysine methylation modulates protein-protein interactions and inhibition of methyltransferase activity

during TCR stimulation alters the interactome of its substrates. Although we proved many aspects of the function of Ezh2-mediated methylation, it might be interesting to test the biological consequence of mutating those lysine residues.

CHAPTER 6: DISCUSSION

In this study, we have explored the cytosolic role of PRC2 in TCR-mediated T cell activation. We showed that PRC2 plays an essential role in TCR-mediated T cell proliferation. In our PRC2 deficient mouse model, peripheral T cells retain wild-type levels of histone modifications and normal gene expression. However, PRC2 deficient T cells showed a signaling defect, independent of its function on histone modification, underscoring the direct impact of PRC2 in signaling events. This observation was substantiated by the use of pharmacological inhibitors of PRC2 targeting its catalytic activity. In addition, we found that cPRC2 was composed of known core components and identified cytosolic interaction partners such as Nck1 and Vav1. Importantly, Ezh2 was associated with the TCR, indicating the direct role of PRC2 for TCR-induced signaling events. In order to understand the molecular mechanism of cPRC2 function in signaling, we relied on proteomic analysis to identify interacting partners in the cytosol as well as the ability of cPRC2 to methylate substrates. We found that cPRC2 function in signaling was mediated by the methylation of its cytosolic substrate, Nck1. Along with Nck1, Ezh2 was self-methylated and these multiple methylation events may regulate protein-protein interactions during stimulation. In conclusion, cPRC2-mediated lysine methylation modulates signaling in T cells by regulating the interactions between Nck1 and Ezh2. We envision a model where cPRC2 may form a macromolecular signaling complex that depends on lysine methylation.

6.1 PRC2 controls T cell proliferation through cytosolic signaling

We showed that genetic ablation or pharmacological inhibition of PRC2 activity leads to a severe defect in T cell proliferation. Several *in vitro* and *in vivo* studies have shown that deletion of Ezh2 causes a reduction in the number of effector T cells and fail to expand in long-term cultures (Yang et al., 2015; Zhang et al., 2014). These reports related the lack of T cell expansion to gene dysregulation by the impairment of PRC2-mediated H3K27me3. In contrast, we show that the impaired proliferation is due to defective signaling. Indeed, we also observed that induction of H3K4 tri-methylation in several genes was significantly reduced in PRC2-deficient T cell upon TCR stimulation. However, H3K4 tri-methylation is not governed by nuclear function of PRC2. Therefore, we concluded that failure of H3K4 tri-methylation induction is due to reduction in signaling capacity. The genes that had the most significant reduction in H3K4 tri-methylation level include *Il2* and *Il2rα*, which are highly relevant to T cell proliferation and survival.

We found that PRC2 deficient T cells had the defective induction of Erk phosphorylation upon TCR stimulation. Since Erk signaling is important for T cell proliferation (D'Souza et al., 2008), the impaired Erk signaling may explain the proliferation defect in PRC2 deficient T cells. Regarding the defect in TCR-induced Erk phosphorylation, one can argue that PRC2 deficient T cells had the developmentally accumulated defect related to Erk activation. Most importantly, we came up with the key argument by using pharmacological inhibitor. Using pharmacological inhibitors ruled out the possible contribution of developmentally accumulated effect to the signaling defect we have seen. Moreover, PMA-induced

signaling was not impaired in the presence of the PRC2 inhibitor, strongly pointing out that PRC2 is involved in specific signaling pathway. Also, the fact that PRC2 deficiency and PRC2 inhibitors did not affect tyrosine phosphorylation events further excluded the potential non-specific behavior of the inhibitor on TCR signaling. All of these evidences suggest that PRC2 plays an essential role in TCR-mediated T cell proliferation by directly controlling signaling pathway. The further study to connect Erk signaling defect to failure of *in vivo* T cell expansion in PRC2 deficient mice requires us to examine the levels of Erk phosphorylation in T cell population.

6.2 Placement of PRC2 in TCR-induced Erk signaling pathway

TCR signaling pathway strongly activates the Erk pathway. PRC2 inhibition did not disrupted PLCγ1 phosphorylation, indicating it controls signaling downstream of PLCγ1. Intact PMA-induced Erk phosphorylation in the inhibitor treated cells further narrows down the potential position of PRC2 in Erk signaling pathway. However, since PLCγ1 is the enzyme responsible for DAG production, which PMA mimics, selective defect from PRC2 deficiency can be only explained by tyrosine phosphorylation independent regulation of PLCγ1 activity by PRC2 or PLCγ1-independent signaling pathway. Another possibility is that PKC fails to be recruited to the plasma membrane bound signaling cluster in PRC2 deficient T cells. Therefore, localized DAG production at the plasma membrane could not activate PKC but PMA treatment could overcome this lack of PKC activation. Assuming that cPRC2 and Vav are on the same pathway, cPRC2 may control membrane translocation of PKC through

Vav-mediated PKC translocation (Villalba et al., 2002; Villalba et al., 2000). When we examined the TCR-induced actin polymerization pathway that was controlled by Ezh2, Ezh2 plays a role upstream of Cdc42, but downstream of Vav tyrosine phosphorylation (Su et al., 2005). As mentioned earlier, Vav is immediately upstream of cdc42, therefore, there also must be an alternative regulatory function of Ezh2 that controls the enzymatic function of Vav independent of tyrosine phosphorylation. To dissect this model, it is necessary to examine the composition of the TCR signaling complex and localization of signaling mediators in the context of PRC2 deficient T cells.

6.3 Contribution of Ezh1 and Ezh2 to T cell immunity

Our *in vitro* and *in vivo* data had some discrepancy with regards to the T cell proliferation phenotype. Ezh2 KO T cells did not exhibit a defect in proliferation upon TCR stimulation *in vitro* while there was almost no expansion of antigen-specific T cells in Ezh2 knockout mice. Two lines of evidence can explain the contradicting results. First, the Ezh2 KO itself has defect in actin dynamics *in vivo* (Gunawan et al., 2015; Su et al., 2005), which can be overcomed by stimulation with anti-CD3/anti-CD28 antibodies. Our previous publication demonstrated that Ezh2 deficient T cells had a defect in APC:T cell conjugate formation. T cell :APC engagement would not be affected by PRC2 deficiency in a system using anti-CD3/anti-CD28 antibodies. To test this possibility, we imaged transgenic T cells with labeled OT-II transferred into RAG-/- mice, followed by immunization. Second, Ezh2 plays an unique role in

controlling death molecules while the signaling defect is only seen in the total absence of both Ezh1 and Ezh2. To validate whether the lack of effector T cells *in vivo* in the EZH2 KO mice can be attributed to cell death or a lack of proliferation, we transferred CFSE-labeled Ezh2 deficient T cells into RAG-/- and challenged the recipient mice with antigens. Probably, due to existence of the redundant enzyme, Ezh1, the phenotype is sensitive to concentration of stimuli and age of the mice that were used. Once both enzymes are ablated, the phenotype becomes more apparent regardless of other variables. A certain degree of redundancy of Ezh1 and Ezh2 in signaling is also further confirmed by Eed deficiency, which has a proliferation defect *in vitro*. Moreover, we have seen more dramatic reduction in TCR-induced Erk phosphorylation by treating GSK503 at the concentration that inhibits Ezh1. Therefore, Ezh1 as well as Ezh2 contribute to signaling.

We showed that Ezh2 up-regulation is much higher than Ezh1 in activated T cells. Although we could not quantify the absolute amount of Ezh1 and Ezh2 in T cells, it can be assumed that cells are differentially utilizing Ezh1 and Ezh2 based on activation status. For example, in resting T cells, Ezh1 plays a significant role in signaling while Ezh2 takes on the dominant role in activated T cells. An earlier report showing the interaction between Ezh1 and ZAP70 (Ogawa et al., 2003), highlights the signaling involvement of Ezh1. Therefore, both Ezh1 and Ezh2 seem to be involved in cytosolic signaling. However, distinct features of Ezh1 and Ezh2 enzymatic activity were reported. For histone, Ezh1 methyltransferase activity is lower than Ezh2 (Margueron et al., 2008). Therefore, one speculation is that activated T cells use Ezh2-PRC2 predominantly, presumably due to the requirement for the higher enzymatic

activity in the activated T cells. We do not know whether this is true for cytosolic substrates but it is likely that such switch system presents in cells. Also, this hypothetical model can explain the different outcomes from Ezh2 deficiency and Ezh1/2 deficiency. In other words, long-term culture *In vitro* or an *in vivo* situation that drives sustained proliferation with rapid expansion. In these situations, Ezh2 may become absolute requirements since cells would be largely relying on Ezh2-mediated cell proliferation rather than utilizing both enzymes.

6.4 Localization of PRC2 in cytosol

We have shown that Ezh2 is associated with TCR in this study. Ezh2 also interacts with the TCR signaling components Nck and Vav1. We also have shown in this study that Nck is required for optimal interaction between Ezh2 and Vav. Interestingly, Ezh2 association with CD3ε disappeared in Vav deficient cells, based on our mass spectrometric analysis. These pieces of data indicate that Ezh2 is localized with the TCR signaling cluster, through Nck that directly interacts with CD3ε and the Nck interacting protein Vav (Pauker and Barda-Saad, 2011; Santiveri et al., 2009). Therefore, it would be interesting if we find co-localization of those three proteins in T cells. To get more understanding how PRC2 is localized to TCR and signaling clusters, it may be necessary to monitor dynamic movement of Ezh2 by imaging techniques. Upon TCR stimulation, TCR initially forms microclusters. Whether PRC2 is included in the microcluster will bolster our argument that PRC2 directly controls TCR signaling in cytosol. Also, if we figure out which area of immunological synapse,

for instance, central supermolecular activation cluster (cSMAC) and peripheral SMAC (pSMAC), Ezh2 is localized to after TCR stimulation, we would be able to elucidate the detailed and specific role of PRC2 in actin skeleton remodeling and TCR signaling. Our preliminary results generated by immunofluorescence show that Ezh2 forms foci rather than diffused in cytosol of activated T cells. If it is reproducible, it strongly suggests that Ezh2 also gets into TCR microclusters and actively transduce the signaling.

6.5 Vav/Nck/Ezh2 complex formation

We have shown that Nck is required for optimal interaction between Vav1 and Ezh2 by co-immunoprecipitation experiments using shRNA-mediated knockdown cells lines. Two possible models exist to explain this result. The first model is that the interaction of Nck with Vav1 or Ezh2 facilitates/stabilize the interaction between Ezh2 and Vav1. Therefore, in this model, it is likely that Vav1, Nck and Ezh2 cooperatively interact with each other to form a trimeric complex. The second model is that the interaction between Vav1 and Ezh2 is indirect and bridged by Nck. In Nck knockdown cell line, the interaction is reduced but not abolished. Therefore, Nck most likely only stabilizes the interaction between Vav1 and Ezh2. But since the knockdown efficiency is not 100%, it is still possible that the remaining Nck can facilitate the interaction. A genetic deletion analysis can address this issue for sure.

6.6 Methylation of cytosolic substrates by PRC2

In our study, we put large efforts into the identification of cPRC2 substrates. We approached this using a candidate-based screening methodology. However, there are several unbiased screening methods for identifying methyltransferase substrates. Also, currently, lysine methylome is actively investigated and it is more obvious that many cellular proteins as well as histone proteins are methylated. One of techniques for approaching this problem is *in vitro* methyltransferase assay with protein arrays (Levy et al., 2011b). This method can give us lists of proteins directly methylated by PRC2. However, often protein arrays do not include all the proteins (>9000 proteins) and high chance to miss the real targets. Also, if the methyltransferase used in the assay is not specific but quite promiscuous, the result may not be recapitulated *in vivo*. For directly approaching to *in vivo* substrates of PRC2, we could pan-methyl lysine specific antibody to enrich the methylated proteins, followed by mass spectrometric analysis (Cao et al., 2013). However, there is weakness here as well since more abundant methylated proteins will be detected and less abundant methylated proteins will be missed. Therefore, filtering step is required to reduce mass spectrometric bias. Perhaps, crosslinking immunoprecipitation of Ezh2 may be helpful for this approach. Also, development of better pan-methyl lysine antibodies is required. We could not provide the stimulus dependent methylation in this study. In Jurkat cells, Nck proteins seem to be methylated even before stimulation. This result may explain why we could not inhibit TCR-induced Erk phosphorylation with the Ezh2 inhibitor in Jurkat cells. Moreover, taking account into low level of methylation in general, we need to develop

better tools to detect methylated Nck in primary T cells. For this purpose, it is necessary to develop anti-methyl Nck antibody.

6.7 Lysine methylation for signaling complex assembly

Our hypothesis is that Ezh2-mediated lysine methylation provides binding modules to cytosolic PRC2 itself to assemble the signaling complex. Indeed, protein-protein interactions related to Nck and Ezh2 were altered by inhibition of Ezh2. It would be interesting if we identify the exact binding partners of the methyl-lysines in Nck and Ezh2. To do so, we can design peptide interaction assays with unmethylated peptides and methylated peptides. For instance, we could incubate T cell lysates with Nck1 K64me1 and K64me0 peptides and examine which proteins come with each peptide, and compare the list. In this way, we would be able to find novel methyl binding proteins.

Our hypothetical model favors TCR-induced lysine methylation and TCR-dependent assembly of a signaling complex controlled by the methylation. The question is how to combine two elements above. The possible mechanism of TCR-dependent assembly of a large signaling complex by PRC2-mediated methylation is the post-translational modification of PRC2 by phosphorylation. The interaction between ZAP-70 and Ezh1 is regulated by phosphorylation of Ezh1 by Lck (Ogawa et al., 2003). This study shows that TCR-dependent signaling pathway actually assembles a signaling complex with PRC2. Additionally, the phosphorylation of Ezh2 was shown to regulate its methyltransferase activity (Cha et al., 2005; Kaneko et al.,

2010; Kim et al., 2013). These studies collectively point out that the activity and interaction with signaling molecules of PRC2 can be regulated by signal-dependent phosphorylation events. Therefore, in our study, phosphorylation of PRC2 components upon TCR stimulation may enhance methylation of its substrates as well as binding to TCR signaling complex.

This study focuses on a novel signaling paradigm that relies on lysine methylation for signaling. Discovery of demethylase (Shi et al., 2004) implicates that lysine methylation may be highly dynamic. Interestingly, our proteomic analysis of Ezh2-IP reveals that LSD1 is associated with Ezh2 before and after TCR stimulation (Figure 5.9 and 5.11). It suggests the possible demethylation on Ezh2 and its targets. Therefore, lysine methyltransferase activity and demethylase activity of PRC2-associated complex may be regulated by stimulation. It is of interest to figure out the dynamics of lysine methylation and address whether there is a turn-off system like phosphatases in phosphorylation cascades although finding demethylases is extremely hard. Our data suggest that initiation of TCR-induced lysine methylation is at least earlier than threonine phosphorylation of Erk, while we do not have any clue for the duration of lysine methylation. Dissection of dynamics of signal-induced lysine methylation will shed light on many aspects of lysine methylation in signaling.

6.8 Involvement of PRC2 in receptor signaling other than TCR signaling

One of the exceptional questions regarding signaling involvement of PRC2 is whether Ezh2 controls signaling downstream of a broad range of cell surface receptors

or specifically of TCR. Previously, several reports suggest that Ezh2 controls non-TCR receptor-mediated signaling events. For example, Ezh2 plays a crucial role in PDGF-induced actin polymerization in MEFs (Su et al., 2005). Also, there was a report showing the reduced FGFR-mediated Erk phosphorylation in Ezh2-deficient ES cells (Tee et al., 2014). Also, it was shown that Ezh2 regulates an integrin-mediated signaling pathway in actin dynamics (Gunawan et al., 2015). Therefore, it seems that the control of receptor-mediated signaling by Ezh2 is universal biological process, rather than the TCR specific phenomenon. As T cell proliferation and survival is also regulated by various cytokine signaling such as IL-2, IL-7 and IL-15, it is of interest to dissect the contribution of PRC2 to cytokine signaling pathways. Particularly, in in vivo autoimmune setting, where cytokines are also largely responsible for T cell expansion, it is possible that loss of Ezh2 leads to amelioration in T cell mediated autoimmune syndrome. In addition to autoimmune settings, T cell driven intestinal inflammation is depending on cytokines as well as microbiome-specific TCR. Therefore, to understand the precise mechanisms by which PRC2 controls T cell immunity *in vivo*, it is essential to address the potential involvement of PRC2 in cytokine signaling pathways.

In this regard, the role of PRC2 in memory T cell response is also an interesting subject. Memory T cells are maintained largely by cytokines. Interestingly, Ezh2 was shown to be important for STAT3 signaling, which can be activated by various cytokines (2013; Dasgupta et al., 2015; Kim et al., 2013). Of note, IL-21-IL-10-STAT3 signaling axis plays a pivotal role in maintenance of memory T cells (Cui et al., 2011). To test the impact of PRC2 on memory T cells, we should be able to

control the timing of Ezh2 inhibition. It can be achieved by utilizing either Cre-ERT2 driven deletion of Ezh2 or pharmacological inhibitions of Ezh2. In summary, studying the role of PRC2 in regulation of cytokine signaling pathways or other receptor signaling pathways will further deepen our understanding of actions of PRC2 *in vivo*. Also, it will help us to develop the therapeutic strategies for treating autoimmune syndromes or adverse effects from anti-tumor immunotherapy with Ezh2 inhibitors.

6.9 Therapeutic implications of PRC2 inhibition

Our work unveiled a novel role of PRC2 in T cell immunity and given that PRC2 activity can be modulated with small molecules, it is an attractive candidate for therapeutic treatment to ameliorate T cell mediated pathogenesis. Indeed, we generated data that Ezh2 inhibition is effective in the treatment of autoimmunity. We tested the therapeutic efficacy of PRC2 inhibition in two different pathological settings, regulatory T cell (Treg) depletion induced inflammation and experimental autoimmune encephalomyelitis (EAE). We depleted Tregs using the previously described $Foxp^{DTR}$ mice with the use of diphtheria toxin which resulted in lymphoproliferative disease (Kim et al., 2007). We treated GSK503 to Treg depleted mice for two weeks and observed that the autoimmune syndrome characterized by lymphadenopathy and splenomegaly disappeared upon GSK503 treatement. Similarly, the symptoms of EAE mice were ameliorated by GSK503 treatment. We treated mice with GSK503 after EAE induction. Compared to solvent treated mice, GSK503 treated mice showed significantly alleviated disease progression. Interestingly, resting cells

were not affected by the drug administration. These data strongly indicate the potential usage of PRC2 inhibitors in stopping unwanted inflammation. In this sense, Ezh2 inhibitors could be used as a drug to treat the autoimmune side effect from immune checkpoint blockade (Weber et al., 2012). However, the timing and specificity of the therapeutic strategies should be considered carefully so that patients would be still benefit from checkpoint blockade without any immunocompromised disease.

Mechanistically, one of the main caveats of *in vivo* experiments using the Ezh2 inhibitor was that it is difficult to distinguish between the impact of Ezh2 inhibition on T cells and other immune cell subsets such as dendritic cells. To bolster our arguments that Ezh2 inhibitors dampened immune responses mainly by controlling T cell expansion, we could treat T cell specific Ezh2 conditional knockout mice with Ezh2 inhibitors for *in vivo* experiments. Then, we can score an additional effect on immune responses, presumably non-T cell subsets, although T cell specific deletion is already dramatically reduced the degree of T cell responses in virus infection models and autoimmune models. By precisely understanding the contribution of the inhibitor to T cell immunity, we could better assess the inhibitor as a therapeutic tool for T cell-mediated autoimmune syndromes.

BIBLIOGRAPHY

(2013). Methylation by EZH2 activates STAT3 in glioblastoma. Cancer discovery *3*, OF21.

Agger, K., Cloos, P.A., Christensen, J., Pasini, D., Rose, S., Rappsilber, J., Issaeva, I., Canaani, E., Salcini, A.E., and Helin, K. (2007). UTX and JMJD3 are histone H3K27 demethylases involved in HOX gene regulation and development. Nature *449*, 731-734.

Aghazadeh, B., Lowry, W.E., Huang, X.Y., and Rosen, M.K. (2000). Structural basis for relief of autoinhibition of the Dbl homology domain of proto-oncogene Vav by tyrosine phosphorylation. Cell *102*, 625-633.

Ahmed, R., Salmi, A., Butler, L.D., Chiller, J.M., and Oldstone, M.B. (1984). Selection of genetic variants of lymphocytic choriomeningitis virus in spleens of persistently infected mice. Role in suppression of cytotoxic T lymphocyte response and viral persistence. The Journal of experimental medicine *160*, 521-540.

Alberola-Ila, J., Forbush, K.A., Seger, R., Krebs, E.G., and Perlmutter, R.M. (1995). Selective requirement for MAP kinase activation in thymocyte differentiation. Nature *373*, 620-623.

Ambler, R.P., and Rees, M.W. (1959). Epsilon-N-Methyl-lysine in bacterial flagellar protein. Nature *184*, 56-57.

Anjum, R., and Blenis, J. (2008). The RSK family of kinases: emerging roles in cellular signalling. Nature reviews Molecular cell biology *9*, 747-758.

Arvey, A., van der Veeken, J., Samstein, R.M., Feng, Y., Stamatoyannopoulos, J.A., and Rudensky, A.Y. (2014). Inflammation-induced repression of chromatin bound by the transcription factor Foxp3 in regulatory T cells. Nature immunology *15*, 580-587.

Baier-Bitterlich, G., Uberall, F., Bauer, B., Fresser, F., Wachter, H., Grunicke, H., Utermann, G., Altman, A., and Baier, G. (1996). Protein kinase C-theta isoenzyme selective stimulation of the transcription factor complex AP-1 in T lymphocytes. Molecular and cellular biology *16*, 1842-1850.

Barber, E.K., Dasgupta, J.D., Schlossman, S.F., Trevillyan, J.M., and Rudd, C.E. (1989). The CD4 and CD8 antigens are coupled to a protein-tyrosine kinase (p56lck) that phosphorylates the CD3 complex. Proceedings of the National Academy of Sciences of the United States of America *86*, 3277-3281.

Barski, A., Cuddapah, S., Cui, K., Roh, T.Y., Schones, D.E., Wang, Z., Wei, G., Chepelev, I., and Zhao, K. (2007). High-resolution profiling of histone methylations in the human genome. Cell *129*, 823-837.

Beguelin, W., Popovic, R., Teater, M., Jiang, Y., Bunting, K.L., Rosen, M., Shen, H., Yang, S.N., Wang, L., Ezponda, T.*, et al.* (2013). EZH2 is required for germinal center formation and somatic EZH2 mutations promote lymphoid transformation. Cancer cell *23*, 677-692.

Bi, K., Tanaka, Y., Coudronniere, N., Sugie, K., Hong, S., van Stipdonk, M.J., and Altman, A. (2001). Antigen-induced translocation of PKC-theta to membrane rafts is required for T cell activation. Nature immunology *2*, 556-563.

Bladt, F., Aippersbach, E., Gelkop, S., Strasser, G.A., Nash, P., Tafuri, A., Gertler, F.B., and Pawson, T. (2003). The murine Nck SH2/SH3 adaptors are important for the development of mesoderm-derived embryonic structures and for regulating the cellular actin network. Molecular and cellular biology *23*, 4586-4597.

Bubeck Wardenburg, J., Pappu, R., Bu, J.Y., Mayer, B., Chernoff, J., Straus, D., and Chan, A.C. (1998). Regulation of PAK activation and the T cell cytoskeleton by the linker protein SLP-76. Immunity *9*, 607-616.

Bunnell, S.C., Diehn, M., Yaffe, M.B., Findell, P.R., Cantley, L.C., and Berg, L.J. (2000). Biochemical interactions integrating Itk with the T cell receptor-initiated signaling cascade. The Journal of biological chemistry *275*, 2219-2230.

Bustelo, X.R. (2000). Regulatory and signaling properties of the Vav family. Molecular and cellular biology *20*, 1461-1477.

Bustelo, X.R. (2001). Vav proteins, adaptors and cell signaling. Oncogene *20*, 6372-6381.

Cao, R., Wang, L., Wang, H., Xia, L., Erdjument-Bromage, H., Tempst, P., Jones, R.S., and Zhang, Y. (2002a). Role of histone H3 lysine 27 methylation in Polycomb-group silencing. Science *298*, 1039-1043.

Cao, X.J., Arnaudo, A.M., and Garcia, B.A. (2013). Large-scale global identification of protein lysine methylation in vivo. Epigenetics *8*, 477-485.

Cao, Y., Janssen, E.M., Duncan, A.W., Altman, A., Billadeau, D.D., and Abraham, R.T. (2002b). Pleiotropic defects in TCR signaling in a Vav-1-null Jurkat T-cell line. The EMBO journal *21*, 4809-4819.

Cha, T.L., Zhou, B.P., Xia, W., Wu, Y., Yang, C.C., Chen, C.T., Ping, B., Otte, A.P., and Hung, M.C. (2005). Akt-mediated phosphorylation of EZH2 suppresses methylation of lysine 27 in histone H3. Science *310*, 306-310.

Chan, A.C., Irving, B.A., Fraser, J.D., and Weiss, A. (1991). The zeta chain is associated with a tyrosine kinase and upon T-cell antigen receptor stimulation associates with ZAP-70, a 70-kDa tyrosine phosphoprotein. Proceedings of the National Academy of Sciences of the United States of America *88*, 9166-9170.

Chan, A.C., Iwashima, M., Turck, C.W., and Weiss, A. (1992). ZAP-70: a 70 kd protein-tyrosine kinase that associates with the TCR zeta chain. Cell *71*, 649-662.

Cho, H.S., Hayami, S., Toyokawa, G., Maejima, K., Yamane, Y., Suzuki, T., Dohmae, N., Kogure, M., Kang, D., Neal, D.E.*, et al.* (2012). RB1 methylation by SMYD2 enhances cell cycle progression through an increase of RB1 phosphorylation. Neoplasia *14*, 476-486.

Chuikov, S., Kurash, J.K., Wilson, J.R., Xiao, B., Justin, N., Ivanov, G.S., McKinney, K., Tempst, P., Prives, C., Gamblin, S.J.*, et al.* (2004). Regulation of p53 activity through lysine methylation. Nature *432*, 353-360.

Clipstone, N.A., and Crabtree, G.R. (1992). Identification of calcineurin as a key signalling enzyme in T-lymphocyte activation. Nature *357*, 695-697.

Costello, P.S., Walters, A.E., Mee, P.J., Turner, M., Reynolds, L.F., Prisco, A., Sarner, N., Zamoyska, R., and Tybulewicz, V.L. (1999). The Rho-family GTP exchange factor Vav is a critical transducer of T cell receptor signals to the calcium, ERK, and NF-kappaB pathways. Proceedings of the National Academy of Sciences of the United States of America *96*, 3035-3040.

Cui, W., Liu, Y., Weinstein, J.S., Craft, J., and Kaech, S.M. (2011). An interleukin-21-interleukin-10-STAT3 pathway is critical for functional maturation of memory CD8+ T cells. Immunity *35*, 792-805.

D'Souza, W.N., Chang, C.F., Fischer, A.M., Li, M., and Hedrick, S.M. (2008). The Erk2 MAPK regulates CD8 T cell proliferation and survival. J Immunol *181*, 7617-7629.

Dasgupta, M., Dermawan, J.K., Willard, B., and Stark, G.R. (2015). STAT3-driven transcription depends upon the dimethylation of K49 by EZH2. Proceedings of the National Academy of Sciences of the United States of America *112*, 3985-3990.

Deak, M., Clifton, A.D., Lucocq, L.M., and Alessi, D.R. (1998). Mitogen- and stress-activated protein kinase-1 (MSK1) is directly activated by MAPK and SAPK2/p38, and may mediate activation of CREB. The EMBO journal *17*, 4426-4441.

Dillon, S.C., Zhang, X., Trievel, R.C., and Cheng, X. (2005). The SET-domain protein superfamily: protein lysine methyltransferases. Genome biology *6*, 227.

Dobenecker, M.W., Kim, J.K., Marcello, J., Fang, T.C., Prinjha, R., Bosselut, R., and Tarakhovsky, A. (2015). Coupling of T cell receptor specificity to natural killer T cell

development by bivalent histone H3 methylation. The Journal of experimental medicine *212*, 297-306.

Downward, J., Graves, J.D., Warne, P.H., Rayter, S., and Cantrell, D.A. (1990). Stimulation of p21ras upon T-cell activation. Nature *346*, 719-723.

DuPage, M., Chopra, G., Quiros, J., Rosenthal, W.L., Morar, M.M., Holohan, D., Zhang, R., Turka, L., Marson, A., and Bluestone, J.A. (2015). The chromatin-modifying enzyme Ezh2 is critical for the maintenance of regulatory T cell identity after activation. Immunity *42*, 227-238.

Ebinu, J.O., Bottorff, D.A., Chan, E.Y., Stang, S.L., Dunn, R.J., and Stone, J.C. (1998). RasGRP, a Ras guanyl nucleotide- releasing protein with calcium- and diacylglycerol-binding motifs. Science *280*, 1082-1086.

Eissenberg, J.C., Morris, G.D., Reuter, G., and Hartnett, T. (1992). The heterochromatin-associated protein HP-1 is an essential protein in Drosophila with dosage-dependent effects on position-effect variegation. Genetics *131*, 345-352.

Eskeland, R., Leeb, M., Grimes, G.R., Kress, C., Boyle, S., Sproul, D., Gilbert, N., Fan, Y., Skoultchi, A.I., Wutz, A.*, et al.* (2010). Ring1B compacts chromatin structure and represses gene expression independent of histone ubiquitination. Molecular cell *38*, 452-464.

Fasolato, C., Hoth, M., and Penner, R. (1993). A GTP-dependent step in the activation mechanism of capacitative calcium influx. The Journal of biological chemistry *268*, 20737-20740.

Faust, C., Schumacher, A., Holdener, B., and Magnuson, T. (1995). The eed mutation disrupts anterior mesoderm production in mice. Development *121*, 273-285.

Fischle, W., Tseng, B.S., Dormann, H.L., Ueberheide, B.M., Garcia, B.A., Shabanowitz, J., Hunt, D.F., Funabiki, H., and Allis, C.D. (2005). Regulation of HP1-chromatin binding by histone H3 methylation and phosphorylation. Nature *438*, 1116-1122.

Fischle, W., Wang, Y., and Allis, C.D. (2003). Binary switches and modification cassettes in histone biology and beyond. Nature *425*, 475-479.

Gil, D., Schamel, W.W., Montoya, M., Sanchez-Madrid, F., and Alarcon, B. (2002). Recruitment of Nck by CD3 epsilon reveals a ligand-induced conformational change essential for T cell receptor signaling and synapse formation. Cell *109*, 901-912.

Gunawan, M., Venkatesan, N., Loh, J.T., Wong, J.F., Berger, H., Neo, W.H., Li, L.Y., La Win, M.K., Yau, Y.H., Guo, T.*, et al.* (2015). The methyltransferase Ezh2 controls cell adhesion and migration through direct methylation of the extranuclear regulatory protein talin. Nature immunology *16*, 505-516.

Hartsough, E.J., Meyer, R.D., Chitalia, V., Jiang, Y., Marquez, V.E., Zhdanova, I.V., Weinberg, J., Costello, C.E., and Rahimi, N. (2013). Lysine methylation promotes VEGFR-2 activation and angiogenesis. Science signaling *6*, ra104.

He, A., Shen, X., Ma, Q., Cao, J., von Gise, A., Zhou, P., Wang, G., Marquez, V.E., Orkin, S.H., and Pu, W.T. (2012). PRC2 directly methylates GATA4 and represses its transcriptional activity. Genes & development *26*, 37-42.

Hirota, T., Lipp, J.J., Toh, B.H., and Peters, J.M. (2005). Histone H3 serine 10 phosphorylation by Aurora B causes HP1 dissociation from heterochromatin. Nature *438*, 1176-1180.

Hobert, O., Jallal, B., and Ullrich, A. (1996). Interaction of Vav with ENX-1, a putative transcriptional regulator of homeobox gene expression. Molecular and cellular biology *16*, 3066-3073.

Hodge, C., Liao, J., Stofega, M., Guan, K., Carter-Su, C., and Schwartz, J. (1998). Growth hormone stimulates phosphorylation and activation of elk-1 and expression of c-fos, egr-1, and junB through activation of extracellular signal-regulated kinases 1 and 2. The Journal of biological chemistry *273*, 31327-31336.

Hogan, P.G., Chen, L., Nardone, J., and Rao, A. (2003). Transcriptional regulation by calcium, calcineurin, and NFAT. Genes & development *17*, 2205-2232.

Huang, J., Perez-Burgos, L., Placek, B.J., Sengupta, R., Richter, M., Dorsey, J.A., Kubicek, S., Opravil, S., Jenuwein, T., and Berger, S.L. (2006). Repression of p53 activity by Smyd2-mediated methylation. Nature *444*, 629-632.

Huang, J., Sengupta, R., Espejo, A.B., Lee, M.G., Dorsey, J.A., Richter, M., Opravil, S., Shiekhattar, R., Bedford, M.T., Jenuwein, T.*, et al.* (2007). p53 is regulated by the lysine demethylase LSD1. Nature *449*, 105-108.

Huang, W., Alessandrini, A., Crews, C.M., and Erikson, R.L. (1993). Raf-1 forms a stable complex with Mek1 and activates Mek1 by serine phosphorylation. Proceedings of the National Academy of Sciences of the United States of America *90*, 10947-10951.

Jain, J., Loh, C., and Rao, A. (1995). Transcriptional regulation of the IL-2 gene. Current opinion in immunology *7*, 333-342.

Jenuwein, T., and Allis, C.D. (2001). Translating the histone code. Science *293*, 1074-1080.

Kamminga, L.M., Bystrykh, L.V., de Boer, A., Houwer, S., Douma, J., Weersing, E., Dontje, B., and de Haan, G. (2006). The Polycomb group gene Ezh2 prevents hematopoietic stem cell exhaustion. Blood *107*, 2170-2179.

Kaneko, S., Li, G., Son, J., Xu, C.F., Margueron, R., Neubert, T.A., and Reinberg, D. (2010). Phosphorylation of the PRC2 component Ezh2 is cell cycle-regulated and up-regulates its binding to ncRNA. Genes & development *24*, 2615-2620.

Katzav, S., Sutherland, M., Packham, G., Yi, T., and Weiss, A. (1994). The protein tyrosine kinase ZAP-70 can associate with the SH2 domain of proto-Vav. The Journal of biological chemistry *269*, 32579-32585.

Kim, E., Kim, M., Woo, D.H., Shin, Y., Shin, J., Chang, N., Oh, Y.T., Kim, H., Rheey, J., Nakano, I.*, et al.* (2013). Phosphorylation of EZH2 activates STAT3 signaling via STAT3 methylation and promotes tumorigenicity of glioblastoma stem-like cells. Cancer cell *23*, 839-852.

Kim, J.M., Rasmussen, J.P., and Rudensky, A.Y. (2007). Regulatory T cells prevent catastrophic autoimmunity throughout the lifespan of mice. Nature immunology *8*, 191-197.

Kishimoto, A., Takai, Y., Mori, T., Kikkawa, U., and Nishizuka, Y. (1980). Activation of calcium and phospholipid-dependent protein kinase by diacylglycerol, its possible relation to phosphatidylinositol turnover. The Journal of biological chemistry *255*, 2273-2276.

Konze, K.D., Ma, A., Li, F., Barsyte-Lovejoy, D., Parton, T., Macnevin, C.J., Liu, F., Gao, C., Huang, X.P., Kuznetsova, E.*, et al.* (2013). An orally bioavailable chemical probe of the Lysine Methyltransferases EZH2 and EZH1. ACS chemical biology *8*, 1324-1334.

Kornberg, R.D. (1974). Chromatin structure: a repeating unit of histones and DNA. Science *184*, 868-871.

Kouzarides, T. (2007). Chromatin modifications and their function. Cell *128*, 693-705.

Koyanagi, M., Baguet, A., Martens, J., Margueron, R., Jenuwein, T., and Bix, M. (2005). EZH2 and histone 3 trimethyl lysine 27 associated with Il4 and Il13 gene silencing in Th1 cells. The Journal of biological chemistry *280*, 31470-31477.

Kurash, J.K., Lei, H., Shen, Q., Marston, W.L., Granda, B.W., Fan, H., Wall, D., Li, E., and Gaudet, F. (2008). Methylation of p53 by Set7/9 mediates p53 acetylation and activity in vivo. Molecular cell *29*, 392-400.

Lee, J.M., Lee, J.S., Kim, H., Kim, K., Park, H., Kim, J.Y., Lee, S.H., Kim, I.S., Kim, J., Lee, M.*, et al.* (2012). EZH2 generates a methyl degron that is recognized by the DCAF1/DDB1/CUL4 E3 ubiquitin ligase complex. Molecular cell *48*, 572-586.

Lee, T.I., Johnstone, S.E., and Young, R.A. (2006). Chromatin immunoprecipitation and microarray-based analysis of protein location. Nature protocols *1*, 729-748.

Lettau, M., Pieper, J., Gerneth, A., Lengl-Janssen, B., Voss, M., Linkermann, A., Schmidt, H., Gelhaus, C., Leippe, M., Kabelitz, D.*, et al.* (2010). The adapter protein Nck: role of individual SH3 and SH2 binding modules for protein interactions in T lymphocytes. Protein science : a publication of the Protein Society *19*, 658-669.

Levy, D., Kuo, A.J., Chang, Y., Schaefer, U., Kitson, C., Cheung, P., Espejo, A., Zee, B.M., Liu, C.L., Tangsombatvisit, S.*, et al.* (2011a). Lysine methylation of the NF-kappaB subunit RelA by SETD6 couples activity of the histone methyltransferase GLP at chromatin to tonic repression of NF-kappaB signaling. Nature immunology *12*, 29-36.

Levy, D., Liu, C.L., Yang, Z., Newman, A.M., Alizadeh, A.A., Utz, P.J., and Gozani, O. (2011b). A proteomic approach for the identification of novel lysine methyltransferase substrates. Epigenetics & chromatin *4*, 19.

Lewis, E.B. (1978). A gene complex controlling segmentation in Drosophila. Nature *276*, 565-570.

Li, G., Margueron, R., Ku, M., Chambon, P., Bernstein, B.E., and Reinberg, D. (2010). Jarid2 and PRC2, partners in regulating gene expression. Genes & development *24*, 368-380.

Li, H., Fischle, W., Wang, W., Duncan, E.M., Liang, L., Murakami-Ishibe, S., Allis, C.D., and Patel, D.J. (2007). Structural basis for lower lysine methylation state-specific readout by MBT repeats of L3MBTL1 and an engineered PHD finger. Molecular cell *28*, 677-691.

Li, M.M., Nilsen, A., Shi, Y., Fusser, M., Ding, Y.H., Fu, Y., Liu, B., Niu, Y., Wu, Y.S., Huang, C.M.*, et al.* (2013). ALKBH4-dependent demethylation of actin regulates actomyosin dynamics. Nature communications *4*, 1832.

Liu, S.K., Fang, N., Koretzky, G.A., and McGlade, C.J. (1999). The hematopoietic-specific adaptor protein gads functions in T-cell signaling via interactions with the SLP-76 and LAT adaptors. Current biology : CB *9*, 67-75.

Margueron, R., Justin, N., Ohno, K., Sharpe, M.L., Son, J., Drury, W.J., 3rd, Voigt, P., Martin, S.R., Taylor, W.R., De Marco, V.*, et al.* (2009). Role of the polycomb protein EED in the propagation of repressive histone marks. Nature *461*, 762-767.

Margueron, R., Li, G., Sarma, K., Blais, A., Zavadil, J., Woodcock, C.L., Dynlacht, B.D., and Reinberg, D. (2008). Ezh1 and Ezh2 maintain repressive chromatin through different mechanisms. Molecular cell *32*, 503-518.

Maurer-Stroh, S., Dickens, N.J., Hughes-Davies, L., Kouzarides, T., Eisenhaber, F., and Ponting, C.P. (2003). The Tudor domain 'Royal Family': Tudor, plant Agenet, Chromo, PWWP and MBT domains. Trends in biochemical sciences *28*, 69-74.

Mazur, P.K., Reynoird, N., Khatri, P., Jansen, P.W., Wilkinson, A.W., Liu, S., Barbash, O., Van Aller, G.S., Huddleston, M., Dhanak, D.*, et al.* (2014). SMYD3 links lysine methylation of MAP3K2 to Ras-driven cancer. Nature *510*, 283-287.

Monks, C.R., Kupfer, H., Tamir, I., Barlow, A., and Kupfer, A. (1997). Selective modulation of protein kinase C-theta during T-cell activation. Nature *385*, 83-86.

Murray, K. (1964). The Occurrence of Epsilon-N-Methyl Lysine in Histones. Biochemistry *3*, 10-15.

Ngoenkam, J., Paensuwan, P., Preechanukul, K., Khamsri, B., Yiemwattana, I., Beck-Garcia, E., Minguet, S., Schamel, W.W., and Pongcharoen, S. (2014). Non-overlapping functions of Nck1 and Nck2 adaptor proteins in T cell activation. Cell communication and signaling : CCS *12*, 21.

O'Carroll, D., Erhardt, S., Pagani, M., Barton, S.C., Surani, M.A., and Jenuwein, T. (2001). The polycomb-group gene Ezh2 is required for early mouse development. Molecular and cellular biology *21*, 4330-4336.

Ogawa, M., Hiraoka, Y., and Aiso, S. (2003). The Polycomb-group protein ENX-2 interacts with ZAP-70. Immunology letters *86*, 57-61.

Paensuwan, P., Hartl, F.A., Yousefi, O.S., Ngoenkam, J., Wipa, P., Beck-Garcia, E., Dopfer, E.P., Khamsri, B., Sanguansermsri, D., Minguet, S.*, et al.* (2016). Nck Binds to the T Cell Antigen Receptor Using Its SH3.1 and SH2 Domains in a Cooperative Manner, Promoting TCR Functioning. J Immunol *196*, 448-458.

Pages, G., Guerin, S., Grall, D., Bonino, F., Smith, A., Anjuere, F., Auberger, P., and Pouyssegur, J. (1999). Defective thymocyte maturation in p44 MAP kinase (Erk 1) knockout mice. Science *286*, 1374-1377.

Pasini, D., Bracken, A.P., Jensen, M.R., Lazzerini Denchi, E., and Helin, K. (2004). Suz12 is essential for mouse development and for EZH2 histone methyltransferase activity. The EMBO journal *23*, 4061-4071.

Pauker, M.H., and Barda-Saad, M. (2011). Studies of novel interactions between Nck and VAV SH3 domains. Communicative & integrative biology *4*, 175-177.

Pawson, T. (1994). SH2 and SH3 domains in signal transduction. Advances in cancer research *64*, 87-110.

Pawson, T., and Gish, G.D. (1992). SH2 and SH3 domains: from structure to function. Cell *71*, 359-362.

Pereira, R.M., Martinez, G.J., Engel, I., Cruz-Guilloty, F., Barboza, B.A., Tsagaratou, A., Lio, C.W., Berg, L.J., Lee, Y., Kronenberg, M.*, et al.* (2014). Jarid2 is induced by TCR signalling and controls iNKT cell maturation. Nature communications *5*, 4540.

Richon, V.M., Johnston, D., Sneeringer, C.J., Jin, L., Majer, C.R., Elliston, K., Jerva, L.F., Scott, M.P., and Copeland, R.A. (2011). Chemogenetic analysis of human protein methyltransferases. Chemical biology & drug design *78*, 199-210.

Roy, E., Togbe, D., Holdorf, A.D., Trubetskoy, D., Nabti, S., Kublbeck, G., Klevenz, A., Kopp-Schneider, A., Leithauser, F., Moller, P.*, et al.* (2010). Nck adaptors are positive regulators of the size and sensitivity of the T-cell repertoire. Proceedings of the National Academy of Sciences of the United States of America *107*, 15529-15534.

Sampath, S.C., Marazzi, I., Yap, K.L., Sampath, S.C., Krutchinsky, A.N., Mecklenbrauker, I., Viale, A., Rudensky, E., Zhou, M.M., Chait, B.T.*, et al.* (2007). Methylation of a histone mimic within the histone methyltransferase G9a regulates protein complex assembly. Molecular cell *27*, 596-608.

Santiveri, C.M., Borroto, A., Simon, L., Rico, M., Alarcon, B., and Jimenez, M.A. (2009). Interaction between the N-terminal SH3 domain of Nck-alpha and CD3-epsilon-derived peptides: non-canonical and canonical recognition motifs. Biochimica et biophysica acta *1794*, 110-117.

Sanulli, S., Justin, N., Teissandier, A., Ancelin, K., Portoso, M., Caron, M., Michaud, A., Lombard, B., da Rocha, S.T., Offer, J.*, et al.* (2015). Jarid2 Methylation via the PRC2 Complex Regulates H3K27me3 Deposition during Cell Differentiation. Molecular cell *57*, 769-783.

Schuettengruber, B., Chourrout, D., Vervoort, M., Leblanc, B., and Cavalli, G. (2007). Genome regulation by polycomb and trithorax proteins. Cell *128*, 735-745.

Secrist, J.P., Karnitz, L., and Abraham, R.T. (1991). T-cell antigen receptor ligation induces tyrosine phosphorylation of phospholipase C-gamma 1. The Journal of biological chemistry *266*, 12135-12139.

Seger, R., Ahn, N.G., Posada, J., Munar, E.S., Jensen, A.M., Cooper, J.A., Cobb, M.H., and Krebs, E.G. (1992). Purification and characterization of mitogen-activated protein kinase activator(s) from epidermal growth factor-stimulated A431 cells. The Journal of biological chemistry *267*, 14373-14381.

Shaw, J.P., Utz, P.J., Durand, D.B., Toole, J.J., Emmel, E.A., and Crabtree, G.R. (1988). Identification of a putative regulator of early T cell activation genes. Science *241*, 202-205.

Shi, Y., Lan, F., Matson, C., Mulligan, P., Whetstine, J.R., Cole, P.A., Casero, R.A., and Shi, Y. (2004). Histone demethylation mediated by the nuclear amine oxidase homolog LSD1. Cell *119*, 941-953.

Strahl, B.D., and Allis, C.D. (2000). The language of covalent histone modifications. Nature *403*, 41-45.

Strahl, B.D., Ohba, R., Cook, R.G., and Allis, C.D. (1999). Methylation of histone H3 at lysine 4 is highly conserved and correlates with transcriptionally active nuclei in Tetrahymena. Proceedings of the National Academy of Sciences of the United States of America *96*, 14967-14972.

Su, I.H., Basavaraj, A., Krutchinsky, A.N., Hobert, O., Ullrich, A., Chait, B.T., and Tarakhovsky, A. (2003). Ezh2 controls B cell development through histone H3 methylation and Igh rearrangement. Nature immunology *4*, 124-131.

Su, I.H., Dobenecker, M.W., Dickinson, E., Oser, M., Basavaraj, A., Marqueron, R., Viale, A., Reinberg, D., Wulfing, C., and Tarakhovsky, A. (2005). Polycomb group protein ezh2 controls actin polymerization and cell signaling. Cell *121*, 425-436.

Takenawa, T., and Suetsugu, S. (2007). The WASP-WAVE protein network: connecting the membrane to the cytoskeleton. Nature reviews Molecular cell biology *8*, 37-48.

Tavares, L., Dimitrova, E., Oxley, D., Webster, J., Poot, R., Demmers, J., Bezstarosti, K., Taylor, S., Ura, H., Koide, H*., et al.* (2012). RYBP-PRC1 complexes mediate H2A ubiquitylation at polycomb target sites independently of PRC2 and H3K27me3. Cell *148*, 664-678.

Tee, W.W., Shen, S.S., Oksuz, O., Narendra, V., and Reinberg, D. (2014). Erk1/2 activity promotes chromatin features and RNAPII phosphorylation at developmental promoters in mouse ESCs. Cell *156*, 678-690.

Tumes, D.J., Onodera, A., Suzuki, A., Shinoda, K., Endo, Y., Iwamura, C., Hosokawa, H., Koseki, H., Tokoyoda, K., Suzuki, Y*., et al.* (2013). The polycomb protein Ezh2 regulates differentiation and plasticity of CD4(+) T helper type 1 and type 2 cells. Immunity *39*, 819-832.

Tuosto, L., Michel, F., and Acuto, O. (1996). p95vav associates with tyrosine-phosphorylated SLP-76 in antigen-stimulated T cells. The Journal of experimental medicine *184*, 1161-1166.

Turner, M., and Billadeau, D.D. (2002). VAV proteins as signal integrators for multi-subunit immune-recognition receptors. Nature reviews Immunology *2*, 476-486.

Vermillion, K.L., Lidberg, K.A., and Gammill, L.S. (2014). Cytoplasmic protein methylation is essential for neural crest migration. The Journal of cell biology *204*, 95-109.

Villalba, M., Bi, K., Hu, J., Altman, Y., Bushway, P., Reits, E., Neefjes, J., Baier, G., Abraham, R.T., and Altman, A. (2002). Translocation of PKC[theta] in T cells is mediated by a nonconventional, PI3-K- and Vav-dependent pathway, but does not absolutely require phospholipase C. The Journal of cell biology *157*, 253-263.

Villalba, M., Coudronniere, N., Deckert, M., Teixeiro, E., Mas, P., and Altman, A. (2000). A novel functional interaction between Vav and PKCtheta is required for TCR-induced T cell activation. Immunity *12*, 151-160.

Wagner, E.J., and Carpenter, P.B. (2012). Understanding the language of Lys36 methylation at histone H3. Nature reviews Molecular cell biology *13*, 115-126.

Wang, H., Wang, L., Erdjument-Bromage, H., Vidal, M., Tempst, P., Jones, R.S., and Zhang, Y. (2004). Role of histone H2A ubiquitination in Polycomb silencing. Nature *431*, 873-878.

Weber, J.S., Kahler, K.C., and Hauschild, A. (2012). Management of immune-related adverse events and kinetics of response with ipilimumab. Journal of clinical oncology : official journal of the American Society of Clinical Oncology *30*, 2691-2697.

Weiss, A., Koretzky, G., Schatzman, R.C., and Kadlecek, T. (1991). Functional activation of the T-cell antigen receptor induces tyrosine phosphorylation of phospholipase C-gamma 1. Proceedings of the National Academy of Sciences of the United States of America *88*, 5484-5488.

Wu, J., Motto, D.G., Koretzky, G.A., and Weiss, A. (1996). Vav and SLP-76 interact and functionally cooperate in IL-2 gene activation. Immunity *4*, 593-602.

Wurm, S., Zhang, J., Guinea-Viniegra, J., Garcia, F., Munoz, J., Bakiri, L., Ezhkova, E., and Wagner, E.F. (2015). Terminal epidermal differentiation is regulated by the interaction of Fra-2/AP-1 with Ezh2 and ERK1/2. Genes & development *29*, 144-156.

Yang, S.H., Shore, P., Willingham, N., Lakey, J.H., and Sharrocks, A.D. (1999). The mechanism of phosphorylation-inducible activation of the ETS-domain transcription factor Elk-1. The EMBO journal *18*, 5666-5674.

Yang, X.P., Jiang, K., Hirahara, K., Vahedi, G., Afzali, B., Sciume, G., Bonelli, M., Sun, H.W., Jankovic, D., Kanno, Y.*, et al.* (2015). EZH2 is crucial for both differentiation of regulatory T cells and T effector cell expansion. Scientific reports *5*, 10643.

Yang, Z., Yik, J.H., Chen, R., He, N., Jang, M.K., Ozato, K., and Zhou, Q. (2005). Recruitment of P-TEFb for stimulation of transcriptional elongation by the bromodomain protein Brd4. Molecular cell *19*, 535-545.

Yap, K.L., and Zhou, M.M. (2010). Keeping it in the family: diverse histone recognition by conserved structural folds. Critical reviews in biochemistry and molecular biology *45*, 488-505.

Zeng, R., Cannon, J.L., Abraham, R.T., Way, M., Billadeau, D.D., Bubeck-Wardenberg, J., and Burkhardt, J.K. (2003). SLP-76 coordinates Nck-dependent Wiskott-Aldrich syndrome protein recruitment with Vav-1/Cdc42-dependent Wiskott-

Aldrich syndrome protein activation at the T cell-APC contact site. J Immunol *171*, 1360-1368.

Zhang, W., Sloan-Lancaster, J., Kitchen, J., Trible, R.P., and Samelson, L.E. (1998). LAT: the ZAP-70 tyrosine kinase substrate that links T cell receptor to cellular activation. Cell *92*, 83-92.

Zhang, Y., Kinkel, S., Maksimovic, J., Bandala-Sanchez, E., Tanzer, M.C., Naselli, G., Zhang, J.G., Zhan, Y., Lew, A.M., Silke, J.*, et al.* (2014). The polycomb repressive complex 2 governs life and death of peripheral T cells. Blood *124*, 737-749.

Zhao, E., Maj, T., Kryczek, I., Li, W., Wu, K., Zhao, L., Wei, S., Crespo, J., Wan, S., Vatan, L.*, et al.* (2016). Cancer mediates effector T cell dysfunction by targeting microRNAs and EZH2 via glycolysis restriction. Nature immunology *17*, 95-103.